

EVALUATION OF EXPOSURE TO COMBUSTION PRODUCTS

For Ruwani and Himaya

**EVALUATION OF EXPOSURE TO COMBUSTION PRODUCTS
USING MULTIDIMENSIONAL CHROMATOGRAPHY AND ULTRA
HIGH RESOLUTION MASS SPECTROMETRY**

By Sujan Fernando, M. Sc.

A Thesis Submitted to the School of Graduate Studies in Partial Fulfilment of the
Requirements for the Degree of Doctor of Philosophy

McMaster University

© Copyright by Sujan Fernando, November 2015

McMaster University

Doctor of Philosophy

Hamilton, Ontario

Chemistry and Chemical Biology

TITLE: Evaluation of Exposure to Combustion Products using Multidimensional Chromatography and Ultra High Resolution Mass Spectrometry.

AUTHOR: Sujan Fernando, M. Sc. (McMaster University)

SUPERVISOR: Professor B. E. McCarry

CO-SUPERVISOR: Dr. K. J. Jobst

NUMBER OF PAGES: xvii, 186

ABSTRACT

This thesis investigates the exposure of humans to organic combustion products. Combustion of natural and anthropogenic materials can lead to highly complex mixtures of gas-phase and particle-bound chemical compounds, whose composition and health effects have been studied extensively. Nevertheless, the analysis of other potentially toxic products remains a challenge due to lack of analytical standards and methodologies. The research that encompasses this thesis is a progression from the analysis of known combustion products to the identification of previously unknown products.

Targeted analytical techniques, such as gas chromatography tandem mass spectrometry (GC-MS/MS), were utilized to evaluate firefighter exposure to wood smoke chemicals during training exercises. The results suggest that a subset of the firefighters were at higher risk of exposure which could be related to specific operational roles and the use of personal protective gear. Comprehensive two-dimensional gas chromatography coupled to time-of-flight mass spectrometry (GC×GC-TOF) was used for the identification of novel wood smoke markers and the results indicate that firefighters are equally exposed to gas-phase and particle phase compounds..

Fourier transform ion cyclotron resonance (FT-ICR) mass spectrometry is a non-targeted technique that is complementary to GC×GC. Together, these tools enabled the identification of a suite of halogenated PAHs (haloPAHs) in samples obtained from the Plastimet Inc. fire, one the largest industrial fires in North America. HaloPAHs are similar in structure to toxic polychlorinated dibenzo-p-dioxins (PCDDs), a notorious class

of toxic chemicals, and they were detected at much higher concentrations. In addition, highly substituted and high molecular weight haloPAHs were detected for the first time in an environmental sample. Finally, negative ion atmospheric pressure chemical ionization (NI-APCI) was explored as an alternative ionization technique for the analysis of mixed bromo/chloro dioxins (PXDDs) in the ash sample. PXDDs, with 1550 possible congeners, are potentially more toxic than their chlorinated counterparts (PCDDs). NI-APCI derived structure diagnostic fragments enabled the differentiation of co-eluting PXDD isomers in the ash sample which has not been possible using traditional ionization techniques (EI/CI) associated with GC-MS.

PREFACE

This thesis consists of five years of research carried out by the author in the field of analytical chemistry. The thesis consists of 6 chapters including an introduction, four manuscript based chapters and a conclusions section. One manuscript has been published while two others have been submitted to peer-reviewed scientific journals for publication. One manuscript is unpublished. The research that encompasses the thesis consists of the analysis of samples from two major studies. The first study focused on assessing firefighter exposure to wood smoke during training exercises while the second examined an ash sample from one of the largest industrial fires in North America using state-of-the-art analytical techniques. All chapters were written by Sujan Fernando with editorial comments by Karl J. Jobst, Philip Britz-Mckibbin, and Brian E. McCarry.

ACKNOWLEDGEMENTS

I would first like to express my gratitude to the late Dr. Brian McCarry. Thank you for accepting me into your research group as a Masters student in 2004 and then as a part-time PhD student in 2010. It is still hard to believe you have passed away and this thesis is a reflection of your teachings for which I am forever grateful. Next, I would like to thank Dr. Karl Jobst. You were a shining light at a moment of darkness and I will never forget all the help and guidance that enabled me to produce a successful thesis.

To all of the McCarry group members both past and present, thank you. The list is long but I need to mention Rong Yang, Julia Gia, Ed Sverko, Birta Asfaw, Libia Saborido, David Dam, Tarlika Persaud, Catherine Amoateng Yemi Sofowate, Ken Chalcraft, Elna Deglint, Ankit Rastogi, Michael Gallea, Lori VandenEnden, Roger Luckham, Fan Fei, Paul Hodgson, David Bowman, Vi Dang, Ashraf Ibrahim and Jonathon Bloomfield. Thank you all for the friendship and help over this long journey. I would also like to thank Dr. Kirk Green of the McMaster Regional Centre for Mass Spectrometry for his support and guidance as well as Leah Allan and Tadek Olech for the many years of friendship. A special thank you to Dr. Philip Britz-McKibbin for all the advice and guidance especially with the firefighter project.

Finally I would like to thank my family. To my mother and father, Uvindra and Bennete Fernando who worked hard to provide me with the opportunities in life to succeed and for the continuing support. I would also like to thank my three sisters for all their support as well as my mother- and father-in-law. To my wonderful wife Ruwani, thank you for all your support and patience especially over the last few years. You have carried more than your share of the load in maintaining a functional home and raising our daughter Himaya. To my loving daughter Himaya, thank you for your patience and understanding. Thathi promises to spend more time with you in the future.

TABLE OF CONTENTS

Abstract.....	iii
Preface.....	v
Acknowledgements.....	vi
Table of Contents.....	vii
List of Figures.....	viii
List of Tables.....	xiv
List of Abbreviations.....	xvi
Chapter 1.....	1
Introduction	
Chapter 2.....	47
Evaluation of firefighter exposure to wood smoke	
Chapter 3.....	85
Identification of novel markers of wood smoke exposures in firefighters using GC×GC-TOF-MS	
Chapter 4.....	118
Identification of the halogenated compounds resulting from the 1997 Plastimet Inc. fire in Hamilton, Ontario, using comprehensive two-dimensional gas chromatography and (ultra)high resolution mass spectrometry	
Chapter 5.....	151
Differentiation of (mixed) Halogenated Dibenzo- <i>p</i> -Dioxins by Negative Ion Atmospheric Pressure Chemical Ionization	
Chapter 6.....	179
Conclusions	

LIST OF FIGURES

Chapter 1

Figure 1. Total ion current (TIC) chromatogram of an ash sample extract from the Plastimet fire (see Chapter 4). The co-eluting compounds give rise to a hump in the chromatogram which complicates comprehensive analysis.

Figure 2. Chemical structures of guaiacol, syringol and the alkylated homologs.

Figure 3. Chemical structures of polychlorinated biphenyls (PCBs), polychlorinated dibenzo-*p*-dioxins (PCDDs), polychlorinated dibenzofurans (PCDFs) and chlorinated polycyclic aromatic hydrocarbons (Cl-PAHs).

Figure 4. The predicted reaction pathway of a radical/molecule coupling of 2,4,5-trichlorophenol leading to the formation of 2,3,7,8-TCDD.

Figure 5 (A) contour plot of a urine sample (B) three-dimensional (3D) surface plot of a specific area of the contour plot (highlighted by a white box). Some of the components that co-elute in the 1st Dimension but are separated in the 2nd Dimension are indicated by the red dots on the 3D surface plot. A projection of the 1st dimension chromatogram is presented. Many minor components are also resolved in this chromatogram that might otherwise be difficult if not impossible to observe much less resolve in a one-dimensional separation.

Figure 6. LECO's Dual-stage Quad Jet Thermal Modulator.

Figure 7. Schematic of the Zoex ZX2 loop modulator.

Figure 8. Reconstructed contour plot of an ash sample extract. The contour plot contains data from 2 different chromatograms which have been overlaid. The top band of compounds correspond to a method with a secondary oven offset of 0°C. The bottom band of compounds correspond to a method with a secondary oven offset of 40°C.

Figure 9. [A] Schematic of a peak from the primary column (blue trace) has been sliced into 3 during the modulation period. [B] The 3 slices have 3 different 1D retention times but the same 2D retention time.

Figure 10. The selected ion monitoring (SIM) and multiple reaction monitoring (MRM) traces for the trimethylsilyl derivative of 1- and 2-hydroxynaphthalene isomers. The MRM method is more selective compared to the SIM method as only the 2 target species are observed in the trace. Furthermore, the MRM method offers better sensitivity due to low background noise in the trace.

Figure 11. Schematic of a time-of-flight mass spectrometer coupled to a GCxGC (diagram courtesy of LECO).

Figure 12. (a) Schematic of the GC transferline and Varian J320MS (diagram courtesy of Varian Inc). (b) Schematic of the hexapole accumulation cell rf ion guide, and ICR cell (diagram courtesy of Varian Inc).

Chapter 2

Figure 1. (a) Total concentration measured for MPs (16 compounds) and (b) PAHs (22 compounds) that highlights the large variability in chemical exposures following training exercises between firefighters at different burn houses from air samples attached to the firefighters ($n=26$), where * indicates that 2 samples were not recovered during training exercises.

Figure 2. The sum of PAHs (16 compounds) and MPs (15 compounds) measured in the pre- and post-exposure wipes from across 5 different body sites for each firefighter are displayed as a box-whisker plot for the five different training exercises, where the insert shows overall changes in whole body chemical exposure for all firefighters ($n=28$). Significance levels are denoted by * $p < 0.05$, ** $p < 0.005$ and *** $p < 0.0005$ using a student's t-test.

Figure 3. Distribution of the total MPs (15 compounds) and PAHs (16 compounds) at the 5 skin sites on the firefighters ($n = 28$). The stack plot shows the net total concentration (ng/cm^2) of the PAH and MP at each skin site sampled on each firefighter following wood smoke exposure during training exercises.

Figure 4. (a) The net increase in the 24 h post-exposure urine of firefighters ($n=28$) for selected MPs (3 compounds) and (b) hydroxy-PAHs (8 compounds/isomers) at five different burn house sites. The net increase in 24 h post-exposure was calculated by first subtracting the pre-exposure value from each of the post-exposure samples followed by the summation of the net concentrations. A value of 1 has been substituted for those firefighters ($n=7$) that did not display a net increase in post exposure for display purposes. The graphic insert in each figure displays a Box-Whisker (*log-scale*) plot for the pre-exposure and net increase in the 24 h post exposure urine levels for MPs and hydroxy-PAHs for all firefighters along with significance levels for fold-change increase using a student's t-test.

Figure 5. The impact of firefighter operational activity during training exercises on measured net total increase in smoke markers excreted in urine (24 h) post-exposure. (a) There was a significant increase in total exposure for firefighters conducting search and

rescue (S&R) activities relative to those primarily involved in fire extinguishing (EXT); (b) a 3D scores plot derived from PLS-DA shows differences in exposure among individual firefighters based on their operational role, whereas (c) variable importance in projection (VIP) rankings show that two alkyl-substituted MPs are significantly elevated in urine among the search and rescue sub-group. All data is *log*-transformed (a) and auto-scaled (b, c) based on net increases in creatinine-normalized concentrations of 3 MPs and 8 OH-PAHs detected in urine. PLS-DA model accuracy was 0.678 with a $R^2 = 0.369$ and $Q^2 = 0.210$ with using leave out-one-at-a-time cross-validation using the first principal component (PC1).

Figure S1. The figure displays the urinary profile of representative hydroxy-PAH compounds from smokers and non-smokers in the US population determined as part of the NHANES study(18). Plotted alongside are the average pre-exposure and post-exposure profiles for 3 firefighters with the highest net increase in post-exposure samples from Figure 4b. This data highlights that the pre-exposure baseline is within the range of the non-smoker profile, whereas the post-exposure data is similar to median values measured for smokers suggestive of significant wood smoke exposure among non-smoking firefighters equipped with bunker gear (*i.e.*, personal protective equipment).

Chapter 3

Figure 1. Total ion current (TIC) 2D chromatogram of [A] wood smoke sample and the corresponding [B] pre-exposure and [C] post-exposure urine samples from an exposed individual presented as a contour plot. The urine samples were more complex compared to the air sample. Also, more peaks were detected in the post-exposure urine than in the pre-exposure urine sample.

Figure 2. A magnified view of a section of a post-exposure urine sample 2D chromatogram (TIC). Many of the co-eluting peaks in the first dimension are resolved in the second dimension.

Figure 3. Three dimensional (3D) surface plot of the 3 pentylguaiacol trimethylsilyl derivatives in smoke and in the pre- and post-exposure urine of an exposed individual.

Figure 4. The electron ionization (EI) mass spectra of the trimethylsilyl (TMS) derivatized guaiacol, methylguaiacol and ethylguaiacol. TMS derivatives of guaiacol and its alkylated homologs have a characteristic fragmentation pattern in which the molecular ion losses successive 15 amu units corresponding to CH_3 losses with the base peak corresponding to the $[\text{M}-2(\text{CH}_3)]^+$ ion.

Figure 5. The EI mass spectra of the tentatively identified trimethylsilyl (TMS) derivatized pentyl guaiacol isomers. The mass spectra follow the same fragmentation pattern as the TMS derivatives of guaiacol and its methyl and ethyl homologs in figure 4.

Figure 6. 3D surface plot of the trimethylsilyl (TMS) derivatized resin acids (6) in smoke and in post-exposure urine of an exposed individual.

Figure 7. A reconstructed 2D chromatogram of selected wood smoke markers identified in the air and in the post-smoke exposure urine of a single firefighter.

Figure 8. The fold increase (in peak area) for the sum of the 6 resin acids, 3 pentylguaiacols, along with the specific markers selected in Chapter 2 which include 3 syringols (syringol, methylsyringol, ethylsyringol) and 8 hydroxyPAHs (metabolites of naphthalene, fluorene and phenanthrene). Pre-exposure urine samples were collected at approximately 9am before the training exercises were conducted which lasted for approximately 30 minutes. All post-exposure urine samples were collected for the next 24hrs and analyzed.

Figure 9. Box-whisker plot of the pre and post-exposure urinary concentrations of MPs, hydroxyPAHs and resin acids in a group of 18 firefighters.

Chapter 4

Figure 1. (a) FT-ICR mass spectrum obtained from an extract of the composite soil sample; (b) Expanded view of the m/z 320 region of the spectrum.

Figure 2. (a) Mass defect plot constructed from the FT-ICR mass spectrum of the soil extract. The structures (left) are tentatively proposed from accurate mass derived elemental compositions (right); (b) Expanded view of the plot focusing on the MD scale between 0.2 and 0.3.

Figure 3. LEFT (a) Total ion and (b-c) Extracted ion chromatograms of the molecular ions of the (mixed) halogenated ANT/PHE and FLU/PYR isomers from GCxGC-HRTOF analysis. RIGHT : Mass spectra with (d) $C_{14}H_6Cl_4^{\bullet+}$ molecular ions; (e) $C_{12}H_5OCl_2Br^{\bullet+}$; and (f) $C_{14}H_6Cl_3Br^{\bullet+}$. The structures are tentatively proposed on the basis of exact mass measurements and EI dissociation behaviour.

Figure S1. Surface plots of the Plastimet soil extract focusing on the region of interest for the identification of 1,3,6,8-tetrachloropyrene. The plot on the top is that of the authentic standard and the plot at the bottom is from the sample.

Figure A1. GCxGC analyses of the crude ash extract using a DB-5 (1D column) and a DB-17 (2D column) configuration. [A] Reconstructed 1D total ion current (TIC) chromatogram. [B] 2D chromatogram presented as a contour plot. The 2D chromatogram shows the separation of the aromatic and halo-aromatic compounds from the unresolved complex mixture (UCM) which is not possible on a standard 1D GC-MS system as depicted by the reconstructed 1D TIC.

Figure A2. GCxGC analyses of the ash sample crude extract using a DB-17 (1D column) and a DB-5 (2D column) configuration. In this case the UCM is located atop of the aromatic band and thus does not interfere with the aromatics.

Figure A3. GCxGC analyses of the ash sample crude extract and Sephadex fractions using a DB-17 (1D column) and a DB-5 (2D column) configuration. [A] Crude sample extract displaying both the aliphatic and aromatic compounds. [B] Sephadex fractions 1-6 which contain the majority of aliphatic compounds. [C] Sephadex fractions 7-12 which contain the majority of aromatic and halo-aromatic compounds.

Chapter 5

Figure 1. The NI-APCI spectra of 2378-TCDD, 2378-TBDD and 2,3-Br₂-,7,8-Cl₂DD. ECPs are observed at m/z 176, and 266 for the 2378-TCDD and 2378-TBDD species. Both of these ECPs are observed for the 2,3-Br₂-,7,8-Cl₂DD

Figure 2. The positive and negative ion APCI analysis of the 1378-, 1234- and 2378-tetra chlorinated dioxins (TCDD) and tetra brominated dioxins (TBDD). [A] displays the molecular ion trace (APCI +ve) for the TCDD isomers and [B] displays the Cl₂ ether cleavage product trace (APCI -ve). [C] displays the molecular ion trace (APCI +ve) for the TBDD isomers and [D] displays the Br₂ ether cleavage product trace (APCI -ve). Note that the TCDDs were separated on a 40m column (DB5-MS) whereas the TBDDs were separated on a 15m column (DB5-MS).

Figure 3. [a] The (M-Cl+O)⁻ chromatogram of the hexachlorinated dioxins (HxCDD) in the Plastimet ash sample along with the Cl₂, Cl₃ and Cl₄ ether cleavage product chromatograms (b-d). The ether cleavage product chromatograms yield the distribution of the chlorines across the 2 benzene rings of the dioxin backbone.

Figure 4. [a] The APCI⁺ MRM trace [(M⁺) → (M-COBr)] transition for the monobromo-trichloro-dioxins (Br₁Cl₃-DD) in the Plastimet ash extract. [b] The NI-APCI Br₁Cl₁ ether cleavage product trace for the same sample. The ether cleavage product trace shows the number of Br₁Cl₃-DD species that have a 2:2 halogen distribution. The toxic 2-Br, 3,7,8-CDD isomer has been identified using an authentic standard.

Figure 5. [a] The APCI⁺ molecular ion chromatogram [b] the (M-Cl+O)⁻ chromatogram [c] Br₁Cl₁ ECP chromatogram [d] Br₁Cl₂ ECP chromatogram and [e] Br₁Cl₃ ECP chromatogram. The ECP chromatograms yield information on the halogen distribution for the 8 unresolved peaks observed.

Figure 6. The percent composition of the halogen distribution for the hexa-, penta- and tetra substituted Br₁Cl_x species. In this case the percent composition for the symmetrical distributions (3:3, 3:2 and 2:2) was favoured over the asymmetrical distributions (4:2, 4:1,4:0 and 3:1) of the halogens for these congener classes.

Figure S1. The Br₂ ECP trace at m/z 266 for a suite of halogenated organics analyzed at a cone gas flow rate of 100L/hr and then at 175L/hr. In this case the increased gas flow into the source helped reduce exhaust backflow resulting in an increase in the S/N as shown for the 2378-TBDD species.

Figure S2. The NI-APCI mass spectrum of 2378-TBDD using nitrogen and then compressed air as the cone gas. The use of compressed air led to a significant increase in the relative abundance of the [M+O]⁻ peak. However, the absolute intensity of the ions including the ECP at m/z 266 were significantly lower compared to the nitrogen spectrum.

LIST OF TABLES

Chapter 2

Table S1. The average airborne concentration of methoxyphenols (16 compounds) and PAHs (22 compounds) from five sampling sessions at four different burn houses/sites across Ontario.

Table S2. The average MP (15 compounds) and PAH (16 compounds) skin loadings (ng/cm^2) measured for all subjects ($n=28$) at five different burn houses used for firefighter training.

Table S3. The pre-exposure and average post exposure concentrations of the selected urinary MP and hydroxy-PAH markers measured for all firefighters ($n=28$) at five different sites. All urine samples were normalized to creatinine using single-spot urine samples collected prior to exposure and 24 h urine post-exposure for each subject.

Chapter 3

Table 1. Compounds identified in wood smoke air samples ($N=5$). 200 compounds were identified using authentic standards and NIST (2008) mass spectral library while 880 compounds were classified as unknowns. The percent abundance in smoke is based on the total peak area for the compounds detected in each compound class.

Table 2. Smoke marker compounds identified in an air sample and in post-exposure urine samples of a firefighter.

Table S1. The metabolites of PAHs, methoxyphenols/derivatives, resin acids and selected novel compounds detected in the post-exposure urine of a single firefighter. Also provided are the concentrations of the compounds in the smoky air and the fold increase in post-exposure urine in comparison to the pre-exposure urinary level.

Chapter 4

Table 1. Concentration of PAH and corresponding halo-PAHs identified in the soil sample.

Table S1. Concentration of selected PAHs and haloPAHs from the ash sample. Compounds were identified and quantified using authentic standards.

Chapter 5

Table 1. A list of the 21 PCDD, PBDD and PXDD/F standards analyzed using APCI. Listed are the observed pseudomolecular ions in NI-APCI mode along with the ether cleavage products (ECP) and its relative abundance (in parenthesis). Also listed are the positive radical cations $[M\bullet+]$ observed by APCI+ mode as well as the estimated instrument detection limits (I.D.L.) for the observed ions. Note that for certain ECP which were detected below 1%, IDLs could not be calculated from the 1pg of material injected on column.

LIST OF ABBREVIATIONS

1-HP	1-hydroxypyrene
2378-TCDD	2,3,7,8-tetrachlorodibenzodioxin
AhR	Aryl hydrocarbon receptor
ANT/PHE	Anthracene/phenanthrene
APCI	Atmospheric pressure chemical ionization
B	Magnetic field
BaP	Benzo[a]pyrene
Br ₁ Cl ₃ -DD	Monobromo-trichloro-dioxin
Br ₁ Cl ₄ -DD	Monobromo-tetrachloro-dioxin
Br ₁ Cl ₅ -DD	Monobromo-pentachloro-dioxin
BTEX	Benzene, toluene, ethylbenzene, xylene
CE	Capillary electrophoresis
CI	Chemical ionization
CID	Collision induced dissociation
CIPAHs	Chlorinated polycyclic aromatic hydrocarbons
CO	Carbon monoxide
DIP	Direct insertion probe
DNA	Deoxyribonucleic acid
ECP	Ether cleavage product
EI	Electron ionization
FLU/PYR	Fluoranthene/pyrene
FT-ICR-MS	Fourier transform ion cyclotron resonance mass spectrometer
FWHM	Full width at half-maximum
GC	Gas chromatography
GC-MS	Gas chromatography-mass spectrometry
GC-MS/MS	Gas chromatography tandem mass spectrometry
GCxGC	Two-dimensional gas chromatography
GCxGC-TOF-MS	Two-dimensional gas chromatography time-of-flight MS
Halo-PAHs	Halogenated polycyclic aromatic hydrocarbons
HCl	Hydrogen chloride
HPLC	High performance liquid chromatography
HRTOF	High resolution time-of-flight
HxCDD	Hexachlorinated dioxins
IDLs	Instrument detection limits
LMCS	Longitudinally modulated cryogenic system
m/z	Mass-to-charge ratio

MD	Mass defect
MP	Methoxyphenols
MRM	Multiple reaction monitoring
MS	Mass spectrometer
NI-APCI	Negative ion atmospheric pressure chemical ionization
PAH	Polycyclic Aromatic Hydrocarbons
PASH	Sulfur containing polycyclic aromatic hydrocarbons
PBDD	Polybrominated dibenzo- <i>p</i> -dioxins
PBDF	Polybrominated dibenzofurans
PCBs	Polychlorinated biphenyls
PCBZ	Polychlorobenzenes
PCDD	Polychlorinated dibenzo- <i>p</i> -dioxins
PCDF	Polychlorinated dibenzofurans
PCN	Polychlorinated naphthalenes
PCP	Polychlorophenols
PM	Particulate matter
PVC	Polyvinylchloride
PXDDs	Mixed bromo/chloro dioxins
PXDDs	Mixed halogenated dibenzo- <i>p</i> -dioxins
PXDFs	Mixed halogenated dibenzofurans
QTOF	Quadrupole-time of flight
R	Mass Resolution
SCBA	Self-contained breathing apparatus
SIM	Selective ion monitoring
SRM	Selective reaction monitoring
TBDD	Tetrabrominated dibenzo- <i>p</i> -dioxins
TCDD	Tetrachlorinated dibenzo- <i>p</i> -dioxins
TEF	Toxic equivalency factors
TEQ	Toxic equivalency quantity
TIC	Total ion current
TOF	Time-of-flight
UCM	Unresolved complex mixture
ν	Cyclotron frequency
VOC	Volatile organic compounds
z	Charge
Δm	Mass difference
ω_c	Angular velocity

CHAPTER ONE

Introduction

1.1 General Background

Humans are exposed to numerous combustion products throughout their life. Exposure varies from common sources such as cigarette smoke, vehicle exhaust, and smog to more extreme events such as fires and occupationally related exposures. A number of studies have evaluated exposure in both global and local settings¹. Global issues involve emissions from urban areas, industries, power plants, waste incineration and large-scale fires. Local issues involve indoor air quality, exposure to biomass burning and local traffic.

Smoke from combustion sources can be very complex and consists of gaseous and particulate bound chemicals. Carbon monoxide (CO) is a common toxic gas produced during combustion processes. The CO levels in smoke from fires range from 0.1 to 10%. The occurrence of CO poisoning is well known^{2,3}. Other toxic gases released in fires include nitrogen oxides, ammonia, phosgene, acrolein, hydrogen cyanide and isocyanates^{4,5}.

Toxic metals have also been detected in the gas-phase as well as the particle-phase of smoke⁶. Lead is one of the major metal contaminants in the environment due to its use in gasoline, paints and batteries. Lead exposure can cause damage to the heart and kidneys and also effect the development of the central nervous system in children⁷. Exposure to

other toxic metals such as beryllium, nickel and chromium in environmental and occupational settings has also been documented⁶.

Volatile organic compounds (VOC) including benzene, toluene, ethylbenzene and xylene (BTEX) are also gas-phase combustion products. BTEX are considered to be very toxic and are produced during numerous combustion processes and these chemicals are present in cigarette smoke. It has been determined that the levels of BTEX in the blood of smokers is on average ten times higher compared to non-smokers⁸. VOCs also pose a threat to air quality and some VOCs are detected at higher levels indoors than in outside air⁹. A major source of indoor VOCs is from off-gassing from new materials¹⁰. Formaldehyde is an example of a VOC which is emitted from building materials such as paints, adhesives and tiles. Formaldehyde is also released at high levels during fires and is known to irritate the mucous membranes of humans¹¹.

Combustion also leads to the production of particulate matter (PM). PM above 1000 μm in diameter is referred to as dust and is often found on surfaces. PM ranging in size from 1000 μm to below 1 μm is found suspended in the air with the smaller diameter PM remaining airborne for a longer period of time than the larger diameter PM¹². Larger diameter PM is generally filtered in the nose. PM smaller than 10 μm (PM₁₀) can penetrate into the lungs while PM smaller than 2.5 μm (PM_{2.5}) can penetrate the lungs and enter the blood stream directly. Exposure to PM is associated with adverse health effects including pulmonary and cardiovascular disease^{12,13}. In a study conducted using ¹³C generated ultrafine particulate (10-100nm) it was found that exposed rats showed

effective translocation of the ultrafine elemental carbon particles from the lungs to the liver within 1 day of inhalation exposure¹⁴.

The dangers associated with PM exposure is further increased by the chemicals bound to the particulate matter¹⁵. The particle-bound chemicals can enter the body and be extracted from the PM and lead to potential toxic effects. Some of these compounds include polycyclic aromatic compounds such as polycyclic aromatic hydrocarbons (PAHs) and methoxyphenols (MPs) as well as halogenated aromatics including polychlorinated biphenyls, dioxins and furans. The volatile fraction of these compounds may be found in the gas-phase as well. The occurrence and toxicity of these compounds will be discussed in more detail in the following sections.

The numerous chemicals that have been identified in the environment represent only a very small fraction of the total chemicals present. In addition, novel compounds continue to be introduced to the environment from various manufacturing processes. This issue is compounded by the presence of impurities in commercial products which can go undetected for many years. For instance, 2,3,7,8-tetrachlorodibenzo-*p*-dioxin (2378-TCDD) was present as an impurity in the infamous herbicide Agent Orange¹⁶. 2378-TCDD is regarded as one to the most toxic chemicals known to exist and is a persistent organic pollutant¹⁷. Comprehensive analysis of environmental samples is thus critical for the identification of toxic chemicals. Comprehensive analysis in this case refers to the ability to resolve all components present in a sample. This is difficult with traditional chromatographic techniques such as gas chromatography-mass spectrometry (GC-MS). For example, Figure 1 displays the total ion current (TIC) chromatogram of an extract of

ash obtained from a fire, at a plastics recycling facility (Plastimet Inc.). Comprehensive analysis is very difficult in this case due to the large number of co-eluting compounds, which gives rise to an unresolved ‘hump’ in the chromatogram. Indeed, one of the goals of this thesis was to develop the necessary analytical techniques required for the deconvolution of complex samples.

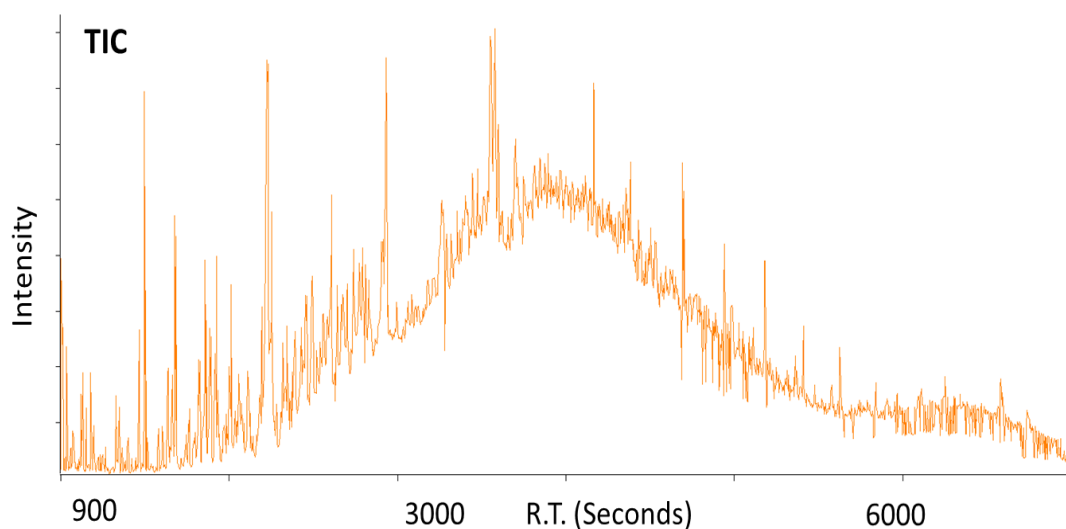


Figure 1. Total ion current (TIC) chromatogram of an ash sample extract from the Plastimet fire (see Chapter 4). The co-eluting compounds give rise to a hump in the chromatogram which complicates comprehensive analysis.

The research that encompasses this thesis is a progression from the analysis of known combustion products to the identification of previously unknown products. As a result both targeted and non-targeted analytical techniques have been utilized. These techniques were used to evaluate the exposure of firefighters to gaseous and particle-bound wood smoke chemicals under controlled training exercises and to analyze the ash fallout from the Plastimet fire, one of the largest industrial fires in North America.

The specific goals of this thesis include:

1. Development of analytical methodologies, specifically multidimensional gas chromatography and high resolution mass spectrometry-based techniques, for targeted and non-targeted analysis of combustion products.
2. Evaluation of firefighter exposure to wood smoke during training exercises using known and novel chemical markers.
3. Identification of halogenated organics in ash fallout from a major industrial fire at a plastic recycling plant (Plastimet Inc).

Firefighter exposures are of significant concern due to the risks posed by both short term and long term occupational exposures to chemicals. Chronic exposure to smoke can lead to significant health problems, including respiratory infections, impaired lung function, cardiac infarctions and cancers¹⁸⁻²⁰. A number of epidemiological studies have identified direct links between firefighters' exposures to toxic chemicals and various cancers^{19,21}. Chemical exposure can occur via inhalation/ingestion or absorption through the skin. Nevertheless, there are only a few studies that have attempted to quantify firefighter exposures using either air measurements or skin concentrations²²⁻²⁵. Even fewer studies have monitored and quantified the air, skin and biochemical markers associated with industrial or trade related diseases^{26,27}. Furthermore, exposure has been evaluated using a limited number of marker compounds. A classical marker of exposure is pyrene, a common PAH and its urinary metabolite 1-hydroxypyrene. However since PAHs are ubiquitous in nature, pyrene is not a specific marker of exposure²⁸⁻³⁰.

A key aspect of the research presented in this thesis is the identification of novel combustion products from fires. The combustion products of interest consist of both gas-phase and particle-phase organics due to their potential toxicity to humans and persistence in the environment. Of the myriad combustion products, those arising from the burning of wood and plastic are of particular interest due to the ubiquitous nature of these materials. The known combustion products of these materials and the toxicities are described in the following sections.

1.2 Combustion Products of Wood

Wood smoke is composed of diverse groups of compounds including sugars, alcohols, sterols, polycyclic aromatic hydrocarbons (PAHs) and numerous lignin breakdown products^{31,32}. Lignin constitutes 18-35% of wood by mass and as a result its breakdown products, including methoxyphenols (MPs), are the most abundant group of compounds found in wood smoke³². The occurrence and distribution of MPs has been studied previously by Simpson *et al.*³³. There are two major types of MPs; guaiacols and syringols (Figure 2). Guaiacols are present in both softwoods and hardwoods, while only syringols are found in hardwoods. It has long been known that guaiacol and its alkylated homologs give rise to the taste while syringol and its alkylated homologs give rise to the aroma in smoked foods³⁴.

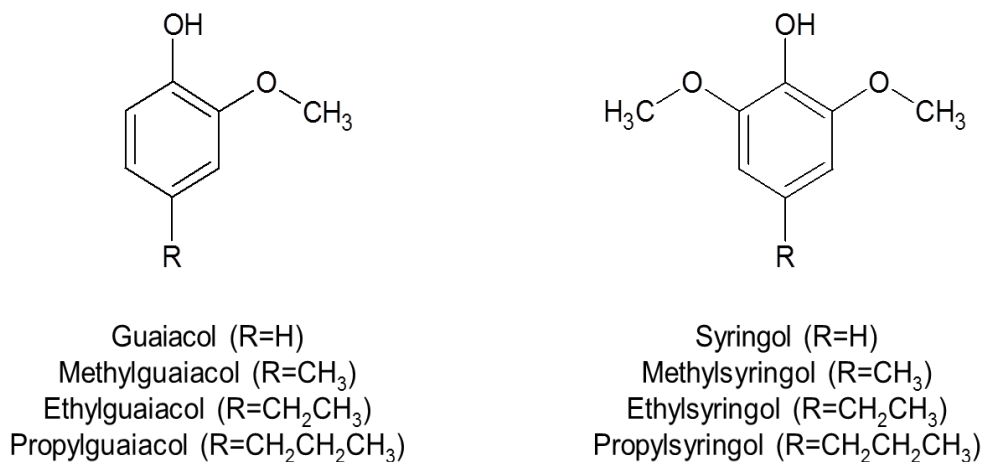


Figure 2. Chemical structures of guaiacol, syringol and the alkylated homologs.

PAHs are a class of organic contaminants that are formed as primary combustion products of carbonaceous fuels such as gasoline, diesel, kerosene, coal and wood^{35,36}. As a result PAHs are ubiquitous in the environment. Common PAHs range from naphthalene (2 rings, 128 Da) to coronene (7 rings, 300 Da). The carcinogenic and mutagenic properties of some PAHs pose a serious threat to humans^{37,38}. PAHs and its urinary metabolites (hydroxyPAHs) have been monitored in many environments and individuals including road pavers, coke plant workers, smokers and members of the general population^{30,39}.

1.3 Combustion Products of Plastic

Plastic fires pose a serious threat to human health due to the nature of the combustion products that are formed⁴⁰. Polyvinylchloride (PVC), a ubiquitous material, is a prime example. Combustion of PVC leads to a wide range of halogenated organics⁴¹ and some of these compounds are known to be toxic, persistent in nature and bioaccumulative¹³⁻¹⁶.

These compounds include polychlorinated biphenyls (PCBs), polychlorinated dibenzo-*p*-dioxins (PCDDs), polychlorinated dibenzofurans (PCDFs) and chlorinated polycyclic aromatic hydrocarbons (Cl-PAHs) (Figure 3).

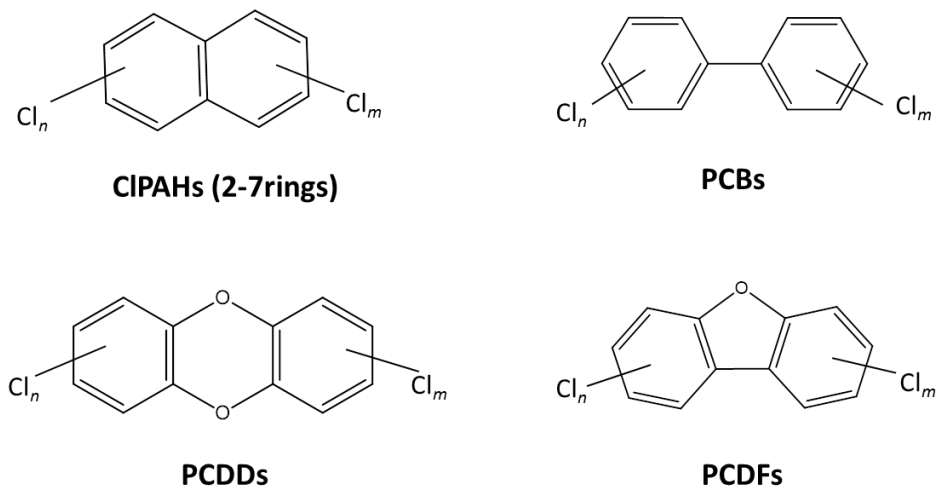


Figure 3. Chemical structures of polychlorinated biphenyls (PCBs), polychlorinated dibenzo-*p*-dioxins (PCDDs), polychlorinated dibenzofurans (PCDFs) and chlorinated polycyclic aromatic hydrocarbons (Cl-PAHs).

It is estimated that approximately 1.4 billion pounds of PCBs were produced between 1929 and 1977 in the U.S. A large portion of these PCBs are used in the electrical utility industry in transformers and capacitors. PCBs were also used as plasticizers in paints and cements, stabilizing additives in flexible PVC coatings of electrical wiring and electronic components. In contrast, PCDDs and PCDFs are thought to be unintentional products of combustion^{42,43}. PCDDs and PCDFs are thought to be produced by thermal conversion processes involving precursor molecules such as polychlorophenols (PCPs), PCBs and polychlorobenzenes (PCBZs)⁴⁴. In the case PCPs, self-condensation⁴⁴ is believed to lead to the formation of PCDD/Fs. The process is thought to involve the coupling of a radical/radical or molecule/radical followed by cyclization of the initial intermediates

followed by chlorination/dechlorination reactions. Figure 4 shows the predicted reaction pathway of a radical/molecule coupling of 2,4,5-trichlorophenol leading to the formation of 2,3,7,8-TCDD⁴⁵. A series of laboratory experiments by Buser, Rappe and colleagues have been able to generate PCDDs and PCDFs from PCBs and PCBZs by heating the latter two types of compounds in sealed ampoules in the presence of air and at different temperatures^{43,44}.

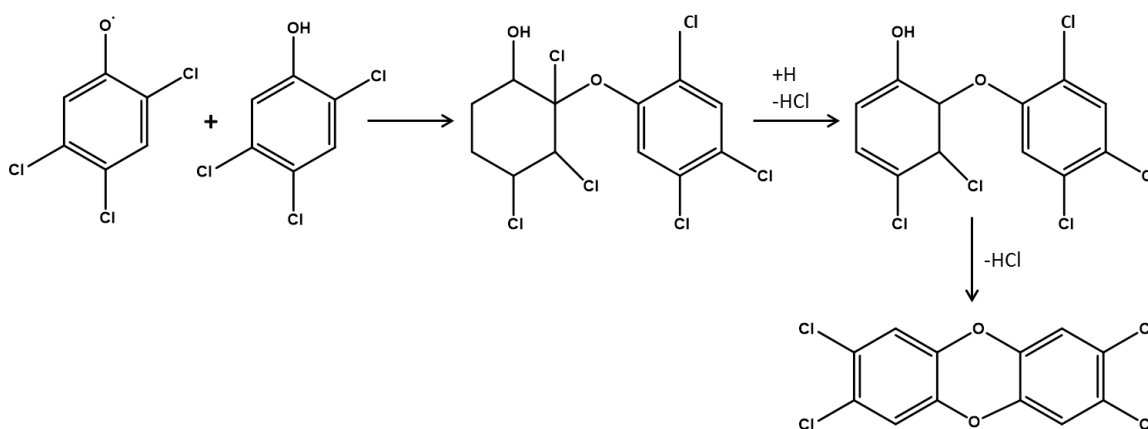


Figure 4. The predicted reaction pathway of a radical/molecule coupling of 2,4,5-trichlorophenol leading to the formation of 2,3,7,8-TCDD⁴⁵.

De novo formation is an alternative mechanism of formation whereby oxidative decomposition of carbonaceous matrix leads to the production of PCDD/Fs. In this case macromolecules with oxygens incorporated into its backbone will yield greater amounts of PCDD/Fs⁴⁶. Decomposition of polymers such as PVC are known to produce high concentrations of PCDD/Fs mainly due to the release of HCl that leads to chlorination of the organics⁴⁶.

Cl-PAHs are believed to be produced from the direct chlorination of the parent PAHs^{37,47}. During fires, higher temperatures favour the production of aromatic compounds such as substituted benzenes and PAHs⁴⁸. Formation of Cl-PAH from PVC combustion was also found to increase with temperature⁴⁹. Wang et al. observed the total concentration of the chlorinated derivatives of the parent PAH naphthalene, biphenyl, fluoranthene, phenanthrene, anthracene, fluoranthene and pyrene increased from 13.58ug/g PVC at 600°C to 101.95ug/g PVC at 900°C⁴⁹. The results suggest that these Cl-PAH were mostly likely formed by the direct chlorination of the parent PAH with hydrogen chloride (HCl) released from the PVC during combustion.

In addition to fires, waste incineration, vehicle exhaust, and various product manufacturing processes lead to the formation and release of halogenated organics into the environment where they persist in air, soil and water^{42,47}. Over the past two decades brominated and mixed bromo/chloro analogues have been detected in the environment due to the increased use of brominated flame retardants (BFRs) in wide variety of products⁵⁰. Manufactured polymers such as PVC contain on average 10% BFRs in an attempt to create more fire-safe products⁵¹. It is reported that plastics including PVC and polypropylene are the largest end users of PBDEs in the world⁵¹. The most common BFR currently used is polybrominated diphenyl ether (PBDE). PBDEs are released to the environment from fires and waste incineration⁵⁰. The degradation and transformation products of PBDEs include polybrominated dibenzo-*p*-dioxins (PBDDs), furans (PBDFs) and their mixed halogenated counterparts (PXDD/Fs)^{50,52}. Given the

similarity in structure to PCBs, PBDEs also have similar toxicity, persistence in nature and bio-accumulation properties⁵⁰.

1.4 Toxicities

Exposure to smoke from fires is often evaluated by monitoring the volatile gases such as carbon monoxide, nitrogen oxides, ammonia, phosgene, acrolein, hydrogen cyanide and isocyanates due to their acute toxicity^{4,5}. In the case of wood smoke, it is the MPs that are most abundant³². However, the toxicities associated with MPs are not well understood even though mid-polar fractions of wood smoke particulate matter containing MPs display high cytotoxicity as demonstrated by glutathione depletion in macrophages relevant to lung immune function^{53,54}. Given the relatively short half-lives of MPs in vivo (4-6hrs) they serve as good biological markers of smoke exposure⁵⁵. As a result, a suite of MPs, both known and novel, have been used to evaluate firefighter exposure to wood smoke in this thesis (Chapter 3 & 4).

PAHs are not very toxic in their native form. The toxicity is as a result of biological activation⁵⁶. Once PAHs enter the body, they are metabolized before being excreted. PAHs are metabolized mainly in the liver via CYP enzymes (Cytochrome P-450). PAHs are initially transformed to epoxides and then to dihydrodiol and phenol derivatives. The diol epoxides of PAHs are mutagenic and react with deoxyribonucleic acid (DNA) to form adducts. When a PAH-DNA adduct is formed at a site critical to the regulation of cell differentiation or growth, this could result in carcinogenesis. The formation of an adduct at a critical site could lead to a mutation during cell replication. Cells that undergo

rapid turnover such as those in the bone marrow, skin and lung tissue are at increased risk of such an event in the case of PAH exposure. The location of the epoxides on a PAH predicts its reactivity and as a result its mutagenicity and carcinogenicity. Benzo[a]pyrene (BaP) is regarded as one of the most potent PAHs. In this thesis, PAH-metabolites were monitored in the urine of exposed firefighters.

Certain halogenated derivatives of PAHs exhibit both carcinogenic and mutagenic properties. Studies on the mutagenicity of ClPAHs have been carried out with *Salmonella typhimurium* TA98 and TA100 in the presence or absence of the S9 activation enzyme system⁵⁷. It was noticed that some ClPAHs exhibit direct-acting mutagenicity in the *Salmonella* system while the parent PAHs exhibit mutagenicity only after biological activation in the presence of the S9 enzyme system. In addition, certain ClPAHs are reported to have other toxic effects, such as tumorigenicity and oncogene activation as reviewed by Fu et al⁵⁸. It's reported that the potencies of 3,8-dichlorofluoranthene and 6-chlorochrysene were 2.0 and 5.7 times greater than that of BaP in the YCM3 cell assay system. Furthermore, it is believed that the toxicity of ClPAHs depends on the regioselectivity and stereoselectivity of the substitutions⁵⁸. In some cases the substitution may block the metabolism of these compounds and inhibit the production of the toxic metabolite intermediates. In other cases where the halogen position on the PAH is remote from the metabolic activation site, halogenation substitution could result in an enhanced metabolic activation and give rise to a more toxic response compared to the parent PAH⁵⁸.

2,3,7,8-tetrachlorodibenzodioxin (2,3,7,8-TCDD) has been described as one of the most toxic chemicals known to exist because of its carcinogenic nature⁴². The potency of 2,3,7,8-TCDD has been determined to be 60 times higher than that of BaP⁴⁷. Common effects of dioxin exposure include immunosuppression, tumor promotion and numerous histopathological changes in body organs⁵⁹. The toxic responses seem to be initiated by the binding of the 2,3,7,8-TCDD to the aryl hydrocarbon receptor (AhR) which regulates the production of Cytochrome P450 and the associated enzymes^{60,61}. The AhR is found in the cytoplasm in a complex with HSP90, XAP2 and P23 protein. Upon binding of a ligand the complex translocate into the nucleus which promotes the enhanced expressions of the CYP1A1 gene which results in the formation of the Cytochrome P450 enzymes. A study conducted on AhR-deficient mice seem to suggest that almost all of the toxic effects of dioxins are initiated by the binding of the 2,3,7,8-TCDD with the AhR⁶². However, the mechanisms involved are not well understood.

Compounds with similar chemical structures to 2,3,7,8-TCDD also have the ability to activate the aryl hydrocarbon receptor and are thus have the potential to be highly toxic⁶³. Studies involving PBDD/Fs and PXDD/Fs have found that some of these compounds have similar toxicities to 2,3,7,8-TCDD⁶³. In fact, some studies have found that PXDD/Fs with substitutions at the 2,3,7,8 positions are potentially more toxic than 2,3,7,8-TCDD^{64,65}. As a result the World Health Organization (WHO) has derived toxic equivalency factors (TEF) for a group of these compounds relative to 2,3,7,8-TCDD. Toxic equivalency quantities (TEQ) are then derived based on the concentration of each compound in a given sample. Furthermore, it has been determined that exposure to

mixtures of these compounds seems to follow an additive model and as such total TEQ values are used to assess toxicity in such cases ⁵⁹. Dioxins however are not good indicator of short-term exposure due to their lipophilic nature. The average half-life of dioxins in humans is approximately 8 years ⁶⁶.

1.5 Analytical Methodologies

One of the major challenges confronted by this thesis was the development of appropriate analytical tools capable of comprehensive analysis of complex environmental and biological samples. Comprehensive analyses of complex samples provide challenges to modern analytical instrumentation which leads to the inability to detect certain compounds, the misidentification of compounds and errors in quantitative analysis ⁶⁷.

High mass resolution mass spectrometry can assist in the identification of components in complex matrices. However, differentiation of isobaric species and structural isomers often requires chromatographic separation ⁶⁸. Resolution of isobaric species and structural isomers is an important issue in toxicology since isomers can display very different toxicities ⁶⁹. Commonly used separation techniques include gas chromatography (GC) for the separation of volatile and semi-volatiles compounds and high performance liquid chromatography (HPLC) and capillary electrophoresis (CE) for the separation of polar and charged compounds. One-dimensional chromatography involves the separation of components using a single column stationary phase whereas multi-dimensional chromatography separations are attained with two or more column

stationary phase chemistries. Multi-dimensional chromatography has become increasingly popular because it can resolve the many components in complex samples that 1D techniques cannot⁷⁰. At present, the most common commercially available multi-dimensional technique is comprehensive two-dimensional gas chromatography (GC×GC), which involves coupling two GC columns of different stationary phases using a modulator⁷¹. Other multi-dimensional techniques involve the combination of two liquid chromatography (LC) columns for two-dimensional liquid chromatography (2D-LC) analyses as well as combination of LC and CE columns⁷². Combination of LC and GC columns is possible in offline configurations⁷³.

The analytical strategy employed in the studies of this thesis involves two complementary analytical techniques:

- (i) GC×GC was used for the separation, followed by detection and identification of the separated components based upon retention and mass spectral characteristics.
- (ii) High resolution mass spectrometry was also used to characterize components on the basis of accurate mass measurements alone, without prior separation. This provided a complementary picture that aided in the interpretation of the complex GC×GC data.

The lion's share of the multi-dimensional chromatography experiments described in this thesis was performed using the LECO Pegasus 4D, which employs a time-of-flight mass spectrometer (TOFMS) as the detector. Complementary high mass resolution experiments were also performed on a Waters GCT time-of-flight instrument, which was modified with a Zoex ZX2 loop modulator to perform GC×GC experiments. Ultrahigh

resolution mass spectrometric experiments were performed on a Varian 920MS Fourier transform ion cyclotron resonance (FT-ICR) mass spectrometer. Descriptions of these techniques are provided in the following sections.

1.5.1 Two-Dimensional Gas Chromatography GC×GC

The key to enhanced separation in GC×GC is the use of two (or more) columns. The choice of stationary phases should be such that they possess orthogonal separation properties, in order to separate compounds which might otherwise co-elute⁷⁴. As a result of this two column configuration, the peak capacity in GC×GC may be approximated as the product of the peak capacity of each individual column. Therefore GC×GC offers much greater peak capacity compared to a conventional 1D-GC.

Figure 5 displays a contour plot and the corresponding three-dimensional (3D) surface plot of a specific area of the contour plot (highlighted by a white box). The black dots on the contour plot are the peak markers. As can be seen from the contour plot there are numerous compounds that co-elute in the 1st dimension, which are nevertheless separated in the 2nd dimension. For example the three peaks indicated by the red dots on the 3D surface plot co-elute in the 1st dimension as indicated by the reconstructed 1D TIC trace in the background. Without separation in the 2nd dimension, the corresponding mass spectrum of the 1D trace would contain the masses of all co-eluting compounds, thus yielding a composite spectrum. Further, the enhanced chromatographic resolution provided by GC×GC allows one to obtain an isomerically pure mass spectrum of each compound, leading to the unambiguous identification and accurate quantification.

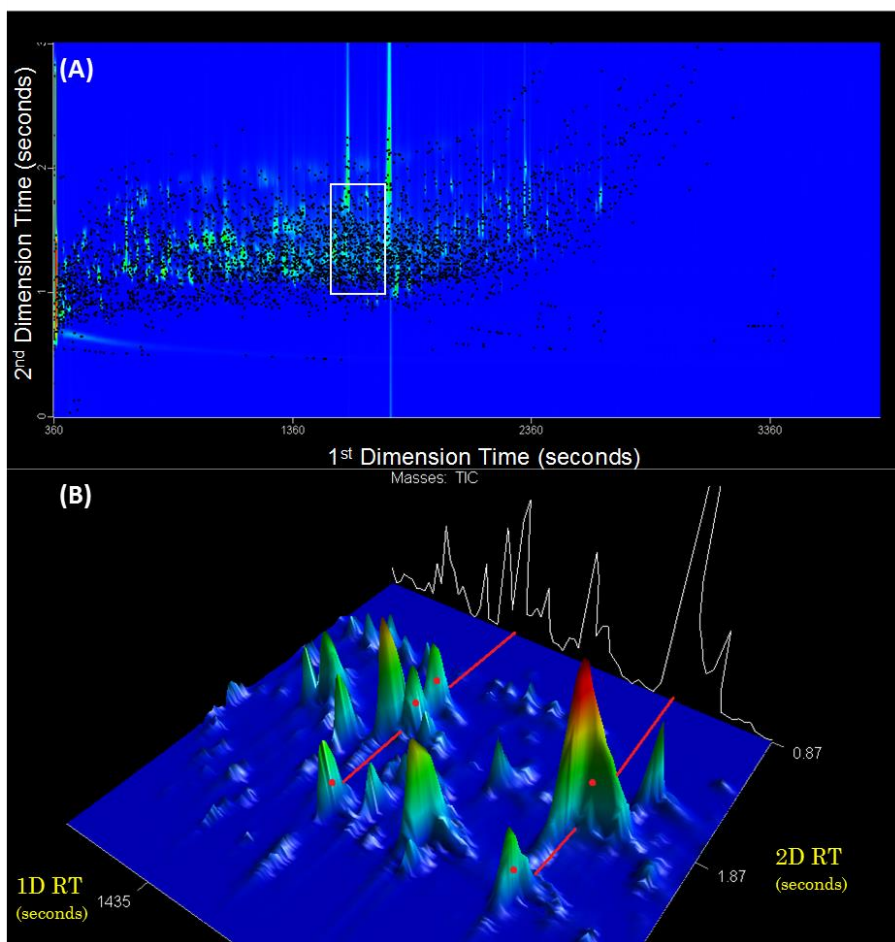


Figure 5 (A) contour plot of a urine sample (B) three-dimensional (3D) surface plot of a specific area of the contour plot (highlighted by a white box). Some of the components that co-elute in the 1st Dimension but are separated in the 2nd Dimension are indicated by the red dots on the 3D surface plot. A projection of the 1st dimension chromatogram is presented. Many minor components are also resolved in this chromatogram that might otherwise be difficult if not impossible to observe much less resolve in a one-dimensional separation.

Early multi-dimensional chromatography was based on heart-cutting techniques whereby a segment of the effluent from one column was collected and re-injected or was redirected onto a second column. The limitation of the heart-cutting technique is that only a specific fraction of the eluent is separated in a secondary column and thus does not provide a comprehensive method of analysis. For comprehensive analysis all components of a sample must be subjected to all dimensions of separation⁷⁴.

The first comprehensive multi-dimensional gas chromatography separation was introduced by J. B. Phillips and Z. Liu in 1991⁷¹. The first modulator developed by Liu and Phillips used a piece of thick film capillary painted with gold paint as a union to connect the primary and secondary columns. The effluent from the (primary column would get trapped in the thick film and would be released to the secondary column by resistive heating of the gold paint. A major limitation of this modulator was that during the heating period to release the trapped analytes, other components eluting from the primary column would also pass through the union to the secondary column. This leads to co-elution of compounds which at one point were separated in the primary column. The issue was resolved by alternatively heating two segments of the capillary union. Dual-stage modulation is used in most modern thermal modulator designs.

Phillips, Dimandja *et al.* developed the first commercially available modulator using a rotating heater bar⁷¹. Similar to their previous design a thick film capillary was used as a union which trapped the effluent from the primary column. A rotating heater was used to heat 2 points of the capillary to a temperature about 100°C higher than the oven temperature. A major limitation of this design was that it was not suited for the analysis of highly volatile compounds as these would not be retained in the capillary. Also, the oven had to be operated at a temperature 100°C below its maximum operating temperature. As a result heater-based modulators are not used today and have given way to cryogenic modulators.

Philip Marriott developed one of the first cryogenic modulators. The longitudinally modulated cryogenic system (LMCS) trapped analytes on a capillary using liquid CO₂

cooling⁷¹. The LMCS consisted of a moveable cooling arm installed around the end segment of the primary column. The cooling arm would cool two different points of the primary column alternately, thereby trapping and focusing the effluent. The arm would first cool one point of the primary column and then move to another point downstream. As the cooling arm moves downstream, the first cooled segment would reach the oven temperature and release the trapped effluent which would travel downstream and be trapped again at the second point. Once the cooling arm moves back to the 1st position, the trapped effluent from the 2nd position would reach oven temperature and be released into the secondary column. This dual stage cryogenic modulation not only trapped a wide variety of analytes but it also improved band broadening giving rise to narrower peaks and thus improving the overall sensitivity of the system. Harynuk and Gorecki developed a cryogenic modulator with no moving parts⁷¹. In this system the modulator consisted of a silicosteel trapping capillary which was housed in a cryo chamber cooled with liquid nitrogen. Most current modulators use this type of design.

Figure 6 displays the thermal modulator by LECO Corporation used in this thesis. The modulator is equipped with a quad jet system composed of 2 hot air jets and 2 cold air jets. The cold air jets of the modulator traps and focuses effluent from the primary column while the hot jets thermally desorb the effluent and injects them into the secondary column. As a result of this trap and purge action of the modulator the peaks that enter the secondary column are much narrower in width resulting in an overall increase in sensitivity.

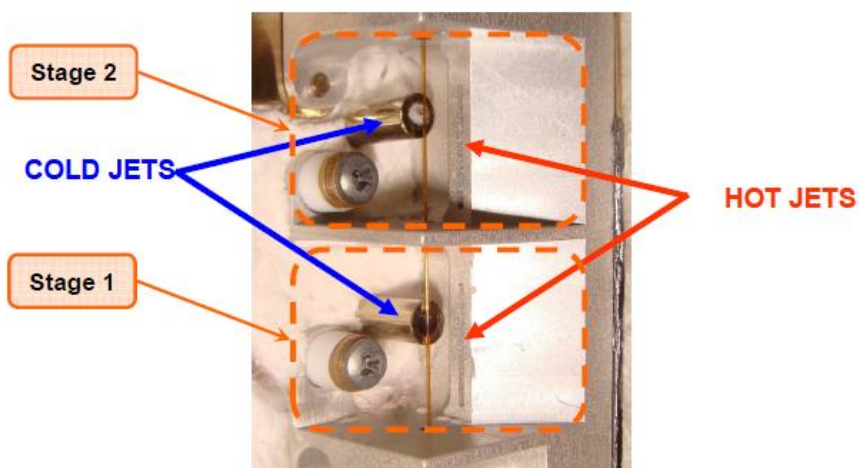


Figure 6. LECO's Dual-stage Quad Jet Thermal Modulator.

The Zoex ZX2 modulator used in this thesis consists of a 2 stage loop. In this design the column is looped twice inside the modular as depicted by the schematic in Figure 7. In this case the cold jets would trap the analytes eluting from the primary column and the hot jets would desorb them. The double loop creates a second stage for trapping and desorbing allowing narrow band of analytes to be injected into the secondary column.

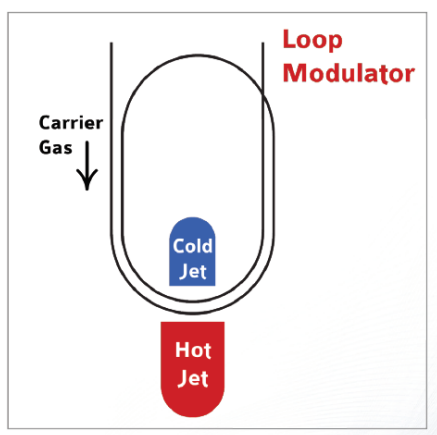


Figure 7. Schematic of the Zoex ZX2 loop modulator.

1.5.1.1 GC×GC Method Optimization

In GC×GC, a shorter secondary column (1-2 m) is used compared to the primary column (15-60 m). A shorter secondary column is necessary to avoid the ‘wrap-around’ of peaks. Wrap-around occurs when a peak from one modulation cycle does not have enough time to exit the secondary column before the beginning of the next cycle (Figure 8). As a result the peak or a part of the peak appears at a very early secondary retention time of the next cycle. Often the secondary column oven is maintained at a higher temperature offset relative to the primary column oven to avoid this wrap-around affect.

Although the secondary oven offset helps eliminate the wrap around affect it could also limit the peak separation in the 2nd Dimension as can be seen in figure 8. The figure displays two GC×GC experiments of the same sample which are superimposed. The band of compounds on the top are from a GC×GC experiment in which the secondary column offset was 0°C. The band at the bottom is from an experiment in which the secondary column offset was 40°C. In this case, an offset of 0°C gives rise to better separation of the components in the second dimension compared to the 40°C offset. However, the 0°C offset does lead to some of the late eluting compounds to wrap around. Therefore the offset must to be optimized to best suit the needs of the analysis.

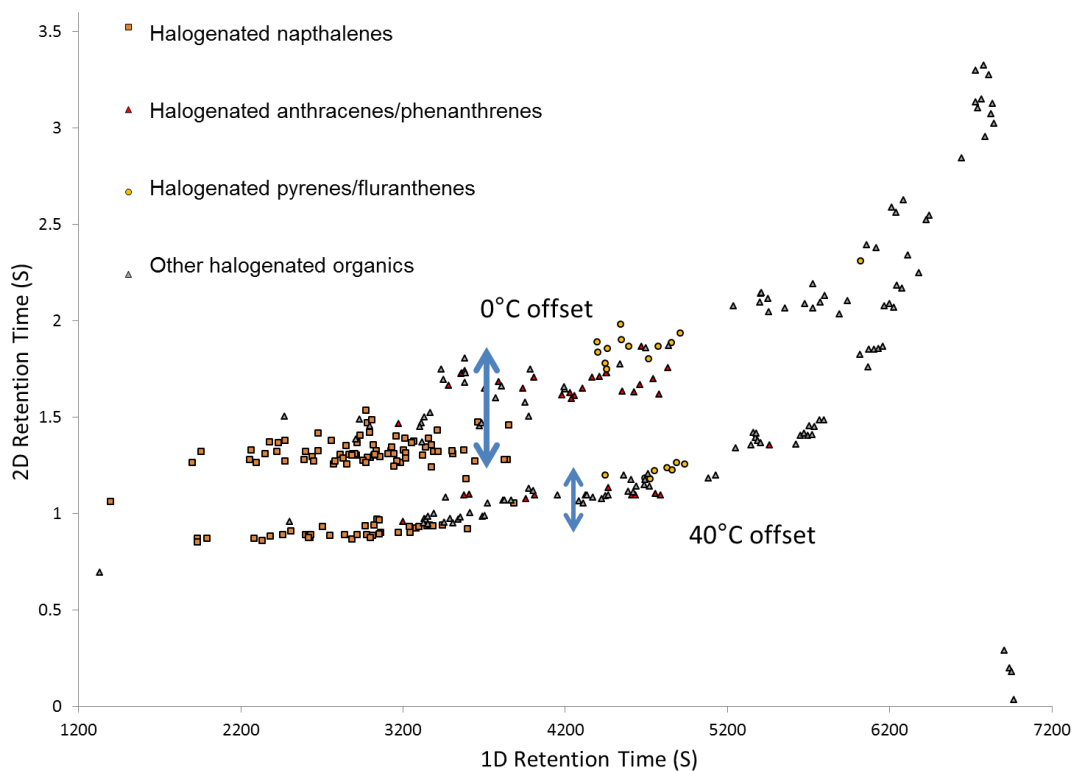


Figure 8. Reconstructed contour plot of an ash sample extract. The contour plot contains data from 2 different chromatograms which have been overlaid. The top band of compounds corresponds to a method with a secondary oven offset of 0°C. In this case wrap-around is observed for a group of peaks observed at a 1D retention time of 7000s and a 2D retention time between 0.1-0.25s. The bottom band of compounds corresponds to a method with a secondary oven offset of 40°C.

At the heart of the GC×GC is the modulator. One of the major parameters that need to be optimized is the modulation period. This refers to the amount of time spent trapping and then releasing the compounds using the cold and hot jets. Typical modulation period ranges between 3-5 seconds, which in turn corresponds to the retention time range for compounds in the second dimension. Longer modulation periods allow more time for the compounds to be eluted off of the secondary column and can be used to eliminate wrap-around effects. However, at longer modulation periods only a few slices of the 1st

Dimension peaks are taken which has the potential to overload the modulator. Also compounds that are separated by less than the modulation period are combined during this period. At short modulation periods the potential for wrap-around increases. However, at shorter modulation periods more slices of the 1st Dimension peaks are taken which decreases the potential to overload the modulator. Figure 9(a) displays a schematic of a peak from the primary column (blue trace) that has been sliced into 3 during the modulation period (red traces). In this case the 3 slices will have 3 different 1D retention times but the same 2D retention time (figure 9b). Since the mass spectrum of each of the slices is identical, the 3 slices are combined and represented as one peak in the resulting 2D contour plot and 3D surface plot.

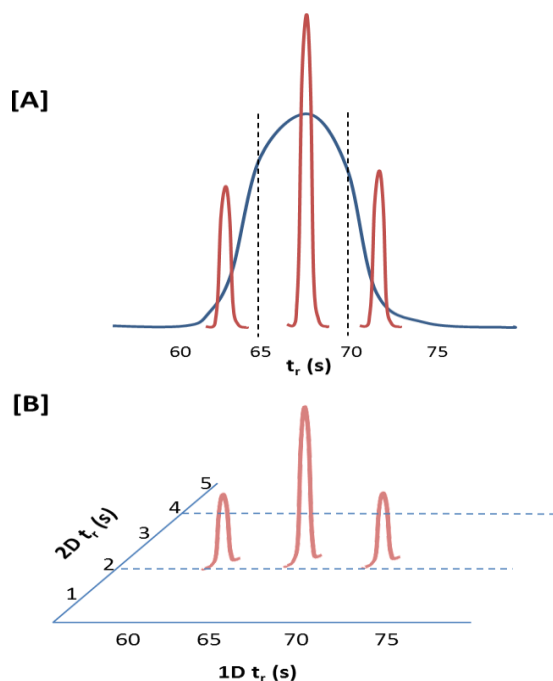


Figure 9. [A] Schematic of a peak from the primary column (blue trace) has been sliced into 3 during the modulation period. [B] The 3 slices have 3 different 1D retention times but the same 2D retention time.

Along with the total modulation period, the user has the ability to change the time associated with the hot and cold jets independently. For example, for a sample with mostly high volatile components one could increase the cold jet time allowing sufficient time for the components to be trapped. On the other hand for a sample with low volatile components, the user can increase the hot jet time in order to thermally desorb these high boiling compounds after they have been trapped. The cold jets are set to a fixed temperature controlled from a Peltier cooling system and typically operate at -80°C . The temperature of the hot jets can be controlled by an offset relative to the secondary oven temperature. An offset in the range of $+15^{\circ}\text{C}$ to 50°C is typically used. The modulator offset can be increased to desorb high boiling point compounds.

The coupling of GC \times GC to mass spectrometry provides another dimension for separation and identification. Mass spectrometry provides the mass to charge ratio (m/z) of eluting compounds. The mass spectrometers coupled to GC \times GC instruments are often equipped with time-of-flight (TOF) mass analyzers. Mass spectrometry will be described in more detail in the following section.

1.5.2 Mass Spectrometry

A mass spectrometer (MS) ionizes molecules and determines the mass to charge ratios (m/z) of the resulting ions. MS can be distinguished by the type of mass analyzers it is equipped with. Some analyzers operate by scanning for ions over a range of m/z while others can simultaneously detect ions over a wide range of m/z . Some analyzers are capable of nominal mass resolution while others offer high mass resolution. Resolution in

this context refers to the ability to distinguish the difference between two masses. Mass resolution (R) can be determined using the following equation:

$$R = m/\Delta m \quad (\text{Equation 1})$$

Where m is the mass of the peaks and Δm is the mass difference between the two peaks. Two peaks are considered resolved in a mass spectrum if the valley between the two peaks is equal to 10% of the weaker peak⁷⁵. Resolution can also be calculated by using the full width at half-maximum (FWHM) of a peak as Δm .

The most common scanning instrument is a quadrupole mass analyzer which offers nominal mass resolution. A quadrupole mass analyzer consists of four circular or hyperbolic rods that are aligned in a parallel formation. The ions passing through the quadrupoles experience an alternating electric field (V) superimposed on a constant field (U)⁷⁶. At any given moment one pair of parallel rods are at a positive potential while the others are held at a negative potential. A positively charged ion travelling through the quadrupole, will be drawn towards the negative rods and as the potential changes it will be deflected away from these same rods. The ratio of U and V is held constant while the amplitude is changed in order to scan for ions of a certain m/z range. Quadrupole instruments can also be operated in selected ion monitoring (SIM) mode for targeted analysis of compounds⁷⁵. In SIM the quadrupole is set to allow the transmission of a single m/z of interest. This gives rise to low background noise in the resulting chromatogram as other ions of different m/z do not reach the detector. Tandem mass spectrometry represents more than one stage of MS analysis. In this case three

quadrupoles are setup in series capable of carrying out collision induced dissociation (CID) experiments⁷⁵. The first quadrupole (Q1) can be set to allow for an ion of a specific m/z to be transmitted. The second quadrupole (Q2) in this case is used as a collision cell whereby a small section of it is filled with an inert gas referred to as the collision gas. The ions being transmitted from Q1 collide with the collision gas giving rise to fragment ions which are then scanned for using the third quadrupole (Q3). This type of MS/MS experiment is commonly referred to as a product ion scan. Fragment information from CID experiments can be used to setup multiple reaction monitoring (MRM) methods. In MRM, Q1 is set to transmit an ion of a specific m/z which is then fragmented in Q2 and a major fragment ion that results is transmitted through Q3 to the detector. MRM experiments are more selective than scanning and SIM experiments since interfering ions which may have the same m/z as the target can be ruled out if they do not give rise to the same fragment ion as the target ion of interest. Figure 10 compares the SIM trace (m/z 216) for the trimethylsilyl derivative of 1 and 2- hydroxynaphthalene isomers to that of the MRM trace (m/z 216 \rightarrow 201) for the same compounds. The SIM trace shows four peaks within the very narrow time period of interest. The MRM trace targeting the same analytes makes identification unambiguous as only the 2 targets analytes of interest are present. Furthermore, the signal-to-noise ratio (S/N) in the MRM trace is on average ten times better compared to the SIM due to the very low baseline noise. MRM experiments often reduce background noise from interfering ions and thus increases the sensitivity of the method.

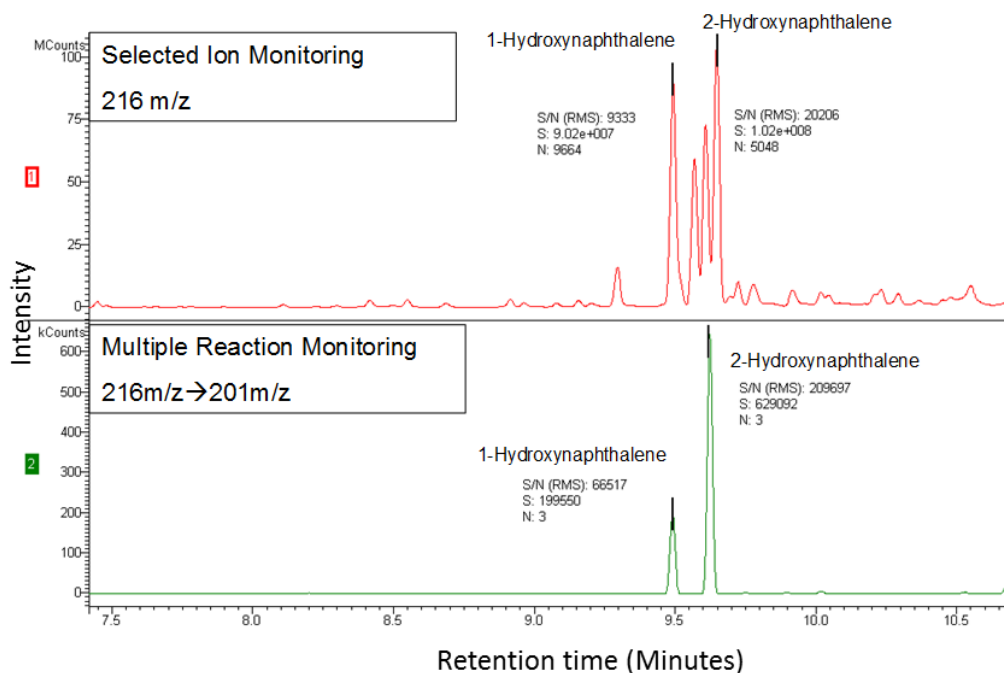


Figure 10. The selected ion monitoring (SIM) and multiple reaction monitoring (MRM) traces for the trimethylsilyl derivative of 1- and 2-hydroxynaphthalene isomers. The MRM method is more selective compared to the SIM method as only the 2 target species are observed in the trace. Furthermore, the MRM method offers better sensitivity due to low background noise in the trace.

The most common analyzer capable of simultaneous detection of an m/z range is the time-of-flight (TOF) instrument. A TOF mass analyzer consists of a flight tube which is used to measure the time it takes for a group of ions to travel its length. Ions of various m/z can be distinguished based on travel time since the velocity of an ion is inversely proportional to the square root of its mass. As a result for a group of ions with the same kinetic energy those with a lower m/z will reach the detector at the end of the flight tube before those with a higher m/z . The major factor that affects mass measurement is a spread in the kinetic energy among ions with the same m/z leaving the ion source⁷⁶. This leads to broad peaks in the mass spectrum since not all ions will reach the detector at the

same time. Delayed pulsed extraction has been used to counter this issue⁷⁶. In this case, the ions are allowed to separate based on their kinetic energy distribution for a brief period of time before an extraction pulse is applied. In this case the ions closer to the pulse as a result of lower kinetic energy will be energized more than ions further away from the pulse which has higher kinetic energy. As a result the ions separated by the kinetic energy distribution will be brought together and will arrive at the detector at the same time.

TOF analyzers are often used for high mass resolution measurements ($R > 10,000$). Mass resolution can be improved with the use of longer flight tubes. Another way to improve mass resolution is by using a reflectron⁷⁶. In this case the ions in the flight tube encounter a retarding electric field which acts as a mirror and deflects the ions back through the flight tube to a detector. Ions of the same m/z but with variable kinetic energies can be corrected since ions with higher energy will penetrate deeper into the reflectron than ions with lower energy. As a result all ions of the same m/z will reach the detector at the same time and thus help improve resolution.

In addition to mass resolution TOF mass analyzers also provide fast acquisition rates since all ions are detected simultaneously. TOF analyzers typically operate at 50-200 spectra per second range. In contrast, scanning instruments such as quadrupoles typically operate below 10 spectra per second rate. The GCxGC (Pegasus 4D) used in the current research was coupled to a TOF-MS (Figure 11). In this case the TOF was utilized for its high acquisition rate since the peak widths obtained on a GCxGC are much narrower (typically 0.1-0.2 seconds) than in a conventional 1D-GC (typically 5-10 seconds). As a

result an analyzer capable of high acquisition rates is needed to collect sufficient data points across the peak to obtain a high quality mass spectrum. TOF analyzers are also used in tandem mass spectrometry systems with quadrupole analyzers (Q-TOF) which offers the added benefit of high mass resolution for CID based experiments⁷⁵.

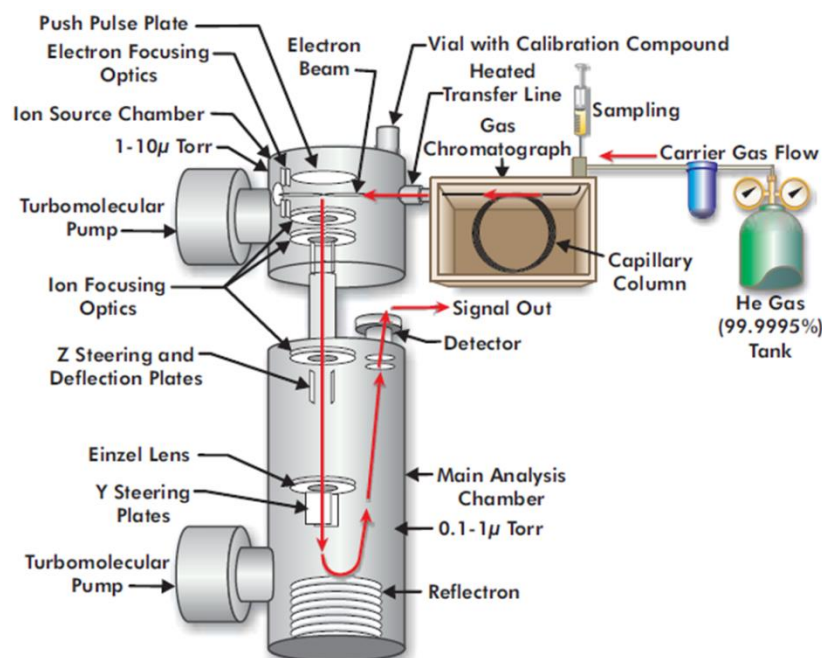


Figure 11. Schematic of a time-of-flight mass spectrometer coupled to a GCxGC (diagram courtesy of LECO).

Ultra-high resolution mass spectrometry ($R > 100,000$) analysis can be carried out on a Fourier transform ion cyclotron resonance mass spectrometer (FT-ICR-MS). FT-ICR developed by Allan Marshall and Mel Comisarow is used to determine the mass-to-charge ratio (m/z) of ions based on its cyclotron frequency in a fixed magnetic field^{77,78,79}. It is known that ions moving perpendicular to an applied uniform magnetic field will travel in a circular orbit as described by Lorentz Force. In a uniform magnetic field

(B) an ion of a mass (m) with a charge (z) will travel in a circular orbit with an angular velocity (ω_c) or cyclotron frequency (ν) defined by the following equation:⁷⁶

$$\omega_c = 2\pi\nu = zB/m \quad (\text{Equation 2})$$

However, the incoherent cyclotron radius of this ion packet is too small to induce a detectable signal. The ions are excited to a larger cyclotron radius by an electric field applied perpendicular to the magnetic field which gives rise to a coherent orbital motion resulting in an increase in the detection efficiency⁷⁷. A signal is detected as an image current on a pair of plates as these excited ions orbit the ICR cell. Since the measured frequency of these ions is inversely proportional to its mass (equation 2), the measured frequency data can be used to obtain its m/z . In addition, the amplitude of the measured sinusoidal frequency is proportional to the number of ions and thus is a measure of its intensity⁷⁷. However this task gets rather complicated as ions of multiple m/z are simultaneously excited by a rapid scan of a large frequency. In this case multiple frequencies are detected as a result of ions of various m/z orbiting in the ICR cell. In this case intensity is measured as a function of time. Fourier transform is used in these cases to convert the signal intensity as a time function into intensity as a function of frequency thus yielding an intensity to m/z plot⁷⁵.

An important feature of equation 2 is that all ions of the same m/z will have the same cyclotron frequency irrespective of their velocity⁷⁷. This is advantageous since additional focusing is not needed to compensate for distributions in kinetic energies as was the case with TOF analyzers in order to achieve high mass resolution. In FT-ICR, mass

resolution is based on the ability to generate distinguishable cyclotron frequencies for a group of ions which is directly proportional to the strength of the applied magnetic field (B). As a result, in order to obtain high mass resolution typically requires superconducting magnets with a strength of 7 Tesla or higher. The FT-ICR-MS instrument used in the current thesis was a Varian 920-MS equipped with a Varian 9.4 Tesla superconducting magnet (Figure 12). The FT-ICR was coupled to a Varian J320-MS triple quadrupole at the front end. The Q1 and Q3 of the triple quadrupole was operated in rf only mode which results in all ions passing through to the hexapole accumulation cell. The accumulated ions are then pulsed ejected as a packet in to the ICR cell.

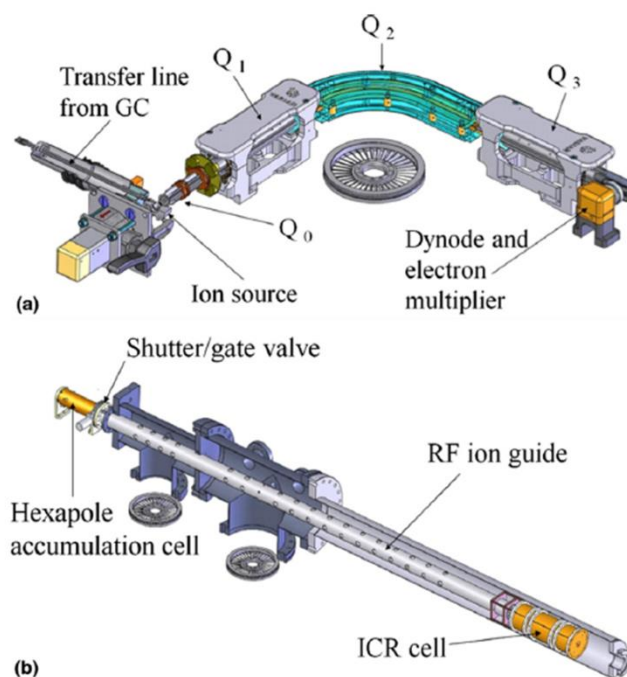


Figure 12. (a) Schematic of the GC transferline and Varian J320MS (diagram courtesy of Varian Inc). (b) Schematic of the hexapole accumulation cell rf ion guide, and ICR cell (diagram courtesy of Varian Inc).

1.5.2.1 Ionization Techniques

Electron ionization (EI) is the most common type of ionization technique associated with GC-MS. In EI high energy electrons (70eV) are emitted from a filament and directed at the effluent from the GC column. The resulting interactions between the electrons and the molecules being eluted leads to an energy transfer to the molecules resulting in its ionization. This leads to the formation of a molecular ion (M^{+}) in which an electron from the molecule is ejected as a result of the energy absorbed⁷⁶. Since the energy absorbed in the interaction with the 70eV electron is much higher than the required ionization energy for a molecule (typically <10eV), this often results in further fragmentation of the molecule⁷⁶. As a result EI is referred to as a hard ionization technique. An EI mass spectrum may display many fragment ions at higher abundance compared to the molecular ion. Thus structural information can be obtained from an EI mass spectrum of a compound based on the observed fragment ions. As a result, mass spectral libraries have been created for numerous chemicals based on the EI mass spectra. The EI mass spectral library created by the National Institute of Standards and Technology (NIST) currently contains spectra for nearly 250,000 compounds (NIST v.14).

The EI mass spectral libraries are an important tool for the identification of unknown compounds. Since EI mass spectra are very reproducible from instrument to instrument under typical source conditions, a mass spectrum of an unknown compound can be searched against the spectral library to obtain a possible match. The match factors are based on algorithms which compare the observed peaks and intensities of a user mass spectrum to those in a library⁸⁰. Since EI mass spectra are often dominated by fragment

ions and contain weak molecular ions, the match factor score is mostly influenced by the observed fragments. Thus a high match factor score (>800) can be obtained in cases even if the molecular ion from the library spectrum does not match with that in the user spectrum⁸¹. Therefore the user must ultimately make the final decision as to whether the match obtained is accurate irrespective of the match score. The ability to obtain a mass spectrum free of interference from other compounds is crucial in this case. Even when a good match is not obtained, structural information can be obtained for the unknown species based on the similarities and differences compared to the library spectrum⁸¹.

An alternative ionization technique associated with GC-MS is chemical ionization (CI). In CI, a reagent gas is introduced to the ion source at a high pressure and ionized using the electrons at 70eV similar to EI. This results in the formation of primary ions which react further with other reagent gas molecules in the source creating an ionization plasma⁷⁶. Molecules of interest introduced into the source will interact with the plasma leading to the formation of both positively and negatively charged ions as a result of proton transfer, hydride abstractions, adduct formation and charge transfer reactions. The choice of reagent gas is based on the proton affinity or electron affinity of the target molecule. Common reagent gases include methane and ammonia. CI is referred to as a soft ionization technique since very little fragmentation is observed compared to EI. As a result a CI mass spectrum may be dominated by the molecular ions (M^{++} or $M^{\bullet-}$) or pseudo molecular ions, e.g. $[M+CH_3]^+$. This can be advantageous in a situation where a molecular ion cannot be observed by EI in order to derive the identity of the compound.

Atmospheric pressure chemical ionization (APCI) is a soft ionization technique analogous to CI but is carried out at atmospheric pressure. In APCI ionization is carried out using a corona needle instead of a filament as is the case with EI and CI. Filaments are not used in this case since they will burn due to the presence of corrosive and oxidizing gases in the atmosphere ⁷⁶. A corona discharge is created by the ionization of molecules within the atmospheric pressure source which leads to the formation of N_2^{*+} or O_2^{*+} (primary ions). Since APCI is traditionally coupled with HPLC these primary ions react further with molecules from the mobile phase giving rise to secondary ions. Similar to CI, both positively and negatively charged ions are formed by APCI as a result of proton transfer, hydride abstractions, adduct formation and charge transfer reactions. Experiments in which APCI was used to couple GC to MS have been reported in the early 1970s by Horning and coworkers and in the 1980s by Korfmacher and Mitchum⁸². However GC-APCI-MS instruments were not made commercially available until recently.

APCI instrument have gained popularity recently since both GC and HPLC systems can be coupled to a single mass spectrometer which is a significant cost reduction compared to having two separate systems. In addition, GC-APCI-MS instruments have offered advantageous features over the traditional EI/CI systems. For instance, APCI often yields an intense molecular ion similar to CI. However, GC-APCI-MS has the advantage of being more sensitive than CI and EI ⁸². As a result an intense molecular ion can be selected as the precursor ion for CID giving rise to selective reaction monitoring (SRM) methods. In EI, the precursor ion selected is often a fragment which affects both the sensitivity and selectivity of the method. However, a major limitation of GC-APCI-MS

systems is the lack of a mass spectral library compared to EI. However, the use of high resolution mass spectrometers can yield elemental compositions for the observed molecular ions that are difficult to identify in EI spectra.

1.6 Thesis Outline

This thesis evaluates the exposure to combustion products using multidimensional chromatography and ultra high resolution mass spectrometry. The research conducted is described in the following four chapters (chapters 2-5).

The second chapter of the thesis consists of a study aimed at evaluating the exposure of firefighters to smoke during training exercises. In this study, air samples, skin wipes and urine samples were collected from a group of firefighters who participated in training exercises at four fire departments across the province of Ontario, Canada. Wood was the primary fuel used in these training exercises and a suite of wood smoke markers were monitored in air (smoke) samples by GC-MS, which included both PAHs and MPs. Skin wipes were obtained from multiple body sites and analyzed for the presence and levels of these marker compounds to evaluate dermal exposure. Next, both pre- and post-exposure urine samples from each firefighter were analyzed by GC-tandem mass spectrometry (GC-MS/MS) for metabolites of the marker compounds in an attempt to quantify overall exposure.

The third chapter of the thesis explores the use of comprehensive two-dimensional gas chromatography mass spectrometry (GC×GC-MS) for the identification of novel markers of wood smoke exposure. Comprehensive analysis of a complex mixture is a very difficult task for traditional one-dimensional chromatographic instrumentation due to the need to separate large number of components present. The purpose of the project was to identify novel smoke marker chemicals in the air and in the post-exposure urine of exposed firefighters and to evaluate the effectiveness of the novel markers compared to those used in Chapter 2.

The fourth chapter of the thesis consists of a study which examined an ash sample from the site of a major industrial fire at a plastic recycling plant (Plastimet Inc.) in Hamilton, Ontario, Canada. Due to the toxic nature of halogenated organics that arise from the burning of plastics this fire raised significant concerns among local residents and health officials. At the time of the fire (1997) numerous samples (air, soil, water) were collected and analyzed for compounds of concern including PAHs, polychlorinated biphenyls (PCBs), polychlorinated dibenzo-*p*-dioxins and dibenzofurans (PCDD/Fs). The goal of the current study was to identify the halogenated organics present in the samples using state-of-the-art analytical instrumentation that was not readily available at the time. The approach undertaken involved probe analysis on an ultra-high resolution mass spectrometer (FT-ICR-MS) for the purpose of rapid identification of contaminants with the aid of mass defect plots followed by GC×GC-TOF-MS analysis for isomer differentiation and quantification.

The fifth chapter of the thesis explores alternative ionization techniques for the analysis of dioxins and furans including chlorine, bromine and mixed bromo/chloro substituted species. The analysis of mixed halogenated dioxins and furans (PXDD/Fs) especially have been hampered by a lack of authentic standards as well as suitable analytical techniques required to resolve the enormous number of potential congeners. Traditional electron ionization (EI) mass spectrometry-based methods are of limited value in part due to the lack of structure diagnostic fragments that are formed. Therefore, differentiation of isomeric species has not been possible in the absence of chromatographic separation. Negative ion atmospheric pressure chemical ionization (NI-APCI) was explored as an alternative ionization technique to derive structure diagnostic fragments using a modern GC-APCI-MS system.

References

1. Brunekreef B. Air pollution and human health: From local to global issues. *Procedia - Soc Behav Sci.* 2010;2(5):6661-6669.
2. Huston CJ. Carbon monoxide poisoning. *Am J Nurs.* 1996;96(1):48.
3. Strohl KP, Feldman NT, Saunders NA., O'connor N. Carbon Monoxide Poisoning in Fire Victims. *J Trauma Inj Infect Crit Care.* 1980;20(1):78-80.
4. Morikawa T. Toxic Hazards of Acrolein and Carbon Monoxide During Combustion. *Journal of Fire Sciences.* 1984;2(April):142-152.
5. Morikawa T. Toxic Gases Evolution from Commercial Building Materials under Fire Atmosphere in a Semi-Full-Scale Room. *J Fire Sci.* 1988;6(2):86-99.
6. Hayes RB. The carcinogenicity of metals in humans. *Cancer Causes Control.* 1997;8(3):371-385.
7. Li M, Cao J, Gao Z, Shen X, Yan C. The trend of lead poisoning rate in Chinese population aged 0–18 years old: a meta-analysis. *BMC Public Health.* 2015;15(1):756.
8. Lin YS, Egeghy PP, Rappaport SM. Relationships between levels of volatile organic compounds in air and blood from the general population. *J Expo Sci Environ Epidemiol.* 2008;18(4):421-429.
9. Cometto-Muñiz JE, Abraham MH. Compilation and analysis of types and concentrations of airborne chemicals measured in various indoor and outdoor human environments. *Chemosphere.* 2015;127:70-86.
10. Chaudhary A, Hellweg S. Including Indoor Offgassed Emissions in the Life Cycle Inventories of Wood Products. 2014.
11. Reisen F, Brown SK. Australian firefighters' exposure to air toxics during bushfire

burns of autumn 2005 and 2006. *Environ Int.* 2009;35(2):342-352.

12. Pope CA, Burnett RT, Thurston GD. Cardiovascular Mortality and Long-Term Exposure to Particulate Air Pollution: Epidemiological Evidence of General Pathophysiological Pathways of Disease. *Circulation.* 2004;109(1):71-77.
13. Fullerton DG, Bruce N, Gordon SB. Indoor air pollution from biomass fuel smoke is a major health concern in the developing world. *Trans R Soc Trop Med Hyg.* 2008;102(9):843-851.
14. Elder A, Gelein R, Lunts A, Kreyling W. Extrapulmonary translocation of ultrafine carbon particles following whole-body inhalation. *Journal of Toxicology and Environmental Health , Part A.* 2002;65:1531-1543.
15. Yu Y, Li Q, Wang H. Risk of human exposure to polycyclic aromatic hydrocarbons: A case study in Beijing, China. *Environ Pollut.* 2015;205:70-77.
16. Stellman JM, Stellman SD, Christian R, Weber T, Tomasallo C. The extent and patterns of usage of Agent Orange and other herbicides in Vietnam. *Nature.* 2003;422:681-687.
17. Schecter A, Birnbaum L, Ryan JJ, Constable JD. Dioxins : An overview. 2006;101:419-428.
18. Ribeiro M, Santos UDP, Bussacos MA, Terra-filho M. Prevalence and Risk of Asthma Symptoms Among Firefighters in Sao Paulo, Brazil: A Population-Based Study. *American Journal of Industrial Medicine.* 2009;269:261-269.
19. Bates MN. Registry-based case-control study of cancer in California firefighters. *Am J Ind Med.* 2007;50(5):339-344.
20. Rosenstock L, Olsen J. Firefighting and Death from Cardiovascular Causes. *The New England Journal of Medicine.* 2013:1261-1263.
21. Kang D, Davis LK. Cancer Incidence Among Male Massachusetts Firefighters , 1987 – 2003. *American Journal of Industrial Medicine.* 2008;335:329-335.

22. Bolstad-Johnson DM, Burgess JL, Crutchfield CD, Storment S, Gerkin R, Wilson JR. Characterization of Firefighter Exposures During Fire Overhaul. *AIHAJ - Am Ind Hyg Assoc.* 2000;61(5):636-641.
23. Reisen F, Brown SK. Australian firefighters' exposure to air toxics during bushfire burns of autumn 2005 and 2006. *Environ Int.* 2009;35(2):342-352.
24. Adetona O, Simpson CD, Onstad G, Naeher LP. Exposure of wildland firefighters to carbon monoxide, fine particles, and levoglucosan. *Ann Occup Hyg.* 2013;57(8):979-991.
25. Miranda AI, Martins V, Cascão P. Monitoring of firefighters exposure to smoke during fire experiments in Portugal. *Environ Int.* 2010;36(7):736-745.
26. Fent KW, Eisenberg J, Evans D, et al. Evaluation of Dermal Exposure to Polycyclic Aromatic Hydrocarbons in Fire Fighters. NIOSH. 2013. Report No. 2010-0156-3196.
27. Laitinen J, Mäkelä M, Mikkola J, Huttu I. Fire fighting trainers' exposure to carcinogenic agents in smoke diving simulators. *Toxicol Lett.* 2010;192(1):61-65.
28. Hansen AM, Mathiesen L, Pedersen M, Knudsen LE. Urinary 1-hydroxypyrene (1-HP) in environmental and occupational studies--a review. *Int J Hyg Environ Health.* 2008;211(5-6):471-503.
29. Strickland P, Kang D. Urinary 1-hydroxypyrene and other PAH metabolites as biomarkers of exposure to environmental PAH in air particulate matter. 1999;108:191-199.
30. Levin JO, Rhen M, Sikström E. Occupational PAH exposure: urinary 1-hydroxypyrene levels of coke oven workers, aluminium smelter pot-room workers, road pavers, and occupationally non-exposed persons in Sweden. *Sci. Total Environ.* 1995, 163 (1-3): 169-77.
31. Simoneit BRT, Rogge WF, Mazurek MA, Standley LJ, Hildemann LM, Cass GR. Lignin pyrolysis products, lignans, and resin acids as specific tracers of plant classes in emissions from biomass combustion. *Environ. Sci. Technol.* 1993, 27 (12): 2533-2541.

32. Nolte CG, Schauer JJ, Cass GR, Simoneit BR. Highly polar organic compounds present in wood smoke and in the ambient atmosphere. *Environ Sci Technol.* 2001;35(10):1912-1919.
33. Clark M, Paulsen M, Smith KR, Canuz E, Simpson CD. Urinary methoxyphenol biomarkers and woodsmoke exposure: comparisons in rural Guatemala with personal CO and kitchen CO, levoglucosan, and PM_{2.5}. *Environ Sci Technol.* 2007;41(10):3481-3487.
34. Soldera S, Sebastianutto N, Bortolomeazzi R. Composition of phenolic compounds and antioxidant activity of commercial aqueous smoke flavorings. *J Agric Food Chem.* 2008;56(8):2727-2734.
35. Baker JE. Source Apportionment of Polycyclic Aromatic Hydrocarbons in the Urban Atmosphere : A Comparison of Three Methods. *Environ. Sci. Technol.* 2003;37(9):1873-1881.
36. Haritash AK, Kaushik CP. Biodegradation aspects of polycyclic aromatic hydrocarbons (PAHs): a review. *J Hazard Mater.* 2009;169(1-3):1-15.
37. Dobbins R., Fletcher R, Benner B. Hoefft S. Polycyclic aromatic hydrocarbons in flames, in diesel fuels, and in diesel emissions. *Combust Flame.* 2006;144(4):773-781.
38. Boffetta P, Jourenkova N, Gustavsson P. Cancer risk from occupational and environmental exposure to polycyclic aromatic hydrocarbons. *Cancer Causes Control.* 1997;8(3):444-472.
39. Grainger J, Huang W, Patterson DG. Reference range levels of polycyclic aromatic hydrocarbons in the US population by measurement of urinary monohydroxy metabolites. *Environ Res.* 2006;100(3):394-423.
40. Blankenship A, Chang DPY, Jones AD, et al. Toxic Combustion By-Products From The Incineration of Chlorinated Hydrocarbons And Plastics. *Chemosphere.* 1994;28(1):183-196.
41. Wang D, Xu X, Chu S, Zhang D. Analysis and structure prediction of chlorinated

- polycyclic aromatic hydrocarbons released from combustion of polyvinylchloride. *Chemosphere*. 2003;53:495-503.
42. Ishaq R, Carina N, Zeb Y, Broman D, Ulf J. PCBs , PCNs , PCDD / Fs , PAHs and Cl-PAHs in air and water particulate samples — patterns and variations. *Chemosphere*. 2003;50:1131-1150.
 43. Morita M, Nakagawa JI, Rappe C. Polychlorinated Dibenzofuran (PCDF) Formation From PCB Mixture by Heat and Oxygen. *Bull. Environm. Contam. Toxicol*. 1978;19:665-670.
 44. Hutzinger O, Choudhry GG, Chittim BG, Johnston LE. Formation of polychlorinated dibenzofurans and dioxins during combustion, electrical equipment fires and PCB incineration. *Environ Health Perspect*. 1985;60:3-9.
 45. Altarawneh M, Dlugogorski BZ, Kennedy EM, Mackie JC. Mechanisms for formation, chlorination, dechlorination and destruction of polychlorinated dibenzo-p-dioxins and dibenzofurans (PCDD/Fs). *Prog Energy Combust Sci*. 2009;35(3):245-274.
 46. Tame NW, Dlugogorski BZ, Kennedy EM. Formation of dioxins and furans during combustion of treated wood. *Prog Energy Combust Sci*. 2007;33(4):384-408.
 47. Horii Y, Ok G, Ohura T, Kannanct K. Occurrence and profiles of chlorinated and brominated polycyclic aromatic hydrocarbons in waste incinerators. *Environ Sci Technol*. 2008;42(6):1904-1909.
 48. Karasek FW, Parsons ML, Hawley-Fedder RA. Products Obtained During Combustion of Polymers under Simulated Incinerator Conditions. *Journal of Chromatography*. 1984;315,211-221.
 49. Wang D, Piao M, Chu S, Xu X. Chlorinated Polycyclic Aromatic Hydrocarbons from Polyvinylchloride Combustion. *Bull. Environm. Contam. Toxicol*. 2001;66:326-333.
 50. Darnerud PO, Eriksen GS, Jóhannesson T, Larsen PB, Viluksela M. Polybrominated Diphenyl Ethers : Occurrence , Dietary Exposure , and Toxicology. *Environmental Health Perspectives*. 2001;109:49-68.

51. Rahman F, Langford KH, Scrimshaw MD, Lester JN. Polybrominated diphenyl ether (PBDE) flame retardants. *The Science of the Total Environment*. 2001;275:1-7.
52. Hites RA. Critical Review Polybrominated Diphenyl Ethers in the Environment and in People : A Meta-Analysis of Concentrations. *Environ. Sci. Technol.* 2004;38(4):945-956.
53. Kuba A, Dronen LC, Picklo MJ, Hawthorne SB. Midpolarity and Nonpolar Wood Smoke Particulate Matter Fractions Deplete Glutathione in RAW 264 . 7 Macrophages. *Chem. Res. Toxicol.* 2006;19:255-261.
54. Kubatova A, Steckler TS, Gallagher JR, Hawthorne SB, Picklo MJ. Toxicity of wide-range polarity fractions from wood smoke and diesel exhaust particulate obtained using hot pressurized water. *Environmental Toxicology and Chemistry*. 2004;23(9):2243-2250.
55. Simpson CD, Naeher LP. Biological monitoring of wood-smoke exposure. *Inhal Toxicol.* 2010;22(2):99-103.
56. Siddens LK, Bunde KL, Harper T, et al. Cytochrome P450 1b1 in polycyclic aromatic hydrocarbon (PAH)-induced skin carcinogenesis: Tumorigenicity of individual PAHs and coal-tar extract, DNA adduction and expression of select genes in the Cyp1b1 knockout mouse. *Toxicol Appl Pharmacol.* 2015;287(2):149-160.
57. Bhatia AL, Tausch H, Stehlik G. Mutagenicity of Chlorinated Polycyclic Aromatic Compounds. *Ecotoxicology and Environmental Safety.* 1987;55:48-55.
58. Fu PP, Tungeln LS Von, Chiu LH. Halogenated - polycyclic aromatic hydrocarbons : A class of Genotoxic environmental pollutants. *Environ. Carcino. & Ecotox. Revs.* 1999;17:71-109.
59. Van den Berg M, Birnbaum LS, Denison M. The 2005 World Health Organization reevaluation of human and mammalian toxic equivalency factors for dioxins and dioxin-like compounds. *Toxicol Sci.* 2006;93(2):223-241.

60. Antos P, Błachuta M, Hrabia A, Grzegorzewska AK, Sechman A. Expression of aryl hydrocarbon receptor 1 (AHR1), AHR1 nuclear translocator 1 (ARNT1) and CYP1 family monooxygenase mRNAs and their activity in chicken ovarian follicles following in vitro exposure to 2,3,7,8-tetrachlorodibenzo-p-dioxin (TCDD). *Toxicol Lett.* 2015;237(2):100-111.
61. Mimura J, Fujii-Kuriyama Y. Functional role of AhR in the expression of toxic effects by TCDD. *Biochim Biophys Acta - Gen Subj.* 2003;1619(3):263-268.
62. Fernandez-Salguero PM, Hilbert DM, Rudikoff S, Ward JM, Gonzalez FJ. Aryl-hydrocarbon Receptor-Deficient Mice Are Resistant to 2, 3, 7, 8-Tetrachlorodibenzo-p-dioxin-Induced Toxicity. *Toxicology and Applied Pharmacology.* 1996;179:173-179.
63. Van den Berg M, Birnbaum LS, Denison M. The 2005 World Health Organization reevaluation of human and Mammalian toxic equivalency factors for dioxins and dioxin-like compounds. *Toxicol Sci.* 2006;93(2):223-241.
64. Weber LW, Greim H. The toxicity of brominated and mixed-halogenated dibenzo-p-dioxins and dibenzofurans: an overview. *J Toxicol Environ Health.* 1997;50(December 2014):195-215.
65. Olsman H, Engwall M, Kammann U. Relative differences in aryl hydrocarbon receptor-mediated response for 18 polybrominated and mixed halogenated dibenzo-p-dioxins and -furans in cell lines from four different species. *Environ Toxicol Chem.* 2007;26(11):2448-2454.
66. Geyer HJ, Schramm K, Anton E, Poiger H, Henkelmann B, Kettrup A. Half-lives of tetra-, penta-, hexa-, hepta-, and octachlorodibenzo-p-dioxins in rats, monkeys and humans — a critical review. *Chemosphere.* 2002;48:631-644.
67. Vendeuvre C, Bertoncini F, Duval L, Duplan J-L, Thiébaud D, Hennion M-C. Comparison of conventional gas chromatography and comprehensive two-dimensional gas chromatography for the detailed analysis of petrochemical samples. *J Chromatogr A.* 2004;1056(1-2):155-162.
68. Focant J-F, Sjödin A, Patterson DG. Improved separation of the 209 polychlorinated biphenyl congeners using comprehensive two-dimensional gas

- chromatography–time-of-flight mass spectrometry. *J Chromatogr A*. 2004;1040(2):227-238.
69. Ohura T. Environmental behavior, sources, and effects of chlorinated polycyclic aromatic hydrocarbons. *ScientificWorldJournal*. 2007;7:372-380.
 70. Kouremenos KA, Pitt J, Marriott PJ. Metabolic profiling of infant urine using comprehensive two-dimensional gas chromatography: Application to the diagnosis of organic acidurias and biomarker discovery. *J Chromatogr A*. 2010;1217(1):104-111.
 71. Górecki T, Panić O, Oldridge N. Recent Advances in Comprehensive Two-Dimensional Gas Chromatography (GC×GC). *J Liq Chromatogr Relat Technol*. 2006;29(7-8):1077-1104.
 72. Evans CR, Jorgenson JW. Multidimensional LC-LC and LC-CE for high-resolution separations of biological molecules. *Anal Bioanal Chem*. 2004;378(8):1952-1961.
 73. Edam R, Blomberg J, Janssen H-G, Schoenmakers PJ. Comprehensive multi-dimensional chromatographic studies on the separation of saturated hydrocarbon ring structures in petrochemical samples. *J Chromatogr A*. 2005;1086(1-2):12-20.
 74. Blumberg L, Klee MS. A critical look at the definition of multidimensional separations. *J Chromatogr A*. 2010;1217(1):99-103.
 75. Ekman, R., Silberring, J., West,am-Brinkman, A.M., Kraj, A. Mass Spectrometry-Instrumentation, Interpretation and Applications. 2009.
 76. Hoffman, E., Stroobant, V. Mass Spectrometry-Principles and Applications. Second Edition 1999.
 77. Marshall AG, Hendrickson CL. Fourier transform ion cyclotron resonance detection: principles and experimental configurations. *Int J Mass Spectrom*. 2002;215:59-75.

78. Comisarow MB, Marshall AG. The early development of Fourier transform ion cyclotron resonance (FT-ICR) spectroscopy. *J Mass Spectrom.* 1996;31(6):581-585.
79. Marshall AG. Milestones in fourier transform ion cyclotron resonance mass spectrometry technique development. *Int J Mass Spectrom.* 2000;200(1-3):331-356.
80. McLafferty FW, Stauffer DB, Zhang M, Loh SY. Comparison of Algorithms and Databases for Matching Unknown Mass Spectra. *J Am Soc Mass Spectrom.* 1998;9:92-95.
81. Sparkman, OD. Evaluating Electron Ionization Mass Spectral Library Search Results. *Am Soc Mass Spectrom.* 1996;7:313-318.
82. Li D-X, Gan L, Bronja A, Schmitz OJ. Gas chromatography coupled to atmospheric pressure ionization mass spectrometry (GC-API-MS): Review. *Anal Chim Acta.* 2015;891:43-61.

CHAPTER TWO

Evaluation of firefighter exposure to wood smoke during training exercises at burn houses

Sujan Fernando¹, Lorraine Shaw¹, Don Shaw¹, Michael Gallea¹, Lori VandenEnden¹, Ron House², Dave Verma¹, Philip Britz-McKibbin^{1*} and Brian McCarry¹

Submitted: *Environ. Sci. Technol.* (Manuscript ID: es-2015-047525)

Author Affiliations:

¹*McMaster University, Department of Chemistry and Chemical Biology, 1280 Main St. W., Hamilton, ON, L8S 4M1 Canada*

²*University of Toronto, 80 St. George St., Toronto, ON, M5S 3H6 Canada*

Author Contributions:

Manuscript prepared by Sujan Fernando with editorial comments provided by Lorraine Shaw, Philip Britz-McKibbin and Brian E. McCarry. The study design was initiated by Sujan Fernando, Lorraine Shaw, Don Shaw, Ron House, Dave Verma and Brian E. McCarry. Sujan Fernando, Lorraine Shaw, Don Shaw, Michael Gallea and Lori VandenEnden participated in sample collection. Sample extraction and cleanup was carried out by Sujan Fernando, Michael Gallea, Lori VandenEnden and Lorraine Shaw. Sample analysis by GC-MS, GC-MS/MS and LC-MS/MS was carried out by Sujan Fernando along with data interpretation.

ABSTRACT

Smoke from wood-fueled fires is one of the most common hazards encountered by firefighters worldwide. Wood smoke is complex in nature and contains numerous compounds, including methoxyphenols (MPs) and polycyclic aromatic hydrocarbons (PAHs), some of which are carcinogenic. Chronic exposure to wood smoke can lead to adverse health outcomes including respiratory infections, impaired lung function, cardiac infarctions and cancers. At training exercises held in burn houses at four fire departments across Ontario, air samples, skin wipes and urine specimens from a cohort of firefighters ($n=28$) were collected prior to and after exposure. Wood was the primary fuel used in these training exercises. Air samples showed that MP concentrations were on average five-fold greater than PAHs. Skin wipe samples acquired from multiple body sites of firefighters indicated whole-body smoke exposure. A suite of MPs (methyl-, ethyl- and propylsyringol) and deconjugated PAH metabolites (hydroxynaphthalene, hydroxyfluorene, hydroxyphenanthrene and their isomers) were found to be sensitive markers of smoke exposure in urine. Creatinine-normalized levels of these markers were significantly elevated ($p < 0.05$) in 24 h post-exposure urine despite large between-subject variations that were dependent on the burn house site and the specific operational roles of firefighters while using personal protective equipment. This work offers deeper insight into potential health risk from smoke exposure among firefighters that is needed for translation of better mitigation policies, including improved equipment to reduce direct skin absorption and standardized hygiene practices implemented at fire services.

INTRODUCTION

Firefighting is one of the most challenging and dangerous professions. Aside from the obvious occupational hazards, firefighters are also confronted with both acute and chronic exposures to chemicals mainly in the form of combustion and pyrolysis products. Long-term exposure to smoke can lead to recurrent health problems, including respiratory infections, impaired lung function, cardiac infarctions and cancers (1-5). A number of epidemiological studies have found direct links between firefighters' exposures to toxic chemicals and various cancers (2,6). The Ontario Industrial Disease Standards Panel Report of 1994 on Cardiovascular Disease and Cancer Among Firefighters recognized a probable connection between firefighting and various cancers, cardiovascular disease and aortic aneurysm (5). As a result, the Government of Ontario (Canada) passed a presumptive legislation in 2007 to include a number of cancers and heart disease as occupational diseases presumed to have been caused by smoke exposure during firefighting. Chemical exposure can occur via inhalation, ingestion or absorption through the skin. However, few studies have quantified chemical exposures using either air measurements or skin concentrations (7-10) while also assessing biochemical markers associated with industrial or trade related diseases (11,12). Further work is needed to identify the routes of smoke exposure in firefighters while validating evidence-based hygiene practices and/or lifestyle interventions that promote risk mitigation.

Polycyclic aromatic hydrocarbons (PAHs) have long been of interest to occupational health and safety because certain PAHs are known to possess mutagenic and carcinogenic properties (13-16). PAHs are formed as by-products of incomplete

combustion of numerous carbonaceous fuels, including wood (17). PAH are oxidized into their hydroxylated metabolites by specific cytochrome P450 isoforms in the liver and are subsequently excreted in urine as their water-soluble glucuronic acid and/or sulfate conjugates (18). One of the classic urinary markers of smoke exposure has been 1-hydroxypyrene (1-HP), which is a major deconjugated metabolite of pyrene for assessment of smoke exposure in various occupational and environmental settings (19-21). However, few studies have investigated whether firefighters' exposure to PAHs in the air is correlated to excretion of 1-HP in their urine, which is needed for occupational risk assessment as compared to other industrial cohorts (22). A disadvantage of 1-HP as a marker of wood smoke exposure is that it is not very selective due to the ubiquitous nature of PAHs in the environment (22,23). Also, pyrene and other higher molecular weight PAHs are preferentially eliminated in the faeces as compared to urine. For instance, oral ingestion of 50 µg of pyrene by rats were found to have 1-HP levels 120-140 times higher in the faeces than in the urine (24). As a result, some studies have expanded their analyses to measure a broader suite of PAH metabolites that are more readily measured in urine after smoke exposure. For example, Edelman *et al.* measured the chemical exposure of firefighters following the World Trade Centre fire (23), including the analysis of 14 different PAH metabolites in blood and urine specimens. However, samples were collected about 3 weeks after the incident with concentrations only slightly greater than background levels in the general population. Also, a recently published NIOSH Health Hazard Report (2013) measured firefighters' exposure to chemicals, including PAHs during two burn exercises (11). However, only one burn

exercise was reported to give rise to increases in urinary hydroxy-PAH metabolites above baseline levels prior to exposure. It should be noted that hydroxy-PAHs reported by NIOSH were measured using ELISA, which is less selective as compared to mass spectrometric (MS)-based techniques. As a result, alternative classes of wood smoke markers are needed to facilitate lifelong exposure studies to better understand the environmental causes of human diseases (25).

A wood smoke exposure study was reported by Dills *et al.* whereby exposure was assessed by monitoring a group of chemicals known as methoxyphenols (MPs) in the air and in the urine of exposed individuals (26). Indeed, wood smoke is composed of diverse groups of compounds including sugars, alcohols, sterols, PAHs, and MPs (27, 28). MPs are the major combustion products of lignin, which constitutes 18-35% of wood by mass. Since the concentrations of the most abundant MPs are on average 5-10 times higher in wood smoke compared to the most abundant PAHs (*e.g.*, naphthalene, phenanthrene),²⁸ MPs are more sensitive markers of wood smoke exposure. For instance, MPs have been used to assess exposure of wildland firefighters (29), where 14 different MP analogs were found to have significantly increased within a sub-set of post-exposure urine samples analyzed. Although the toxicity of MPs are not well understood, mid-polar fractions of wood smoke particulate matter containing MPs have been reported to be cytotoxic due to glutathione depletion in macrophages that can adversely impact lung immune function (30, 31). However, some classes of MPs are also widely used as additives in the food industry, such as guaiacol, syringol and their alkylated homologs that give rise to the taste and aroma of smoked foods (32). As a result, the selection of specific MP markers of

smoke exposure depend on the type of wood burned and experimental conditions used to conduct human exposure studies, including dietary exclusion criteria for volunteers (33). In this work, firefighter's exposure to wood smoke was evaluated during training exercises in burn houses at four different sites across Ontario. For the first time, exposure to wood smoke was assessed by monitoring an expanded suite of PAHs and MPs in the air, on the skin, as well as their corresponding metabolites excreted in urine over 24 h. Wood smoke exposure was evaluated for individual firefighters equipped with personal protective equipment, which was found to be dependent on their operational duties during training exercises, as well as hygiene practices adopted by different regional fire services.

EXPERIMENTAL

Chemicals and Reagents. *N*-methyl-*N*-(trimethylsilyl)trifluoroacetamide (MSTFA) >98.5%, β -glucuronidase (from *Helix Pomatia*, Type Hp-2, aqueous solution, > 1.0 x 10⁵ units/mL) and sodium acetate (Reagent plus 99%) were purchased from Sigma-Aldrich (Canada & USA). The PAH standards (see Supporting Information section) were purchased from Chiron AS (Norway). Phenanthrene-d₁₀ (98%), pyrene-d₁₀ (98%) and chrysene-d₁₂ (98%) were purchased from Cambridge Isotope Laboratories (USA). Guaiacol, methylguaiacol, ethylguaiacol, propylguaiacol, syringol, methylsyringol, eugenol, isoeugenol (cis/trans), acetovanillone, acetosyringone, sinapyl aldehyde, along with the hydroxyl-PAHs were purchased from MRI (USA). Dichloromethane (distilled-in-glass), water (HPLC), methanol (HPLC), toluene (HPLC) and acetonitrile (HPLC) were purchased from Caledon (Canada). Ethylsyringol, propylsyringol, butylsyringone,

propylsyringone, guaiacyl acetone, guaiacol-d₄ (98%), syringol-d₆ (98%) and acetosyringone-d₆ (98%) were generously gifted by Christopher D. Simpson.

Study Design and Sample Collection. This study was granted ethics approval by the Research Ethics Board at McMaster University. All firefighters completed a written questionnaire to assess health status, previous smoke exposures and lifestyle information prior to training exercises (**Appendix 1** in the Supplemental Information). Wood smoke air samples along with skin wipes and urine samples were collected from firefighters while performing normal training exercises at burn houses. A total of 28 firefighter volunteers (24 males and 4 females) from four different fire departments across Ontario (Burlington, Toronto, Hamilton, Ottawa) took part in this study. Samples were collected on different days over a period of a year from training facilities located at each regional fire service. One fire department (Hamilton) was sampled twice, however the training exercise involved different participants. As a result, samples were collected from a cohort derived from five independent training exercises. All training exercises were conducted in enclosed structures known as “burn houses”. The items burned inside the burn houses consisted of untreated wood including pine and oak as well as straw. The firefighters wore their full bunker gear and self-contained breathing apparatus (SCBA) throughout the entire exercise. The SCBA was not removed until the fire was extinguished and the firefighters were at least 60 feet from the burn house to eliminate any possibility of inadvertent inhalation exposures. Air samples were collected by attaching samplers on the firefighter’s protective gear before entering the burn house. The gas and particle-phase of the air (smoke) were sampled using a Teflon® filter and XAD-2 tube attached to a

personal air sampling pump (2 L/min flow rate), respectively. Both air fractions were extracted together representing total concentrations of organic combustion by-products sampled within burn houses. Once the wood was set on fire inside the burn house, a group of about 5 firefighters would enter the structure. A subset (2-3) of these firefighters would extinguish the fire while the others would conduct a simulated search and rescue operation. The training sessions lasted approximately 30 min. Skin wipes were collected by wiping the skin with alcohol wipes before and after the training exercises. The specific locations on the body sampled include the wrist, neck, forehead, back and fingers. A single-spot urine sample was collected from each firefighter immediately before the training exercise (pre-exposure/baseline) followed by collection of urine specimens for the next 24 h after the training exercise (post-exposure). In all cases, mid-stream urine samples were collected into sterilized 50 mL collection cups. Samples were then stored in a -20°C freezer until analysis prior to analysis. All of the firefighters were non-smokers, as reported in a lifestyle questionnaire. Due to potential dietary interferences, all firefighters were requested to refrain from eating of BBQ food, sauces or smoke-flavoured products. Also, whenever possible, firefighters were requested to refrain from direct exposure to smoke 24 h prior to sampling and during the 24 h post-exposure sampling period at the workplace. The 28 firefighters who participated in the study were grouped according to the fire departments at which they were sampled. These groups were designated as AFD, BFD, CFD, DFD and EFD. Firefighters belonging to each group were randomly assigned a number following the group designate (AFD1, AFD2, etc.) for the purpose of anonymity.

Air Sample Workup. For XAD tube extraction, the contents of the tube were emptied into a vial containing 2 mL acetonitrile (ACN) and extracted by gentle agitation for 30 min. The filters were placed in a vial to which was added 3 mL of dichloromethane (DCM). Extraction was performed by sonication for 20 min. The extract was then filtered using a 0.45 μm syringe filter. A 1 mL aliquot of the extract was solvent exchanged into 1 mL of ACN by nitrogen blown down. A sample aliquot (50 μL) of the tube and filter extract was derivatized with MSTFA (40 μL) in order to form trimethylsilyl derivatives with MPs by heating at 60°C for 30 min. Pyrene-d₁₀ (10 μL , 10 ng/ μL) was added to the derivatized sample as an internal standard prior to analysis. Field blank samples were also collected within burn houses prior to the start of training exercises, which were found to contain less than 1% of target compounds measured in the air during firefighting activities. Breakthrough of volatiles from the XAD tube was evaluated by analyzing the front portion of the sorbent material separately from the back portion of the sorbent which was separated by glass wool. In all cases less than 5% breakthrough was observed.

Skin Wipe Sample Workup. Skin sampling was carried out by wiping the exposed skin with 3 successive alcohol (isopropanol) wipes. An approximately 30 cm² area of exposed skin demarcated by a foil cut-out was sampled at a specific body site using alcohol wipes. Whatman filter papers (7 cm diameter) used as the wipes were pre-extracted in DCM. Three successive wipes from each site were combined and extracted together. Each wipe was spiked with 10 μL of recovery standard prior to accelerated solvent extraction (ASE 300, Dionex, Sunnyvale, CA, USA). The recovery standard consisted of guaiacol-d₄, syringol-d₆, acetosyringone-d₆, phenanthrene-d₁₀ and chrysene-d₁₂ each at a concentration

of 10 ng/ μ L in ACN. ASE was carried out using DCM at 110°C at 10.3 MPa with heating time of 5 min and a static extraction of 5 min for 3 extraction cycles. 1 mL of toluene was added to the DCM extract obtained by ASE. The extract was then blown down to the 1 mL toluene mark using a Rotovap. A 50 μ L aliquot of the extract was derivatized by the addition of 40 μ L MSTFA followed by heating at 60°C for 30 min. An internal standard, pyrene-d₁₀ (10 μ L, 10 ng/ μ L), was added to the derivatized sample prior to analysis.

Urine Sample Workup. All urine samples were filtered using a 0.45 μ m syringe filter prior to cleanup. Then, 5 mL of 0.100 M sodium acetate buffer, pH 5.5 was added to a 3 mL aliquot of the filtered urine, followed by 20 μ L of a recovery standard mix consisting of guaiacol-d₄, syringol-d₆, acetosyringone-d₆ and ¹³C₆ 1-hydroxypyrene each at 1 ng/ μ L. 10 μ L of β -glucoridase/sulfatase was added to the sample and the sample was allowed to incubate at 37°C for 17-18 h in order to fully deconjugate hydroxy-PAH metabolites. Varian Focus SPE cartridges (50 mg, 6 mL) were used for the cleanup of deconjugated urine samples. The SPE cartridges were conditioned with 1 mL methanol followed by 1 mL water at a flow rate of 10 mL/min. The sample was then loaded at a flow rate of 1 mL/min. After the sample was loaded the cartridge was rinsed with 1 mL of water followed by 20% methanol in 0.100 M sodium acetate buffer, pH 5.5. Next, the sorbent of the cartridge was dried by aspirating air through it for 5 min followed by nitrogen blow down for 5 min to ensure that there was no residual water in the cartridge. Contents of the cartridge were then eluted with 5 mL of DCM at 0.5 mL min⁻¹. The 5 mL DCM extract was put through a sodium sulfate packed Pasteur pipette (1-2 g sodium sulfate) to remove any residual water. The dried sample was then blown down to 50 μ L and derivatized by

the addition of 40 μL MSTFA at 60°C for 30 min. An internal standard, pyrene-d₁₀ (10 μL , 10 ng/ μL), was added to the derivatized sample prior to analysis.

GC-MS and GC-MS/MS Analysis. The air and skin wipe samples were analyzed on an Agilent 6890N Gas Chromatograph (GC) coupled to an Agilent 5973N Mass Selective Detector (MSD). Both air and skin samples were analyzed using a selected ion monitoring (SIM) method. A suite of MPs and PAHs were targeted in both the air and skin samples (see Supporting Information for method details and target compound list). Urine samples were analyzed on a Varian CP-3800 GC coupled to a Varian 1200L triple quadrupole mass spectrometer, operated in multiple reaction monitoring (MRM) mode when using GC-MS/MS. A suite of MPs and hydroxy-PAHs were analyzed in human urine specimens (refer to Supplemental Information for method details and target compound list). Recovery data based on four spiked stable-isotope internal standards for all samples analyzed ranged from 63-121%, including guaiacol-d₄ (63 \pm 13), syringol-d₆ (75 \pm 11), acetosyringone-d₆ (121 \pm 11) and 1-hydroxypyrene-¹³C₆ (85 \pm 10). Quantification was performed using response factors relative to an internal standard (pyrene-d₁₀). All urine data is presented normalized to creatinine to correct for variations in hydration status. Creatinine was measured in all urine samples using a liquid chromatograph-mass spectrometry method in order to correct for hydration status (refer to Supplemental Information). All univariate statistical analyses were carried out using Microsoft Excel and OriginLab software, whereas multivariate statistical analyses using partial least squares-discriminate analysis (PLS-DA) on *log*-transformed and autoscaled data (*i.e.*, MP and PAH concentrations measured within a sample were mean-centred and

normalized to their standard deviation) were performed using MetaboAnalyst 3.0 (34). PLS-DA on preprocessed data was used to reduce data dimensionality while maximizing data covariance for subject classification (*i.e.*, search & rescue vs. fire extinguishing activity) as depicted within a scores plot, whereas a variable importance in projection (VIP) is used to rank each variable (*i.e.*, PAH or MP concentration) in the PLS-DA model projected onto the first principal component (PC1) axis.

RESULTS AND DISCUSSION

Exposure to Airborne Wood Smoke Markers in Burn Houses. The total airborne concentrations of MPs (16 compounds) and PAHs (22 compounds) from the personal air samplers attached to the 28 firefighters are shown in **Figure 1**. There was a high degree of correlation between the total MP and total PAH concentrations for all firefighters sampled reflected by a coefficient of determination (R^2) of 0.884 and $p = 0.000905$. Overall, the total airborne MP levels within the burn houses were about 5-fold higher than that of PAHs with average concentrations of $(1500 \pm 1380) \mu\text{g m}^{-3}$ and $(280 \pm 190) \mu\text{g m}^{-3}$ respectively, which is consistent with previous data involving the combustion of wood (35). The most abundant MPs consisted of syringol, guaiacol and their alkyl/acetone derivatives, whereas naphthalene, phenanthrene, fluoranthrene and pyrene were the predominate PAHs measured in air samples (refer to **Table S1** in the Supplemental Information). The total amount of chemical exposure for firefighters within the same group/site (*i.e.*, burn house) varied on average by 3-fold between-subjects with the exception of members from the CFD group who were found to have over a 10-fold

greater total air exposure. Indeed, certain members of the CFD and EFD groups were exposed to the highest overall airborne concentrations of PAH and MPs, whereas members from BFD group had the lowest levels. The overall difference in smoke exposure among all firefighters in this study was as high as 50-fold, likely due to the type and amount of wood burned, temperature of the fire and burning techniques (wet versus dry), as well as different burn house layout and ambient conditions during training exercises that were performed throughout the year.

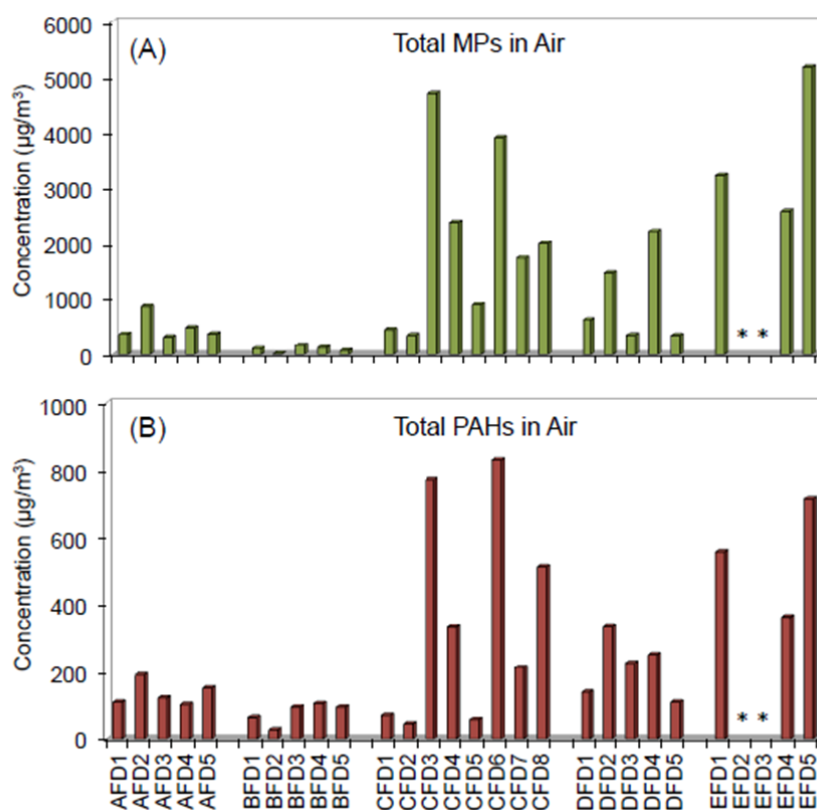


FIGURE 1. (a) Total concentration measured for MPs (16 compounds) and (b) PAHs (22 compounds) that highlights the large variability in chemical exposures following training exercises between firefighters at different burn houses from air samples attached to the firefighters ($n=26$), where * indicates that 2 samples were not recovered during training exercises.

In addition, the specific role played by each firefighter during the training session was also a likely factor impacting smoke exposure. For instance, three members of the CFD group (1, 2 and 5) had significantly lower airborne concentrations compared to the rest of the group. Two of these members (1 and 5) were identified from questionnaires as being members of the fire extinguishing group, whereas the others were part of the search and rescue group. Similar trends were observed with the other groups with the members carrying out the fire extinguishing duties (AFD1, AFD4, BFD1, BFD2, DFD1 and DFD3) having lower levels of airborne chemicals as compared to most of the search and rescue members. Overall, firefighters who extinguished the fire had lower airborne concentrations of wood smoke markers possibly because they were able to deflect the smoke away thereby reducing their effective chemical exposure. Thus, there was significant between-subject and between-site variability in smoke exposure as measured from active air sampling devices on the firefighters, which also reflected their exact operational roles during training exercises.

Wood Smoke Skin Deposition After Exposure in Burn House. To determine skin exposure for firefighters while wearing full bunker gear equipment, wipe samples were collected from five different body sites on each participant before and after the training exercises. Samples were collected from the wrist, neck, forehead, back and fingers. The total sum of the PAHs (16 compounds) and MPs (15 compounds) in the pre- and post-exposure wipes across the 5 body sites of each firefighter were measured. Overall, skin loadings for total MPs and PAHs increased significantly with an average 4-fold change following exposure relative to baseline in all firefighters sampled ($p = 6.8 \times 10^{-9}$) as

depicted by the inset of **Figure 2**. The CFD group, which had the highest overall airborne concentrations of smoke markers, also had the highest loadings of the markers deposited on skin. Also, the difference between the lowest skin loading of chemicals and the highest skin loading was approximately 3-fold, which was significantly lower than the variance measured for air concentration levels of the same chemicals at different sites. These results suggest a saturation effect on the skin at high airborne concentrations.

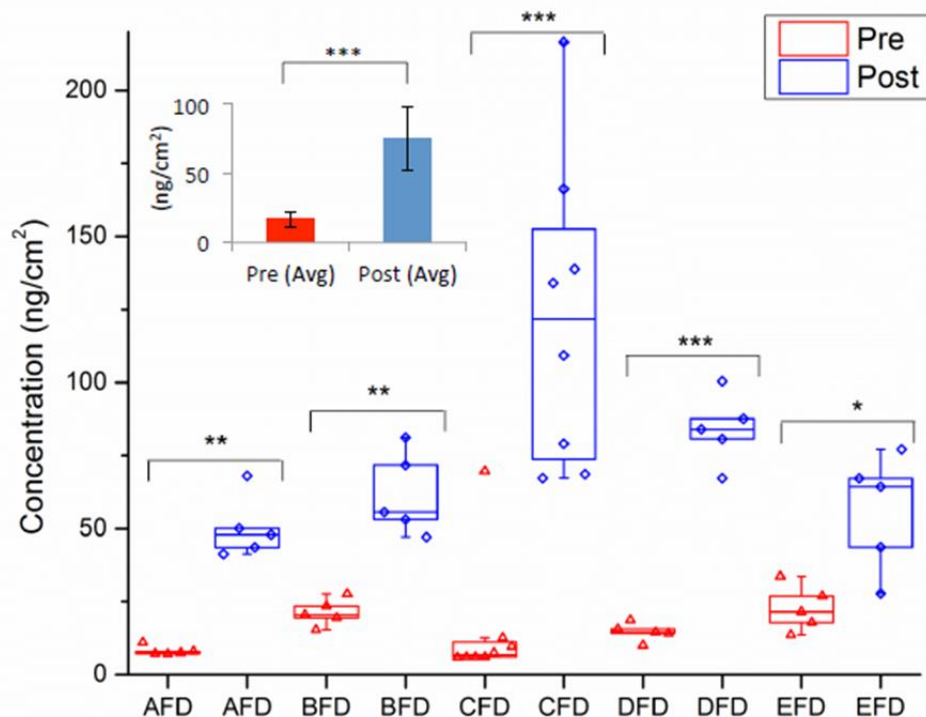


FIGURE 2. The sum of PAHs (16 compounds) and MPs (15 compounds) measured in the pre- and post-exposure wipes from across 5 different body sites for each firefighter are displayed as a box-whisker plot for the five different training exercises, where the insert shows overall changes in whole body chemical exposure for all firefighters ($n=28$). Significance levels are denoted by * $p < 0.05$, ** $p < 0.005$ and *** $p < 0.0005$ using a student's t-test.

Next, the distribution of smoke marker compounds across the five different skin sites was also evaluated. **Figure 3** depicts the net increase in smoke marker levels on the five different skin sites as a stack plot. The total concentration of PAHs (16 compounds) and MPs (15 compounds) at the 5 different skin sites were, in most cases, nearly identical for each firefighter (refer to **Table S2** in the Supplemental Information). It was observed that the only skin site that had a significantly higher loading of chemicals ($p < 0.05$) deposited from wood smoke was the fingers. These results imply that the volatile wood combustion products have penetrated the bunker gear and deposited on the skin uniformly irrespective of the site. These findings are consistent with the NIOSH study, which detected 6 PAHs at similar levels on five different body sites for firefighters (*i.e.*, arm, neck, face, scrotum and fingers) indicative of “whole-body” exposure.¹¹ It is postulated that the fingers in most cases had a higher loading compared to the other sites likely because the firefighters would remove their gloves and use their bare hands to remove their SCBA and other protective gear. In the process, they would transfer residue/soot onto their fingers. Also, given the high temperatures and physical exertion while wearing full bunker equipment in burn houses, most firefighters were sweating extensively following the training exercise, which likely had the effect of distributing chemical exposure uniformly across the body.

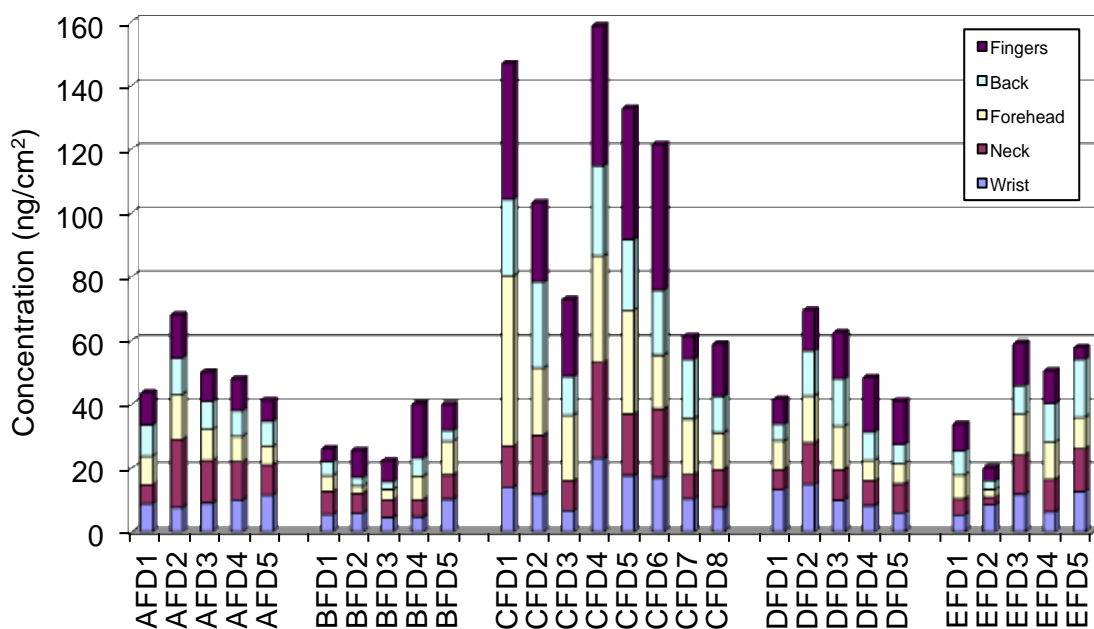


FIGURE 3. Distribution of the total MPs (15 compounds) and PAHs (16 compounds) at the 5 skin sites on the firefighters ($n = 28$). The stack plot shows the net total concentration (ng/cm^2) of PAH and MP deposition at each skin site as sampled on each firefighter following wood smoke exposure during training exercises in burn houses.

Urinary Excretion of Firefighters Upon Acute Wood Smoke Exposure. Urinary metabolites of PAHs and MPs were also analyzed for firefighters to confirm absorption of chemicals and their elimination as a result of smoke exposure during training exercises even while using personalized protective equipment. Certain PAHs generated a number of hydroxy-PAH isomers that were detectable in the urine. For example, naphthalene often gives rise to both 1- and 2-hydroxynaphthalene positional isomers in urine. Of the 22 and 16 PAHs originally measured in the air and from skin wipe extracts respectively, only 10 hydroxy-PAHs derived from 5 parent PAHs were detected in urine when using GC-MS/MS after enzymatic deconjugation and solid-phase extraction. In this case, low

molecular weight hydroxy-PAHs were primarily detected in urine samples. However, metabolites of pyrene (1-hydroxypyrene) and fluoranthene (3-hydroxyfluoranthene) were detected in less than 50% of the firefighters sampled, whereas higher molecular weight PAH metabolites were not detected due to their low concentration levels in urine. For instance, the method detection limit for 1-hydroxypyrene in urine samples was 5 ng/g creatinine, which was inadequate for most urine samples analyzed. As a result these compounds were excluded in the data analysis. Unlike the PAHs, MPs are excreted in urine at much higher concentration levels as their glucuronide or sulfate conjugates without further oxidative modifications (29). In the case of the MPs, 16 compounds were detected in air/skin samples, as well as excreted in urine. However, guaiacol, eugenol, and acetovanillone were present at relatively high concentrations levels ($> 100 \mu\text{g/g}$ creatinine) in pre-exposure urine samples likely because these compounds are present in many food additives (32) despite providing dietary restriction instructions to participants in this study. In fact, a previous wood smoke exposure study also found these MPs to be present at high levels in the urine samples of individual subjects prior to exposure (33), thus were not considered as reliable wood smoke markers for occupational health applications.

Given their widely different abundances in air, different mechanisms of elimination/metabolism and various background sources, a sub-group of MPs and hydroxy-PAHs were selected as more specific markers of wood smoke exposure based on the following criteria: (i) compounds were present at low pre-exposure levels in the urine ($< 10 \mu\text{g/g}$ creatinine), (ii) markers significantly increased (*e.g.*, > 2 -fold; $p < 0.05$) during the post-exposure period, and (iii) compounds were detected in at least 60% of

firefighters. Based on these selection criteria, a group of 3 MPs were chosen, namely methylsyringol, ethylsyringol and propylsyringol. The wood smoke exposure study by Dills *et al.* (26) proposed using 5 MPs, which included the 3 from this work along with syringol and propylguaiacol. However, the latter MPs did not satisfy our three criteria as reliable urinary smoke-exposure markers. Similarly, urinary hydroxy-PAH compounds selected as reliable smoke markers in this study included 1- and 2-hydroxynaphthalenes, 2-, 3- and 9-hydroxyfluorenes along with 2-, 3- and 4-hydroxyphenanthrene isomers. Thus, urinary data presented in the following discussion will be based on the total concentrations of these specific wood smoke markers as normalized to creatinine in order to correct for differences in total urine volume collected. **Figure 4** displays the net change in concentration in the 24 h post-exposure urine samples of firefighters based on selected MPs (3 compounds) and hydroxy-PAHs (8 compounds/isomers) relative to baseline (pre-exposure). The net change in post-exposure samples were determined by first subtracting the pre-exposure concentrations from each of the post exposure samples for a given participant followed by the summation of the net changes in concentration of all the post-exposure samples (refer to **Table S3** in the Supporting Information). Of the 28 firefighters sampled, 25 showed a net increase in the marker compounds in post-exposure samples. Overall, a significant correlation was found between post-exposure MP and hydroxy-PAH levels in the urine samples of all the firefighters as reflected by a correlation for determination (R^2) of 0.523 and $p = 0.036$. The box-whisker plot insets in **Figure 4** display the pre-exposure and average post-exposure marker concentrations for all firefighters. A more significant net increase was observed for hydroxy-PAHs ($p = 0.0285$)

as compared to the MPs ($p = 0.0564$) among the firefighters. The plot also depicts the high variability in marker compound excretion measured between subjects.

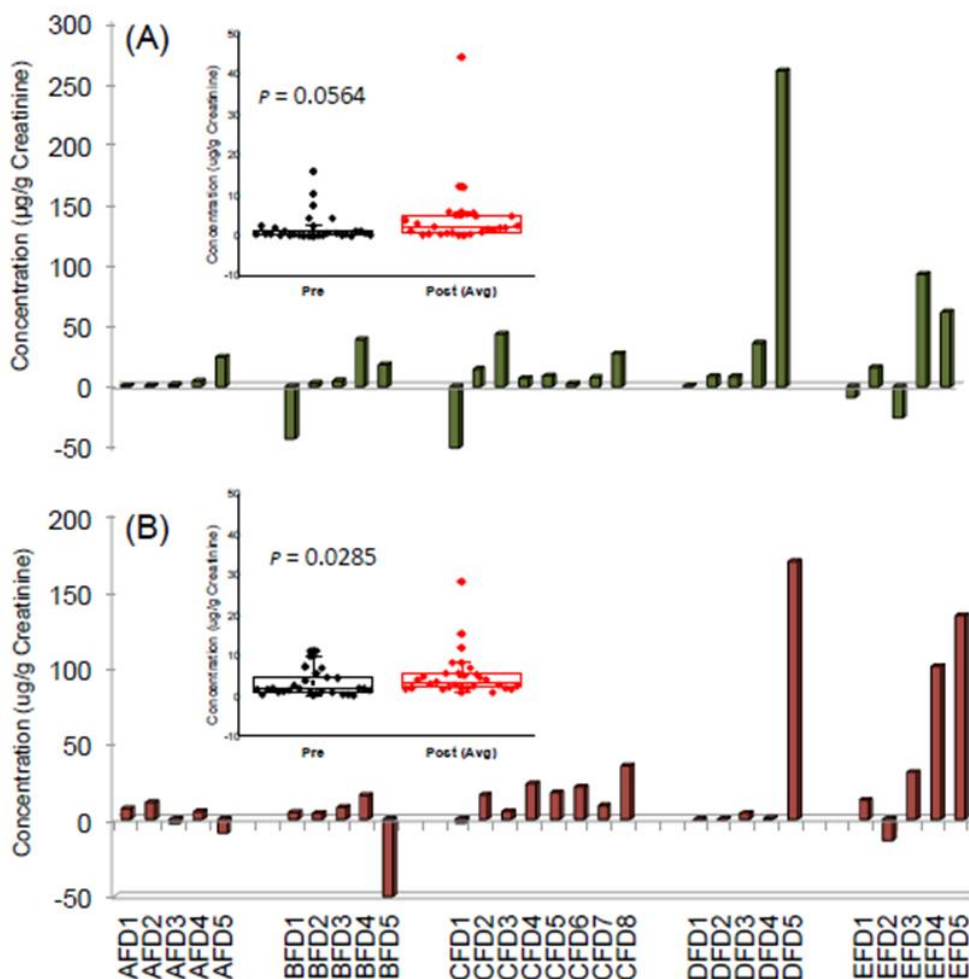


FIGURE 4. (a) The net change in the 24 h post-exposure urine of firefighters ($n=28$) for selected MPs (3 compounds) and (b) hydroxy-PAHs (8 compounds/isomers) at five different burn house sites. The net change in 24 h post-exposure was calculated by first subtracting the pre-exposure value from each of the post-exposure samples followed by the summation of the net concentrations. The graphic insert in each figure displays a Box-Whisker plot for the pre-exposure and the average post exposure urine concentrations for MPs and hydroxy-PAHs for all firefighters along with significance levels for fold-change increase using a student's t-test (paired).

It was observed that in each of the five different cohorts sampled, 1-2 firefighters had significantly higher post-exposure marker levels in their urine than the rest of the cohort. In fact, three individual firefighters had extremely high excretion levels of MPs and hydroxy-PAHs over the period of 24 h after exposure (*i.e.*, DFD5, EFD4 and EFD5) that was not related to their measured air/skin exposures. Since there are no occupational exposure limits available for MPs in urine, comparisons were made to relevant studies in literature. Recently, wood smoke exposure studies conducted on adult volunteers ($n = 9$) over 2 h in a yurt-like structure were reported without any protective gear (26) with post-exposure urine samples collected over 24 h. These individuals were reported to undergo on average a 2.1-fold increase in concentration from baseline (2.1 $\mu\text{g/g}$ creatinine) to average 24 h post-exposure levels (4.5 $\mu\text{g/g}$ creatinine). In the current study, the 25 firefighters who had a net increase in post-exposure urine displayed a 8.2-fold increase in concentration from baseline (0.7 $\mu\text{g/g}$ creatinine) to average 24 h post-exposure levels (5.8 $\mu\text{g/g}$ creatinine). In fact, the 3 firefighters from the current study with the highest net increase displayed a nearly 40-fold increase in concentration from baseline (0.6 $\mu\text{g/g}$ creatinine) to average 24 h post-exposure levels (23.4 $\mu\text{g/g}$ creatinine). These results seems to indicate that these firefighters, despite wearing their bunker gear and SCBA still had an exposure value that exceeded the levels for subjects breathing smoke unprotected for 2 h and the impact was especially high for a subset of participants.

As is the case with the MPs, there are no occupational exposure limits available for hydroxy-PAH levels in urine, and as a result comparisons were made to relevant studies in literature. The urinary hydroxy-PAH levels of the firefighters from the present study

were compared to those observed in a study conducted by the Center for Disease Control and Prevention as part of the US National Health and Nutrition Examination Survey (NHANES) (18). The NHANES study determined the urinary hydroxy-PAH levels of more than 2,700 people in the US covering a wide range of age, sex, race/ethnicity in order to establish reference range concentrations in the US population. The subjects sampled were divided into subsets of smokers and non-smokers and their hydroxy-PAH values for a suite of compounds were examined. Smokers were shown to have elevated levels of hydroxy-PAH compared to non-smokers. **Figure S1** (Supplemental Information) shows urinary profiles for a selected number of hydroxy-PAH compounds from smokers and non-smokers in the US population determined as part of the NHANES study. Also plotted are the average pre-exposure and post-exposure profiles for the 3 firefighters with the highest net increase in concentration of hydroxy-PAHs from **Figure 4b**. This data suggests that the pre-exposure profile of these firefighters is within the range of the non-smoker profile, whereas their post-exposure profile is similar to the smoker profile from the NAHNES data reflecting significant wood smoke exposure.

Firefighter Smoke-Exposure Risk Assessment. The data were evaluated to determine if a relationship exists between the marker compound concentrations in the air, skin and urine. A correlation was observed for MP and PAH concentrations in the air and on the skin. With the exception of the members of the EFD group, the total group concentrations of the marker compounds correlate very well ($R^2 = 0.980$, $p = 0.042$) with the lowest airborne group (BFD) having the lowest skin loadings and the highest airborne group (CFD) having the highest skin loadings. However, no such correlation is observed

between wood smoke marker concentrations in the air or deposition loading on skin with their excretion in urine. A correlation matrix of MP and (hydroxy)-PAH measured consistently in air, skin and urine samples in this study is included in the Supplemental Information (**Figure S2**). These unexpected findings suggest that the firefighters with the highest post-exposure urinary MP and hydroxy-PAH levels may have been exposed to a larger dose of wood smoke as compared to other firefighters. To the best of our knowledge, all the SCBA units were functioning and installed properly and none of the firefighters removed the SCBA while inside the training unit. However, some of the firefighters may have been inadvertently exposed to smoke via inhalation possibly due to momentary dislodgement of the SCBA while carrying out their operational duties within the burn house.

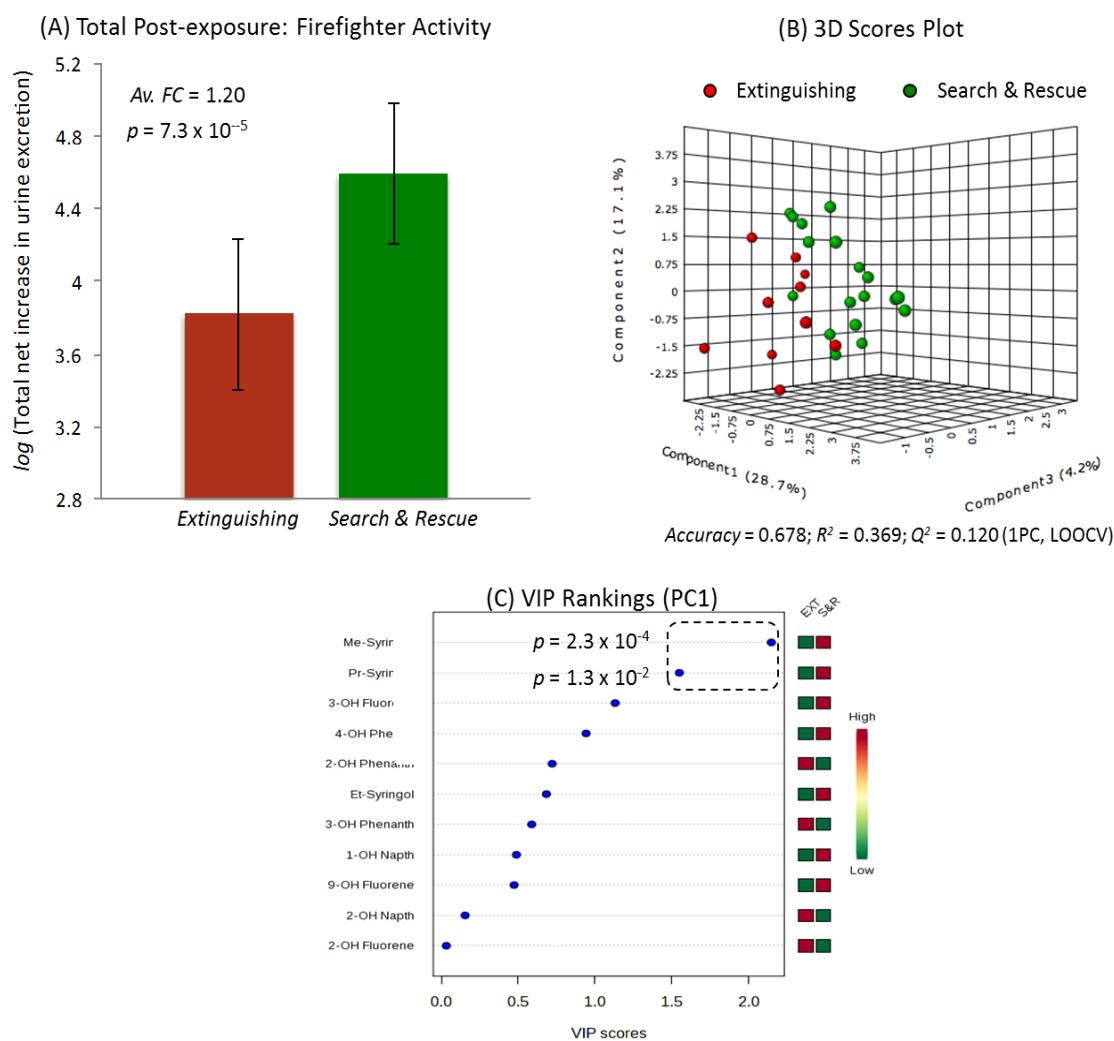


FIGURE 5. The impact of firefighter operational activity during training exercises on measured net total increase in smoke markers excreted in urine (24 h) post-exposure. (a) There was a significant increase in total exposure for firefighters conducting search and rescue (S&R) activities relative to those primarily involved in fire extinguishing (EXT); (b) a 3D scores plot derived from PLS-DA shows differences in exposure among individual firefighters based on their operational role, whereas (c) variable importance in projection (VIP) rankings show that two alkyl-substituted MPs are significantly elevated in urine among the search and rescue sub-group. All data is *log*-transformed (a) and auto-scaled (b, c) based on net increases in creatinine-normalized concentrations of 3 MPs and 8 OH-PAHs detected in urine. PLS-DA model accuracy was 0.678 with a $R^2 = 0.369$ and $Q^2 = 0.210$ with using leave out-one-at-a-time cross-validation using the first principal component (PC1).

As a result, the role of each of the firefighters in the training exercises was re-examined to determine a possible relationship to the level of exposure. At each fire station sampled, firefighter roles were classified as being part of the fire extinguisher group or part of the search and rescue group. **Figure 5(a)** shows that firefighters conducting search and rescue activities during training exercises overall had a significantly higher total net increase in chemical exposure (1.20-fold, $p = 7.3 \times 10^{-5}$) as reflected by MP and hydroxy-PAH metabolites excreted in urine over 24 h relative to fire extinguishing participants. Despite significant between-subject and between-site variability in chemical exposure, supervised multivariate analysis using partial least squares-discriminate analysis (PLS-DA) of *log*-transformed/autoscaled data highlights that many firefighters conducting search and rescue operations during training exercises excreted higher amounts of most MPs and hydroxy-PAH metabolites in their urine, notably methylsyringol ($p = 0.00023$) and propylsyringol ($p = 0.013$) as shown in **Figure 5(b) and (c)**. These results suggest that some members of the search and rescue group were at a higher risk for exposure compared to the fire extinguishing group.

Thus, a major source of exposure risk is related to the specific operational role of firefighters and how this activity may potentially impact the performance of their personal protective equipment. Future study designs should include direct monitoring of physiological responses (*e.g.*, body temperature, heart rate) coupled with tracking of firefighter movements during training exercises to better understand these confounding factors that impact exposure risk. In addition, sampling for possible air exposure within SCBA equipment during training is also needed to confirm whether some firefighters are

at increased risk to exposure. Indeed, hygiene practices and cleaning procedures for bunker gear across different regional fire services remain unstandardized across Ontario, which may contribute to large differences in chemical exposures between subjects. A limitation of this study is that only single spot/mid-stream urine samples were collected from firefighters at baseline, whereas an average exposure was assessed for each subject over a 24 h post-exposure period. Comprehensive analysis of other classes of urinary metabolites beyond traditional wood smoke markers are also needed to better evaluate risk assessment for firefighters as a result of lifelong occupational exposure. This is urgently needed to mitigate whole body exposure during repeated training exercises in burn houses, as well as acute exposures in real-world industrial/residential fires containing far more toxic and bioaccumulative combustion by-products, such as dioxins, furans and other novel halogenated organics (36).

References

1. Ribeiro M, Santos, Bussacos MA, Terra-filho M. Prevalence and risk of asthma symptoms among firefighters in Sao Paulo, Brazil: a population-based study. *Am. J. Ind. Med.* **2009**, *52* (3): 261-269.
2. Bates MN. Registry-based case-control study of cancer in California firefighters. *Am. J. Indus. Med.* **2007**, *50* (5): 339-344.
3. Rosenstock L, Olsen J. Firefighting and death from cardiovascular causes. *N. Engl. J. Med.* **2007**, *356* (12): 1261-1263.
4. Kales SN, Soteriades ES, Christoudias SG, Christiani DC. Firefighters and on-duty deaths from coronary heart disease: a case control study. *Environ. Health* **2003**, *2*: 14.
5. Guidotti TL. Evaluating causality for occupational cancers: the example of firefighters. *Occup. Med. (Lond)*. **2007**, *57* (7): 466-471.
6. Kang D, Davis LK. Cancer incidence among male massachusetts firefighters, 1987 – 2003. *Am. J. Ind. Med.* **2008**, *51* (5): 329-335.
7. Bolstad-Johnson DM, Burgess JL, Crutchfield CD, Storment S, Gerkin R, Wilson JR. Characterization of firefighter exposures during fire overhaul. *Am. Ind. Hyg. Assoc.* **2000**, *61* (5): 636-641.
8. Reisen F, Tiganis BE. Australian firefighters' exposure to air toxins during bushfire burns of autumn 2005 and 2006. *Environ. Int.* **2009**, *35* (2): 342-352.
9. Adetona O, Simpson CD, Onstad G, Naeher LP. Exposure of wildland firefighters to carbon monoxide, fine particles, and levoglucosan. *Ann. Occup. Hyg.* **2013**, *57* (8): 979-991.
10. Miranda AI, Martins V, Cascão P, *et al.* Monitoring of firefighters exposure to smoke during fire experiments in Portugal. *Environ Int.* **2010**, *36* (7): 736-745.
11. Fent KW, Eisenberg J, Evans D, *et al.* Evaluation of dermal exposure to polycyclic aromatic hydrocarbons in firefighters. *Health Hazard Evaluation Report No. 2010-0156-3196*. **December 2013**.
12. Laitinen J, Mäkelä M, Mikkola J, Huttu I. Firefighting trainers' exposure to carcinogenic agents in smoke diving simulators. *Toxicol. Lett.* **2010**, *192* (1): 61-65.

13. Bhatia AL, Tausch H, Stehlik G. Mutagenicity of chlorinated polycyclic aromatic compounds. *Ecotoxicol. Environ. Safety* **1987**, *14 (1)*: 48-55.
14. Papa E, Pilutti P, Gramatica P. Prediction of PAH mutagenicity in human cells by QSAR classification. *SAR QSAR Environ. Res.* **2008**, *19 (1-2)*: 115-127.
15. Delgado-Saborit JM, Stark C, Harrison RM. Carcinogenic potential, levels and sources of polycyclic aromatic hydrocarbon mixtures in indoor and outdoor environments and their implications for air quality standards. *Environ. Int.* **2011**, *37 (2)*: 383-392.
16. Boffetta P, Jourenkova N, Gustavsson P. Cancer risk from occupational and environmental exposure to polycyclic aromatic hydrocarbons. *Cancer Causes Control* **1997**, *8 (3)*: 444-472.
17. Baker JE. Source apportionment of polycyclic aromatic hydrocarbons in the urban atmosphere: a comparison of three methods. *Environ. Sci. Technol.* **2003**, *37 (9)*: 1873-1881.
18. Li Z, Sandau CD, Romanoff LC. Concentration and profile of 22 urinary polycyclic aromatic hydrocarbon metabolites in the US population. *Environ Res.* **2008**, *107 (3)*: 320-331.
19. Hansen AM, Mathiesen L, Pedersen M, Knudsen LE. Urinary 1-hydroxypyrene (1-HP) in environmental and occupational studies-a review. *Int. J. Hyg. Environ. Health* **2008**, *211 (5-6)*: 471-503.
20. Strickland P, Kang D. Urinary 1-hydroxypyrene and other PAH metabolites as biomarkers of exposure to environmental PAH in air particulate matter. *Toxicol Lett.* **1999**, *108 (2-3)*: 191-199.
21. Levin JO, Rhcn M, Sikstrdm E. Occupational PAH exposure: urinary 1-hydroxypyrene levels of coke oven workers, aluminium smelter pot-room workers, road pavers, and occupationally non-exposed persons in Sweden. *Sci. Total Environ.* **1995**, *163 (1-3)*: 169-77.
22. Caux C, O'Brien C, Viau C. Determination of firefighter exposure to polycyclic aromatic hydrocarbons and benzene during firefighting using measurement of biological indicators. *Appl. Occup. Environ. Hyg.* **2002**, *17 (5)*: 379-386.
23. Edelman P, Osterloh J, Pirkle J. Biomonitoring of chemical exposure among New York City firefighters responding to the World Trade Center fire and collapse. *Environ Health Perspect.* **2003**, *111 (16)*: 1906-1911.

24. Jacob J, Bruneb H, Gettbarn G, Grimmef D. Urinary and faecal excretion of pyrene and hydroxypyrene by rats after oral , intraperitoneal, intratracheal or intrapulmonary application. *Cancer Lett.* **1989**, *46 (1)*: 15-20.
25. S.M. Rappaport and M. T. Smith, Environment and disease risks. *Science* **2010**, *330 (6003)*: 460-461.
26. Dills RL, Paulsen M, Ahmad J, Kalman DA, Elias FN, Simpson CD. Evaluation of urinary methoxyphenols as biomarkers of woodsmoke exposure. *Environ. Sci. Technol.* **2006**, *40 (7)*: 2163-2170.
27. Simoneit BRT, Rogge WF, Mazurek MA, Standley LJ, Hildemann LM, Cass GR. Lignin pyrolysis products, lignans, and resin acids as specific tracers of plant classes in emissions from biomass combustion. *Environ. Sci. Technol.* **1993**, *27 (12)*: 2533-2541.
28. Nolte CG, Schauer JJ, Cass GR, Simoneit BR. Highly polar organic compounds present in wood smoke and in the ambient atmosphere. *Environ. Sci. Technol.* **2001**, *35 (10)*: 1912-1919.
29. Neitzel R, Naeher LP, Paulsen M, Dunn K, Stock a, Simpson CD. Biological monitoring of smoke exposure among wildland firefighters: a pilot study comparing urinary methoxyphenols with personal exposures to carbon monoxide, particulate matter, and levoglucosan. *J. Expos. Sci. Environ. Epidemiol.* **2009**, *19 (4)*: 349-358.
30. Kuba A, Dronen LC, Picklo MJ, Hawthorne SB. Midpolarity and nonpolar wood smoke particulate matter fractions deplete glutathione in RAW 264.7 macrophages. *Chem. Res. Toxicol.* **2006**, *19 (2)*: 255-261.
31. Kubatova A, Steckler TS, Gallagher JR, Hawthorne SB, Picklo MJ Sr. Toxicity of wide-range polarity fractions from wood smoke and diesel exhaust particulate obtained using hot pressurized water. *Environ. Toxicol. Chem.* **2004**, *23 (9)*: 2243-2250.
32. Soldera S, Sebastianutto N, Bortolomeazzi R. Composition of phenolic compounds and antioxidant activity of commercial aqueous smoke flavorings. *J. Agric. Food Chem.* **2008**, *56 (8)*: 2727-2734.
33. Simpson CD, Naeher LP. Biological monitoring of wood-smoke exposure. *Inhal. Toxicol.* **2010**, *22 (2)*: 99-103.
34. Xia J, Sinelnikov IV, Han B, Wishart, DS. MetaboAnalyst 3.0-making metabolomics more meaningful. *Nucl. Acids Res.* **2015**, *43(W1)*: W251-W257.

35. Schauer, JL, Kleeman, MJ, Cass, GR, Simoneit, BRT. Measurement of emissions from air pollution sources. 3. C1-C29 organic compounds from fireplace combustion of wood. *Environ Sci Technol.* **2001**, 35 (9):1716-1728.
36. Fernando S, Jobst KJ, Taguchi VY, Helm PA, Reiner EJ, McCarry BE. Identification of the halogenated compounds resulting from the 1997 Plastimet Inc. fire in Hamilton, Ontario, using comprehensive two-dimensional gas chromatography and (ultra)high resolution mass spectrometry. *Environ. Sci. Technol.* **2014**, 48 (18): 10656-10663.

Supplementary Information

GC-MS Method for Analysis of Smoke Exposure in Air and Skin Wipe Sample Extracts. Analysis was carried out on an Agilent 6890GC coupled to an Agilent 5973MSD. Analysis was carried out on an Agilent J&W DB-17ht column (30 m x 0.25 mm x 0.15 μ m). The injector was set to 250°C and operated in splitless mode. A 1 μ L injection of the sample was made. The starting oven temperature was 50°C and increased to 300°C using a continuous gradient of 8°C/min. Temperature was held at 300°C for 15 min resulting in a total run time of 46 min. The MSD was operated in selective ion monitoring (SIM) mode. The quantifying and qualifying ions for each of the target compounds are summarized below.

Methoxyphenols	Quan Ion	Qual Ion	PAHs	Quan Ion	Qual Ion
Guaiacol	166	196	Naphthalene	128	102
MethylGuaiacol	180	210	2-MethylNaphthalene	142	115
EthylGuaiacol	194	224	1-MethylNaphthalene	142	115
Syringol	196	226	Acenaphthylene	152	124
PropylGuaiacol	209	238	Biphenyl	154	128
Eugenol	206	236	Acenaphthene	154	126
Methylsyringol	210	240	Fluorene	166	139
Isoeugenol	206	236	Phenanthrene	178	152
Ethylsyringol	224	254	Fluoranthene	202	101
Propylsyringol	238	268	Pyrene	202	101
Acetovanillone	223	238	Benzo[ghi]fluoranthene	226	113
Guaiacylacetone	209	252	Benzo[c]phenanthrene	228	114
Acetosyringone	238	268	Cyclopenta[cd]pyrene	226	113
Butylsyringone	253	282	Benz[a]anthracene	228	114
Propylsyringone	253	296	Chrysene	228	114
Synapaldehyde	222	280	Benzo[b]fluoranthene	252	126
			Benzo[j]fluoranthene	252	126
			Benzo[k]fluoranthene	252	126
			Benzo[a]fluoranthene	252	126
			Benzo[e]pyrene	252	126
			Benzo[a]pyrene	252	126
			Perylene	252	126

GC-MS/MS Method for the Analysis of Smoke Exposure Markers in Urine. Due to the lower levels of smoke markers and their oxidized metabolites/conjugates and their isomers in urine, analysis was carried out on a Varian CP-3800GC coupled to a Varian 1200L triple quadrupole MS. Analysis was carried out on an Agilent J&W DB-17ht column (30 m x 0.25 mm x 0.15 μ m). The injector was set to 250°C and operated in splitless mode. A 1 μ L injection of the sample was made. The starting oven temperature was 40°C and increased to 300°C using a continuous gradient of 8°C/min. Temperature was held at 300°C for 2 min resulting in a total run time of 35 min. The MS was operated in multiple reaction monitoring (MRM) mode. The collision gas used was argon at a collision cell pressure of 1.5 torr. The MRM transitions for the target compounds are listed below. The target compounds were the trimethyl silyl derivatives of the listed methoxyphenols and hydroxyl-PAHs.

Methoxyphenols	MRM Transition	Collision Energy (V)
Guaiacol	196-->181	10
Methylguaiacol	210-->180	10
Ethylguaiacol	224-->209	10
Syringol	226-->211	10
Eugenol	236-->206	10
Isoeugenol	236-->206	10
Propylguaiacol	238-->223	15
Acetovanillone	238-->223	10
Methylsyringol	240-->210	10
Ethylsyringol	254-->239	10
Propylsyringol	268-->239	15
Guaiacylacetone	252-->209	10
Acetosyringone	268-->253	15
Butylsyringone	282-->267	15
Propylsyringone	296-->281	10
Sinapylaldehyde	280-->265	10

Hydroxy-PAHs	MRM Transition	Collision Energy (V)
1-OH Naphthalene	216-->201	10
2-OH Naphthalene	216-->201	10
9-OH Fluorene	254-->165	15
3-OH Fluorene	254-->165	15
2-OH Fluorene	254-->165	15
4-OH Phenanthrene	266-->235	25
3-OH Phenanthrene	266-->235	25
2-OH Phenanthrene	266-->235	25
3-OH Fluoranthene	290-->259	30
1-OH Pyrene	290-->259	30

LC-MS Method for the Analysis of Creatinine in Urine Samples. Due to the large variations in hydration status among firefighters, creatinine was used to normalize the concentration levels for all smoke marker compounds measured in urine. Analysis was carried out on a Waters 2690 HPLC coupled to a Waters Quattro Ultima triple quadrupole mass spectrometer. Analysis was carried out on a Kinetex 2.6u XBC18 column (50 x 2.1 mm). Mobile phase used was a 50:50 water and acetonitrile containing 0.1% formic acid at a flow rate of 0.2 mL/min with an isocratic elution for 5 min. Urine samples were diluted by 1000-fold in mobile phase and a 2 μ L injection was made. Prior to injection, each sample was spiked with creatinine-d₃ and quantification was carried out using internal calibration method. A five-point calibration curve was made ranging in concentration from 0.1 to 10 μ g/mL. MRM was carried out for the creatinine (114→86) as well as creatinine-d₃ (117→89). Argon was used as the collision gas with a collisional energy for precursors ions set at 20V.

TABLE S1. The average airborne concentration of methoxyphenols (16 compounds) and PAHs (22 compounds) from five sampling sessions at four different burn houses/sites across Ontario.

Average Airborne Concentrations ($\mu\text{g}/\text{m}^3$)										
Methoxyphenols	AFD (n=5)	STDEV	BFD (n=5)	STDEV	CFD (n=8)	STDEV	DFD (n=5)	STDEV	EFD (n=3)	STDEV
Guaiacol	80	16	29	13	429	302	185	86	479	77
Methylguaiacol	65	21	20	12	121	86	109	58	408	62
Ethylguaiacol	56	21	11.3	7.5	174	124	89	47	332	69
Syringol	72	36	11.9	9.9	513	498	199	191	568	354
Eugenol	13.6	4.3	2.8	1.8	29	21	18.6	8.6	96	25
Isoeugenol	36	22	3.9	2.8	97	117	77	45	335	152
Propylguaiacol	12.9	4.4	2.2	1.5	23	18	21	15	93	36
Acetovanillone	7.3	7.6	2.7	1.0	15	14	23	17	172	68
Methylsyringol	36	19	8.4	7.7	164	166	104	104	145	91
Ethylsyringol	33	31	3.6	2.2	104	102	165	156	237	126
Propylsyringol	22	N/A	1.9	1.3	52	52	43	46	49	23
Guaiacylacetone	30	17	9.2	5.1	134	131	56	45	416	167
Acetosyringone	27	12	9.7	2.0	127	105	133	55	222	70
Butylsyringone	7.9	3.8	3.2	1.6	38	28	28	25	ND	N/A
Propylsyringone	ND	--	0.3	0.0	8.1	5.0	2.4	1.2	35	16
Synapaldehyde	5.8	N/A	ND	N/A	4.0	0.6	15	17	ND	N/A
Total	504		120		2032		1268		3587	
PAHs										
Naphthalene	46	12	38	13	108	107	110	26	119	20
2-methylnaphthalene	5.2	4.4	6.6	2.8	28	26	27.4	8.1	37.6	8.9
1-methylnaphthalene	6.7	1.4	4.5	1.5	16	16	10.0	6.3	19.6	4.8
Acenaphthylene	11.1	3.2	5.9	2.5	32	31	27.6	8.3	33	11
Biphenyl	5.1	1.5	4.1	1.6	12	12	10.0	2.1	14.6	5.6
Acenaphthene	2.6	1.5	ND	N/A	1.0	0.7	1.9	0.4	2.7	2.7
Fluorene	4.2	1.4	2.0	1.0	15	12	8.6	2.6	18.7	6.1
Phenanthrene	16.9	7.3	11.8	6.1	45	47	28.6	7.0	76	34
Fluoranthene	8.4	3.4	3.6	2.1	26	24	13.5	2.3	47	17
Pyrene	9.9	3.9	4.2	2.4	26	24	14.1	2.1	45	22
Benzo[ghi]fluoranthene	1.2	N/A	0.5	0.2	5.6	3.0	2.2	0.3	12.8	2.7
Benzo[c]phenanthrene	0.5	N/A	0.2	0.1	2.0	0.9	0.8	0.2	10.6	3.6
Cyclopenta[cd]pyrene	1.6	0.3	0.2	0.1	7.4	5.3	5.3	0.8	10.6	3.4
Benz[a]anthracene	1.9	0.7	0.7	0.4	13	15	3.5	0.4	17.5	7.8
Chrysene	2.2	0.8	1.1	0.5	7.5	5.1	3.8	0.6	21.9	7.8
Benzo[b]fluoranthene	0.8	0.2	0.3	0.2	3.8	2.2	1.5	0.2	9.7	3.4
Benzo[j]fluoranthene	0.5	0.2	0.2	0.1	2.7	1.8	1.3	0.2	7.0	2.7
Benzo[k]fluoranthene	0.7	0.2	0.3	0.1	2.7	1.8	1.3	0.2	10.5	5.3
Benzo[a]fluoranthene	0.2	0.1	0.1	N/A	1.8	1.1	0.5	0.1	5.8	3.3
Benzo[e]pyrene	0.7	0.2	0.3	0.2	2.3	1.7	1.2	0.2	8.9	4.8
Benzo[a]pyrene	1.0	0.4	0.3	0.2	4.9	3.0	2.0	0.3	14.3	7.3
Perylene	0.2	0.1	0.1	0.0	0.8	0.5	0.4	0.1	5.0	3.1
Total	128		85		364		277		548	

TABLE S2. The average MP (15 compounds) and PAH (16 compounds) skin loadings (ng/cm²) measured for all subjects (n=28) at five different burn houses used for firefighter training.

Methoxyphenols (ng/cm ²)	Wrist		Neck		Forehead		Back		Fingers	
	Mean	Std Dev	Mean	Std Dev	Mean	Std Dev	Mean	Std Dev	Mean	Std Dev
Guaiacol	0.42	0.58	0.44	0.60	0.46	0.64	0.44	0.62	0.49	0.63
Methylguaiacol	0.18	0.26	0.26	0.34	0.28	0.38	0.21	0.34	0.31	0.41
Ethylguaiacol	0.29	0.23	0.38	0.29	0.37	0.26	0.31	0.27	0.72	0.63
Syringol	0.45	0.41	0.63	0.51	0.47	0.37	0.46	0.40	1.64	2.24
Eugenol	0.59	0.47	0.70	0.53	0.68	0.53	0.78	0.68	0.82	0.72
Isoeugenol	0.02	0.03	0.08	0.14	0.02	0.02	0.02	0.04	0.13	0.26
Propylguaiacol	0.05	0.13	0.07	0.13	0.07	0.15	0.06	0.12	0.09	0.15
Acetovanillone	0.53	0.84	0.41	0.57	0.58	1.02	0.32	0.52	0.81	1.39
Methylsyringol	0.11	0.12	0.28	0.59	0.09	0.10	0.06	0.07	0.64	0.84
Ethylsyringol	1.50	2.04	1.87	2.54	2.31	3.81	2.07	3.21	2.96	3.40
Propylsyringol	0.04	0.07	0.07	0.11	0.04	0.13	0.09	0.27	0.16	0.28
Guaiacylacetone	0.61	1.05	0.62	0.47	0.64	0.57	0.46	0.43	1.48	2.14
Acetosyringone	0.25	0.25	0.39	0.33	0.73	1.06	0.47	0.70	0.66	0.60
Butylsyringone	0.32	0.25	0.35	0.28	0.45	0.36	0.35	0.29	0.50	0.53
Propylsyringone	0.31	0.26	0.59	0.55	0.88	1.41	1.08	1.46	0.51	0.45
PAHs										
Naphthalene	1.33	2.11	1.11	1.82	1.26	1.68	1.39	2.24	1.19	1.17
2-methylnaphthalene	0.45	0.39	0.45	0.40	0.47	0.43	0.48	0.46	0.47	0.40
1-methylnaphthalene	0.15	0.14	0.16	0.14	0.17	0.16	0.19	0.17	0.17	0.19
Fluorene	0.15	0.13	0.14	0.07	0.13	0.09	0.15	0.09	0.16	0.13
Phenanthrene	1.03	0.61	0.99	0.51	1.04	0.72	1.00	0.64	1.16	0.84
Fluoranthene	0.32	0.20	0.38	0.23	0.37	0.31	0.31	0.24	0.47	0.32
Pyrene	0.22	0.16	0.34	0.27	0.30	0.27	0.23	0.22	0.41	0.33
Benz[a]anthracene	0.19	0.22	0.30	0.35	0.42	0.60	0.31	0.44	0.26	0.22
Chrysene	0.08	0.11	0.09	0.08	0.10	0.10	0.08	0.13	0.12	0.09
Benzo[b]fluoranthene	0.07	0.11	0.05	0.05	0.05	0.06	0.03	0.07	0.07	0.07
Benzo[i]fluoranthene	0.04	0.06	0.03	0.02	0.03	0.04	0.03	0.05	0.03	0.02
Benzo[k]fluoranthene	0.05	0.09	0.07	0.08	0.10	0.13	0.10	0.15	0.05	0.05
Benzo[a]fluoranthene	0.06	0.12	0.07	0.10	0.15	0.20	0.12	0.18	0.03	0.05
Benzo[e]pyrene	0.06	0.09	0.07	0.06	0.12	0.14	0.08	0.11	0.06	0.05
Benzo[a]pyrene	0.05	0.08	0.04	0.05	0.08	0.11	0.05	0.07	0.03	0.03
Perylene	0.04	0.06	0.02	0.02	0.03	0.04	0.03	0.04	0.01	0.00

TABLE S3. The pre-exposure and average post exposure concentrations of the selected urinary MP and hydroxy-PAH markers measured for all firefighters ($n=28$) at five different sites. All urine samples were normalized to creatinine using single-spot urine samples collected prior to exposure and 24 h urine post-exposure for each subject.

FF Code	Concentration (ng/g Creatinine)			
	Methoxyphenols		Hydroxy-PAHs	
	Pre	Post (avg)	Pre	Post (Avg)
AFD1	7.8	151	770	2131
AFD2	0.1	145	895	2680
AFD3	20.7	346	5617	5037
AFD4	16.1	777	1253	2067
AFD5	20.8	4824	3899	2136
BFD1	15934	5373	4536	5650
BFD2	212	710	1837	2481
BFD3	601	1026	898	1604
BFD4	318	5084	2608	4540
BFD5	4265	5449	9778	3522
CFD1	10316	394	4486	3987
CFD2	82.6	1663	1382	3131
CFD3	622	5942	305	932
CFD4	1191	2316	1094	4915
CFD5	220	1442	348	2792
CFD6	153	518	1066	4024
CFD7	430	1910	204	1970
CFD8	1879	5702	1834	6943
DFD1	0.1	280	1889	2093
DFD2	312	2002	7037	8380
DFD3	1284	2908	11211	11952
DFD4	540	4938	1639	1746
DFD5	1095	44230	1818	5457
EFD1	2366	1246	295	1834
EFD2	598	2545	7374	5651
EFD3	7485	3878	11122	15508
EFD4	499	12077	1383	2607
EFD5	222	12295	1621	28432

Supplemental Figures.

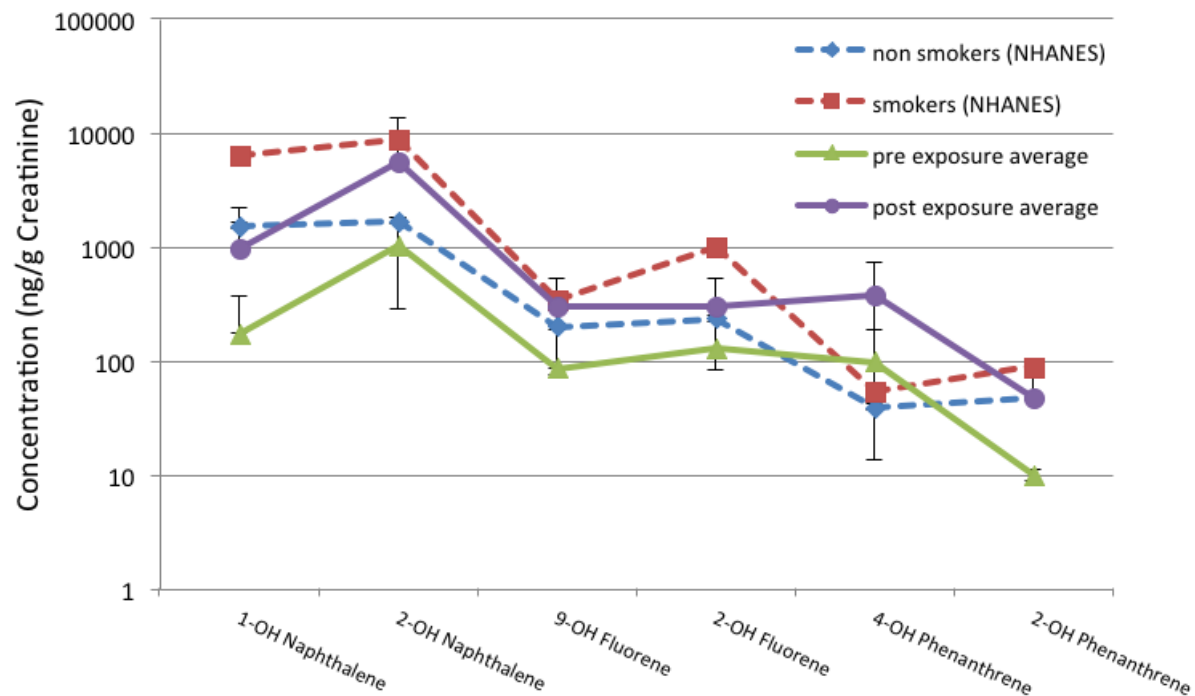


FIGURE S1. The figure displays the urinary profile of representative hydroxy-PAH compounds from smokers and non-smokers in the US population determined as part of the NHANES study(18). Plotted alongside are the average pre-exposure and post-exposure profiles for 3 firefighters with the highest net increase in post-exposure samples from Figure 4b. This data highlights that the pre-exposure baseline is within the range of the non-smoker profile, whereas the post-exposure data is similar to median values measured for smokers suggestive of significant wood smoke exposure among non-smoking firefighters equipped with bunker gear (*i.e.*, personal protective equipment).

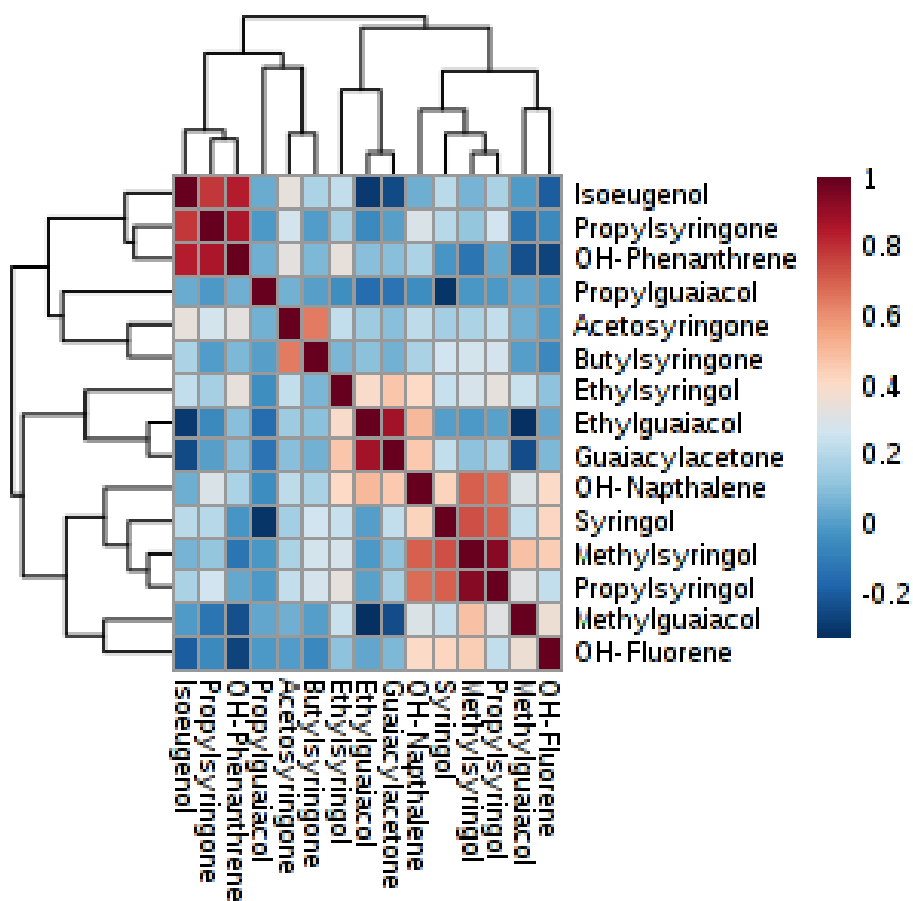


FIGURE S2. A correlation matrix highlighting the relationship between major MPs and (OH)PAHs consistently detected in air, skin and urine samples from firefighters following smoke exposure during exercise trials in burn houses.

CHAPTER THREE

Identification of Novel Markers of Wood Smoke Exposures in Firefighters using GC×GC-TOF-MS

Sujan Fernando¹, Jonathon Bloomfield¹, Lorraine Shaw¹, Don Shaw¹, Philip Britz-McKibbin^{1*} and Brian McCarry¹

Author Affiliations:

¹McMaster University, Department of Chemistry and Chemical Biology, 1280 Main Street West, Hamilton, ON, L8S 3S2

Author Contributions:

Manuscript prepared by Sujan Fernando with editorial comments provided by Philip Britz-McKibbin and Brian E. McCarry. Sujan Fernando, Lorraine Shaw, Don Shaw, and Jonathon Bloomfield participated in sample collection. Sample extraction and cleanup was carried out by Sujan Fernando and Jonathon Bloomfield. Sample analysis by GC×GC-TOF-MS was carried out by Sujan Fernando along with data interpretation. Sample analysis by GC-MS/MS was carried out by Sujan Fernando and Jonathon Bloomfield.

Abstract

Wood smoke is complex in nature and poses a serious health risk to those exposed including firefighters. Traditional chromatographic techniques have been able to identify a number of the main components of wood smoke including methoxyphenols (MPs) and polycyclic aromatic hydrocarbons (PAHs), a subset of which have subsequently been used as urinary markers of exposure. However, these markers are often present in secondary sources including foods which gives rise to elevated urinary background levels and thus complicates exposure assessment. As a result extracts from wood smoke air samples and urine samples of exposed firefighters were analyzed using a comprehensive two-dimensional gas chromatograph coupled to a time-of-flight mass spectrometer (GC×GC-TOF-MS) to identify novel markers of exposure. Compounds identified in air (wood smoke) included PAHs, MPs, various other lignin breakdown products, resin acids and novel substances some of which were detected in the post-exposure urines of the firefighters. A number of the novel markers identified were found to be present exclusively in the particle-phase of smoke for which there are very few markers that currently exist. Tandem mass spectrometry experiments were developed and used to monitor the urines of a group of firefighters (N=18) for both novel and previously used markers. These data showed that both gas-phase and particulate-bound chemicals were excreted in the urine, clearly indicative of exposures to these substances.

Introduction

Comprehensive analyses of complex mixtures provide challenges to modern analytical instrumentation due to the need to separate large numbers of components present¹. This often leads to the inability to detect certain compounds, the misidentification of compounds and errors in quantitative analysis. Even though high resolution mass spectrometry can assist in the identification of components within complex matrices with or without chromatographic separation, isobaric species and structural isomers can only be identified once they have been resolved chromatographically². The ability to resolve isobaric species and structural isomers is important in toxicological assessment since isomers often display different toxicities³.

Commonly used separation techniques include gas chromatography (GC) for the separation of volatile compounds; high performance liquid chromatography (HPLC) and capillary electrophoresis (CE) for the separation of polar and charged compounds. One-dimensional chromatography involves the separation of components using a single column whereas multi-dimensional chromatography involves separation on two or more columns. Multi-dimensional chromatography has become increasingly popular due to the inability of one-dimensional techniques to fully resolve the components in complex samples⁴. Comprehensive two-dimensional gas chromatograph (GC×GC) is the most common commercially available multi-dimensional instrument, and it consists of the two GC columns in series for enhanced separation⁵. Other multi-dimensional techniques involve the combination of two liquid chromatography (LC) columns for two-

dimensional liquid chromatography (2D-LC) analyses as well as combination of LC and CE columns⁶. Combinations of LC and GC columns has been carried out in offline configurations⁷. The multi-dimensional chromatography system used in the current work is a comprehensive two-dimensional gas chromatograph coupled to a time-of-flight mass spectrometer (GC×GC-TOF-MS, LECO Pegasus 4D).

GC×GC has been utilized for the analysis of fragrances⁸, petroleum products^{9,10} and numerous environmental¹¹⁻¹⁴ and biological samples¹⁵⁻¹⁷. The enhanced separation of GC×GC offers the opportunity to analyze complex samples with minimal cleanup¹². Dalluge et al. was able to detect up to 30,000 peaks from cigarette smoke by the direct introduction of the smoke to a GC×GC-TOF-MS¹⁸. One of the major challenges however is the deconvolution and identification of the large number of peaks detected. The ordered nature of the resulting two-dimensional (2D) chromatogram is extremely useful in this case⁵. Related compounds typically appear as distinct bands as is the case with the analysis of petroleum whereby the alkanes, alkenes and aromatics can be distinguished⁹. The structured 2D chromatograms have also been used for the identification of volatiles in urine¹⁶. In this case the chromatographic separation of compound classes greatly benefited the identification of analytes in the complex urine matrix. GC×GC has also been used for pattern recognition purposes¹⁹ and forensics¹⁴.

In the current study, air samples from wood based fires along with urines from exposed firefighters were analyzed by GC×GC-TOF-MS for the identification of novel markers of exposure. Wood based fires are one of the most common types of fires encountered by firefighters in their profession. Exposure to smoke leads to numerous

health problems including respiratory infections, impaired lung function and cancers²⁰. Wood smoke is composed of diverse groups of chemicals including sugars, alcohols, sterols, lignin breakdown products and polycyclic aromatic hydrocarbons (PAHs)^{21,22}. Since lignin constitutes 18-35% of wood by mass²³, the major lignin breakdown products known as methoxyphenols (MPs) have been used as markers of wood smoke exposure in recent studies^{20,23,24}. Some of these MPs are responsible for the aroma and taste of the smoke and are found in foods²⁵.

PAHs are by-products of many carbonaceous fuels including wood. The carcinogenic and mutagenic properties of some PAH poses a serious exposure risk²⁶. 1-hydroxypyrene, a metabolite of the PAH pyrene has been used as a classical marker of exposure in many individuals including road pavers, coke plant workers, smokers and members of the general population²⁷. Over the past few years a larger suite of PAHs and corresponding metabolites have been used to asses' exposure^{28,29}. Similar to MPs, PAHs are also present in foods. For example, BBQ sauces and smoked foods contain high levels PAHs and MPs²⁵. The ubiquitous nature of PAHs also complicates assessing exposure from a specific source. For example, it is known that cigarette smoke gives rise to various PAHs thus the urine of smokers often contains elevated hydroxyPAH levels compared to non-smokers²⁷. Another classical marker of wood smoke exposure is levoglucosan, a pyrolysis product of cellulose³⁰. Levoglucosan has been used as a marker for particle-bound organic compounds due to its high abundance in the smoke. However, due to its presence in food the pre-exposure levels of levoglucosan in urine is often high and thus is not a desirable marker of exposure³⁰.

As a result, dietary restrictions must be established and enforced in studies which attempt to assess exposure to wood smoke using the markers that currently exist. The goal of the current study was to utilize GC×GC-TOF-MS as a discovery tool to identify novel markers of wood smoke exposure by analyzing air (smoke) and urine samples of exposed firefighters during training exercises.

Experimental

Chemicals and Reagents

N-methyl-*N*-(trimethylsilyl)trifluoroacetamide (MSTFA) >98.5%, β -glucuronidase (from *Helix Pomatia*, Type Hp-2, aqueous solution, > 1.0 x 10⁵ units/mL), sodium acetate (Reagent plus 99%), sinapyl alcohol, homovanilyl alcohol, coniferyl alcohol, 4-hydroxyethanol and 4-hydroxybenzoic acid were purchased from Sigma-Aldrich (Canada & USA). The 16 EPA priority PAH standard mix was purchased from Chiron AS (Norway). Phenanthrene-d₁₀ (98%), pyrene-d₁₀ (98%) and chrysene-d₁₂ (98%) were purchased from Cambridge Isotope Laboratories (USA). Guaiacol, methylguaiacol, ethylguaiacol, propylguaiacol, syringol, methylsyringol, eugenol, isoeugenol (cis/trans), acetovanillone, acetosyringone, sinapyl aldehyde, along with the hydroxyl-PAHs were purchased from MRI (USA). Dichloromethane (distilled-in-glass), water (HPLC), methanol (HPLC), toluene (HPLC) and acetonitrile (HPLC) were purchased from Caledon (Canada). Pimaric acid, isopimaric acid, sandaracopimaric acid, dehydroabietic acid and 7-oxodehydroabietic acid were purchased from Helix Biotech (Canada). Abietic acid was purchased from Alfa Aesar (USA). Ethylsyringol, propylsyringol,

butylsyringone, propylsyringone, guaiacyl acetone, guaiacol-d₄ (98%), syringol-d₆ (98%) and acetosyringone-d₆ (98%) were generously gifted by Christopher D. Simpson.

Study Design and Sample Collection

Selected wood smoke air samples along with urines from exposed firefighters were analyzed by GC×GC-TOF-MS for the identification of novel markers of exposure. These samples were obtained from a previous study described in detail in Chapter 2. Briefly, the wood smoke air samples and urine from an exposed group of firefighters were collected during firefighter training exercises conducted in enclosed structure known as burn houses. Air samples were collected by attaching samplers on the firefighter's protective gear before entering the burn house. Both gas and particle-phase of the air were sampled using a XAD tube and filter attached to a pump. Once the items (untreated wood including pine and oak as well as straw) were set on fire inside the burn house, the firefighters would enter the structure and put out the fire followed by a search and rescue operation. The training session lasted approximately 30 minutes. A pre-exposure urine sample was collected from each firefighter prior to the training exercise followed by all urine samples for 24 hours after the training exercise. It was requested that the firefighters involved in the study do not consume any BBQ food, sauces or flavoured products as well as refrain from smoking 24hrs prior to the sampling as well as during the sampling period.

Following the GC×GC-TOF-MS identification of novel markers of wood smoke exposure, a multiple reaction monitoring (MRM) method was developed to monitor the

novel urinary markers along with the specific markers used in the previous study (Chapter 2) in a second firefighter exposure study. The second study involved 18 different firefighters and was a follow up to the first study that focused more specifically on exposure due to leaks of the self-contained breathing apparatus (SCBA) used by the firefighters. The training exercises were conducted in the same manner described above. In this case a 24hr pre-exposure urine sample was collected from each firefighter followed by all urine samples for 24hrs post-exposure. The post-exposure urine samples were combined into 0-6hrs, 6-12hrs and 12-24hrs periods. The same dietary and smoking restrictions were set in place.

Sample Extraction

Wood Smoke Air Samples

For XAD tube extraction, the contents of the tube were emptied into a vial containing 2 mL acetonitrile (ACN) and extracted by gentle agitation for 30 min. The filters were placed in a vial to which was added 3 mL of dichloromethane (DCM). Extraction was performed by sonication for 20 min. The extract was then filtered using a 0.45 μ m syringe filter. A 1 mL aliquot of the extract was solvent exchanged into 1 mL of ACN by nitrogen blown down. A sample aliquot (50 μ L) was derivatized with MSTFA (40 μ L) in order to form trimethylsilyl (TMS) derivatives with any alcohols, phenol and acids present in the sample extract by heating at 60°C for 30 min. Pyrene-d₁₀ (10 μ L, 10 ng/ μ L) was added to the derivatized sample as an internal standard prior to analysis. Field

blank samples were also collected within burn houses prior to the start of training exercises, which were found to contain less than 1% of target compounds measured in the air during firefighting activities.

Urine Samples

All urine samples were filtered using a 0.45 μL syringe filter prior to cleanup. Then, 5 mL of 0.100 M sodium acetate buffer, pH 5.5 was added to a 3 mL aliquot of the filtered urine, followed by 20 μL of a recovery standard mix consisting of guaiacol- d_4 , syringol- d_6 , acetosyringone- d_6 and $^{13}\text{C}_6$ 1-hydroxypyrene each at 1 $\text{ng}/\mu\text{L}$. 10 μL of β -glucuronidase/sulfatase was added to the sample and the sample was allowed to incubate at 37°C for 17-18 h in order to fully deconjugate metabolites. Varian Focus SPE cartridges (50 mg, 6 mL) were used for the cleanup of deconjugated urine samples. The SPE cartridges were conditioned with 1 mL methanol followed by 1 mL water at a flow rate of 10 mL/min. The sample was then loaded at a flow rate of 1 mL/min. After the sample was loaded the cartridge was rinsed with 1 mL of water followed by 20% methanol in 0.100 M sodium acetate buffer, pH 5.5. Next, the sorbent of the cartridge was dried by aspirating air through it for 5 min followed by nitrogen blow down for 5 min to ensure that there was no residual water in the cartridge. Contents of the cartridge were then eluted with 5 mL of DCM at 0.5 mL min^{-1} . The 5 mL DCM extract was put through a sodium sulphate packed Pasteur pipette (1-2 g sodium sulphate) to remove any residual water. The dried sample was then blown down to 50 μL and derivatized by the addition of 40 μL MSTFA at 60°C for 30 min. An internal standard, pyrene- d_{10} (10 μL , 10 $\text{ng}/\mu\text{L}$), was added to the derivatized sample prior to analysis.

Recovery data based on spiked labeled standards for all samples analyzed ranged from 70-114%. Quantification was performed using response factors relative to an internal standard (pyrene-d₁₀).

Instrumental Analysis

The multi-dimensional chromatography system used in the current research is a comprehensive two-dimensional gas chromatograph coupled to a time-of-flight mass spectrometer (GC×GC-TOF-MS, LECO Pegasus 4D). The column set used was a DB-5MS (60m x 0.25mm x 0.15µm) in the first dimension followed by a DB-17ht (1m x 0.1mm x 0.1µm) in the second dimension. Quantitative analysis was carried out by MRM on a Bruker CP3800 GC coupled to a Bruker 320MS triple quadrupole mass spectrometer. Analysis was carried out on a DB-17ht (30m x 0.25mm x 0.15µm) column. Method information is described in detail in the supplementary information (SI).

Results and Discussion

GCxGC-TOF-MS Analysis

Approximately 1100 peaks were detected (S/N>50) in the wood smoke air samples (N=5) of which approximately 200 compounds were identified using authentic standards and NIST (2008) mass spectral library. Compounds identified using the mass spectral library had a match factor of at least 80%. Compounds with match factors below 80% were classified as ‘unknowns’ and consists of nearly 900 of the peaks detected. Table 1 provides a breakdown of the compounds identified which include the number of compounds detected for each chemical class along with percent (%) composition in

smoke. The % composition was calculated by dividing the total peak area for each compound class by the total peak area for all peaks detected. The majority of the identified peaks were alkanes/alkenes (77 compounds) which represent nearly 11% abundance in smoke. It should be noted that many of the peaks were classified as alkanes/alkenes even when the library match factor was below 80% as these compounds would elute as a distinct band in the 2D chromatogram and also due to the characteristic ions in its mass spectrum. MPs and its derivatives (57 compounds) were the most abundant group at 12%. The MP derivatives in this case consisted of alcohols and acids of guaiacol/syringol and were described by C.G. Nolte et al. (2001) in their analysis of wood smoke²².

Table 1. Compounds identified in wood smoke air samples (N=5). 200 compounds were identified using authentic standards and NIST (2008) mass spectral library while 880 compounds were classified as unknowns. The percent abundance in smoke is based on the total peak area for the compounds detected in each compound class.

Compound Class	Number of compounds detected in smoke	% Abundance in smoke
PAH	10	1
Methoxyphenols and derivatives	57	12
Resin Acids	6	1
Anhydro Sugars	3	3
Alkanols and Sterols	13	1
Alkanoic Acids	34	5
Alkanes & Alkenes	77	11
Unknowns	880	66

Urine samples were more complex compared to the smoke samples as the number of peaks detected in the urines ranged from 4000 to 20000 ($S/N > 50$). The contour plots in Figure 1 displays the total ion current (TIC) chromatograms of an air (smoke), pre- and a selected post-exposure urine sample of an individual firefighter. Many more peaks were detected in the urine samples compared to the wood smoke air sample. The complexity of the urine sample is better depicted in Figure 2 which focuses on a specific region of the post-exposure urine sample. There are many compounds which co-elute in the first dimension but were separated in the second dimension. This separation was crucial for identifying wood smoke chemicals that were excreted in the urine.

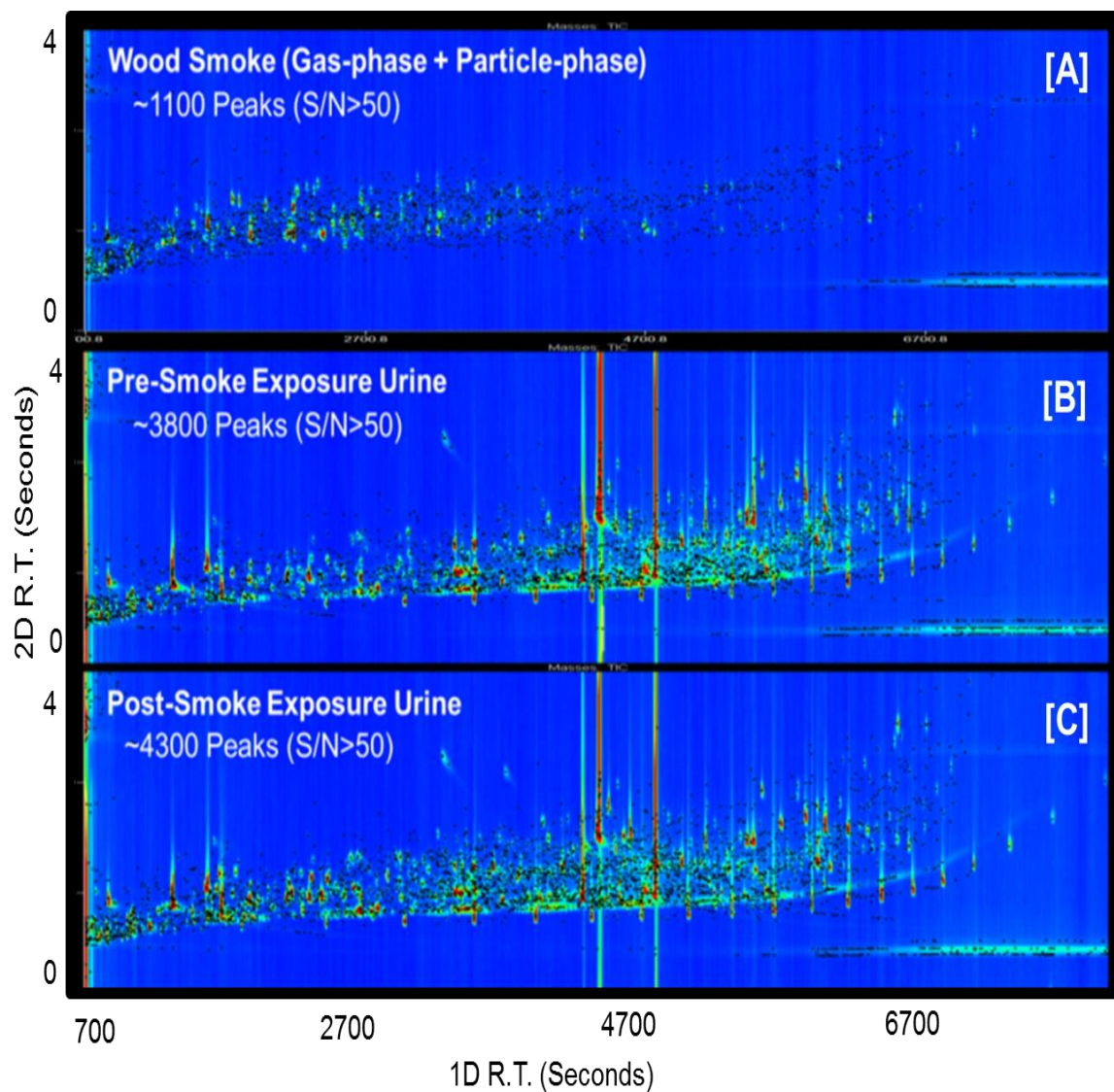


Figure 1. Total ion current (TIC) 2D chromatogram of [A] wood smoke sample and the corresponding [B] pre-exposure and [C] post-exposure urine samples from an exposed individual presented as a contour plot. The urine samples were more complex compared to the air sample. Also, more peaks were detected in the post-exposure urine than in the pre-exposure urine sample.

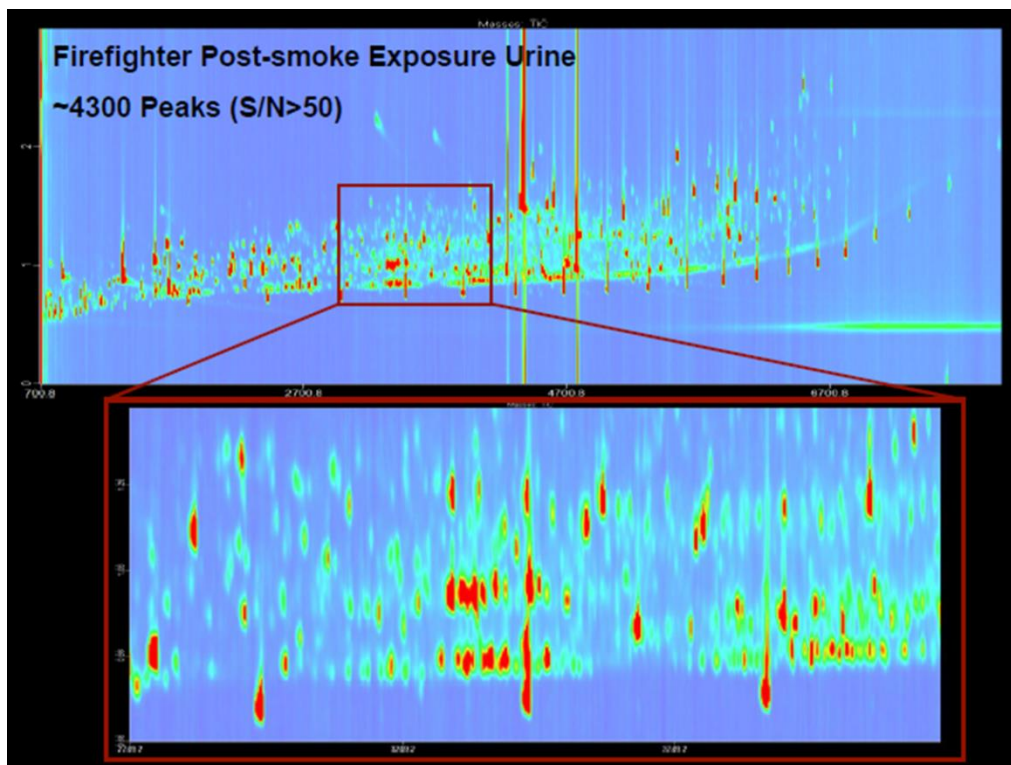


Figure 2. A magnified view of a section of a post-exposure urine sample 2D chromatogram (TIC). Many of the co-eluting peaks in the first dimension are resolved in the second dimension.

One of the major challenges at hand was the identification of the numerous wood smoke chemicals in the air that were excreted in the urine. The Statistical Compare feature of the LECO ChromaTOF software was utilized for this purpose. The Statistical Compare feature aligns the peaks identified in each data file based on 1st and 2nd dimension retention times and mass spectral similarity. Air and urine samples were blank corrected prior to data alignment. Data alignment helps reduce the complexity of the data and provides a starting point to wood smoke marker identification in urine. It should be noted that the alignment of data is useful when identifying chemicals in the smoke that are structurally unchanged in the deconjugated urine and therefore have the same or

similar retention times. This feature is not useful for compounds that are structurally modified *in vivo* prior to excretion in the urine such as PAHs which are hydroxylated³¹. In this case the retention times and mass spectra will differ between the parent molecules in the smoke and the corresponding metabolites in the urine.

A low mass spectral match factor (>60%) was used for the data alignment since despite the enhanced separation there were numerous co-eluting peaks in the urine which resulted in poor quality mass spectra. In order to simplify the task at hand, only the 60 most intense unknown peaks were selected as ‘novel markers’ in the Statistical Compare analysis. These 60 peaks represented nearly 80% of the peak area abundance of the approximately 900 unknowns detected in smoke. Table 2 displays the number of compounds detected in the wood smoke as well as in the post-exposure urines of a firefighter. Of the 60 novel compounds in the air, 23 were detected in the post-exposure urines. Of these 23 compounds, 3 were of particular interest since their pre-exposure concentration in urine was very low and increased significantly in the post-exposure urines analyzed (Figure 3). The compounds have been tentatively identified as structural isomers of pentylguaiacol (labelled C5G1, C5G2 and C5G3). The compounds were identified based on mass spectral interpretation as standards for these compounds did not exist at the time of analysis. Figure 4 displays the electron ionization (EI) mass spectra for the trimethylsilyl (TMS) derivatives of guaiacol, methylguaiacol and ethylguaiacol which are previously known MPs and were identified using authentic standards. In this case, TMS derivatized guaiacol and its alkylated homologs have a characteristic fragmentation pattern in which the molecular ion losses successive 15 atomic mass units

(amu) corresponding to CH₃ losses with the base peak corresponding to the [M-2(CH₃)]⁺ ion. The tentatively identified TMS derivatized pentylguaiacol isomers follow the same fragmentation pattern in its mass spectra (Figure 5).

A group of 6 resin acids were also detected in the smoke samples and the corresponding urine samples of the firefighters (Figure 6). Many of the resin acids were not present in pre-exposure urine and only appeared in the post exposure urine of these individuals. The presence of resin acids in coniferous softwood species has been documented previously²². However resin acids have not been monitored in urine previously as a potential smoke marker to the best of our knowledge. The resin acid identities have been confirmed with the use of authentic standards. These include pimaric acid, isopimaric acid, sandaracopimaric acid, abietic acid, dehydroabietic acid and 7-oxodehydroabietic acid.

Table 2. Smoke marker compounds identified in an air sample and in post-exposure urine samples of a firefighter.

Compound Class	Number of compounds detected in smoke	Number of compounds detected in urine
PAH	10	3
Methoxyphenols and Derivatives	57	24
Resin Acids	6	6
Anhydro sugars	3	3
Alkanols and Sterols	13	10
Alkanoic Acids	34	26
Alkanes & Alkenes	77	30
Unknowns	880	20 of 60

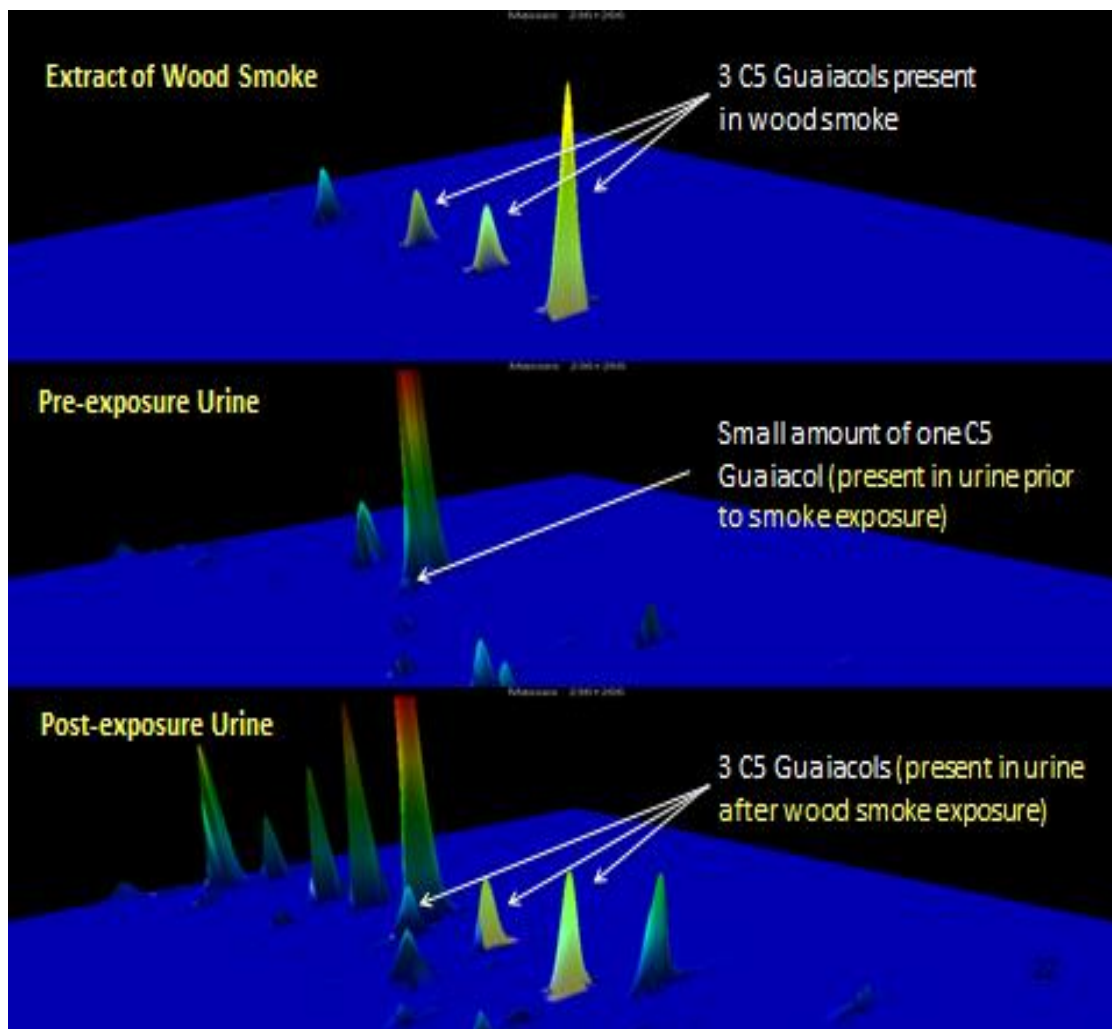


Figure 3. Three dimensional (3D) surface plot of the 3 pentylguaiacol trimethylsilyl derivatives in smoke and in the pre- and post-exposure urine of an exposed individual.

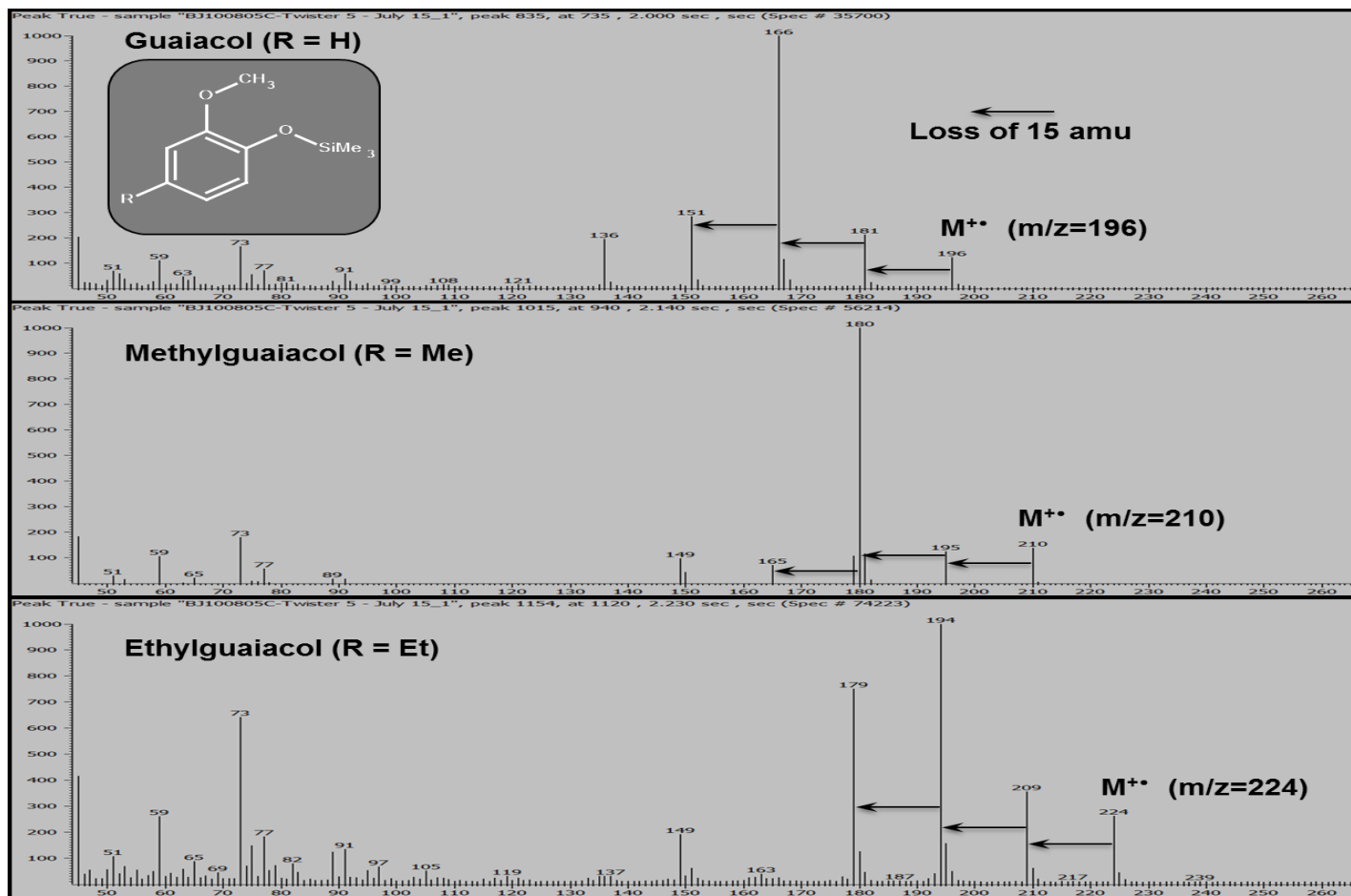


Figure 4. The electron ionization (EI) mass spectra of the trimethylsilyl (TMS) derivatized guaiacol, methylguaiacol and ethylguaiacol. TMS derivatives of guaiacol and its alkylated homologs have a characteristic fragmentation pattern in which the molecular ion losses successive 15 amu units corresponding to CH₃ losses with the base peak corresponding to the [M-2(CH₃)]⁺ ion.

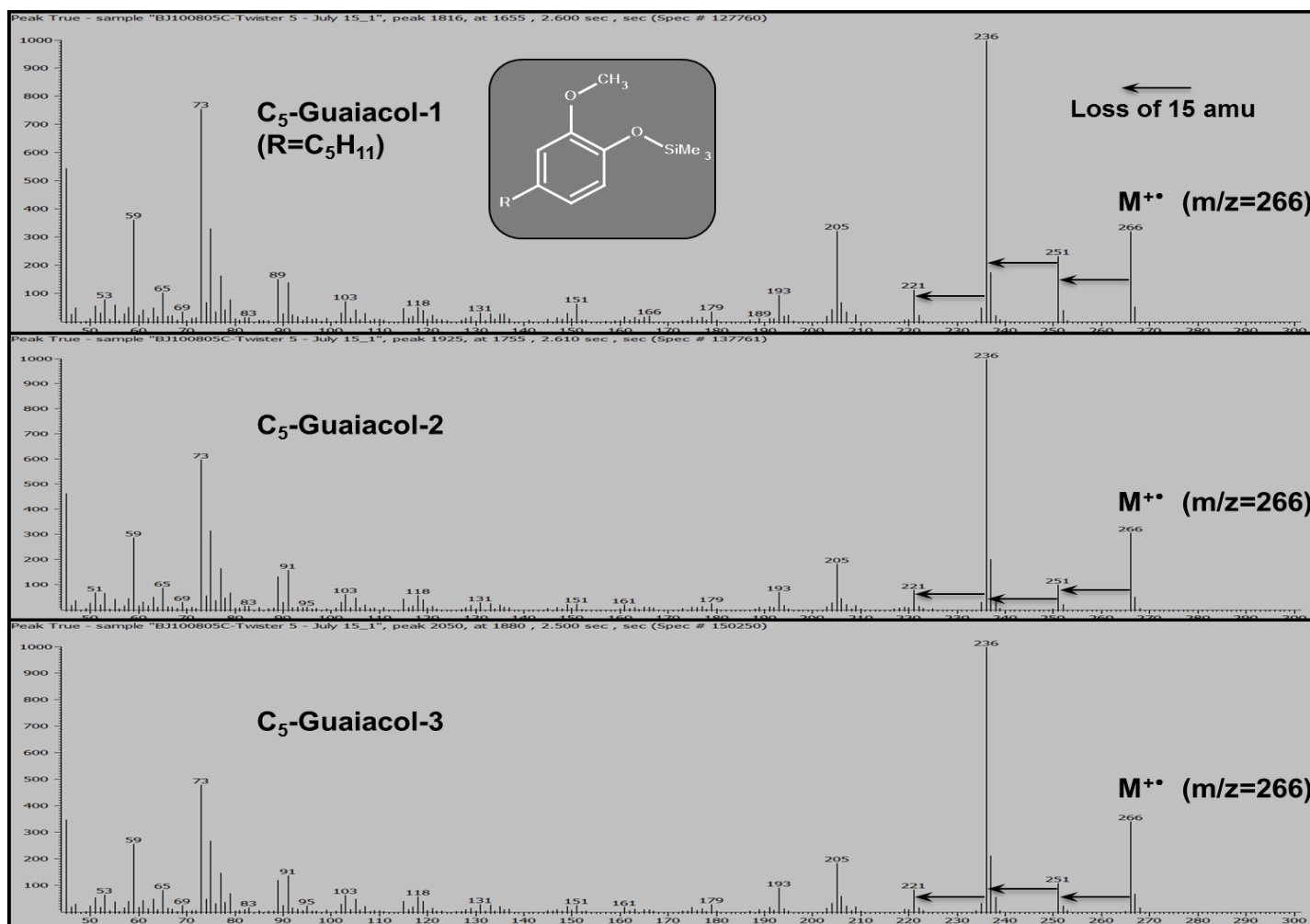


Figure 5. The EI mass spectra of the tentatively identified trimethylsilyl (TMS) derivatized pentyl guaiacol isomers. The mass spectra follow the same fragmentation pattern as the TMS derivatives of guaiacol and its methyl and ethyl homologs in figure 4.

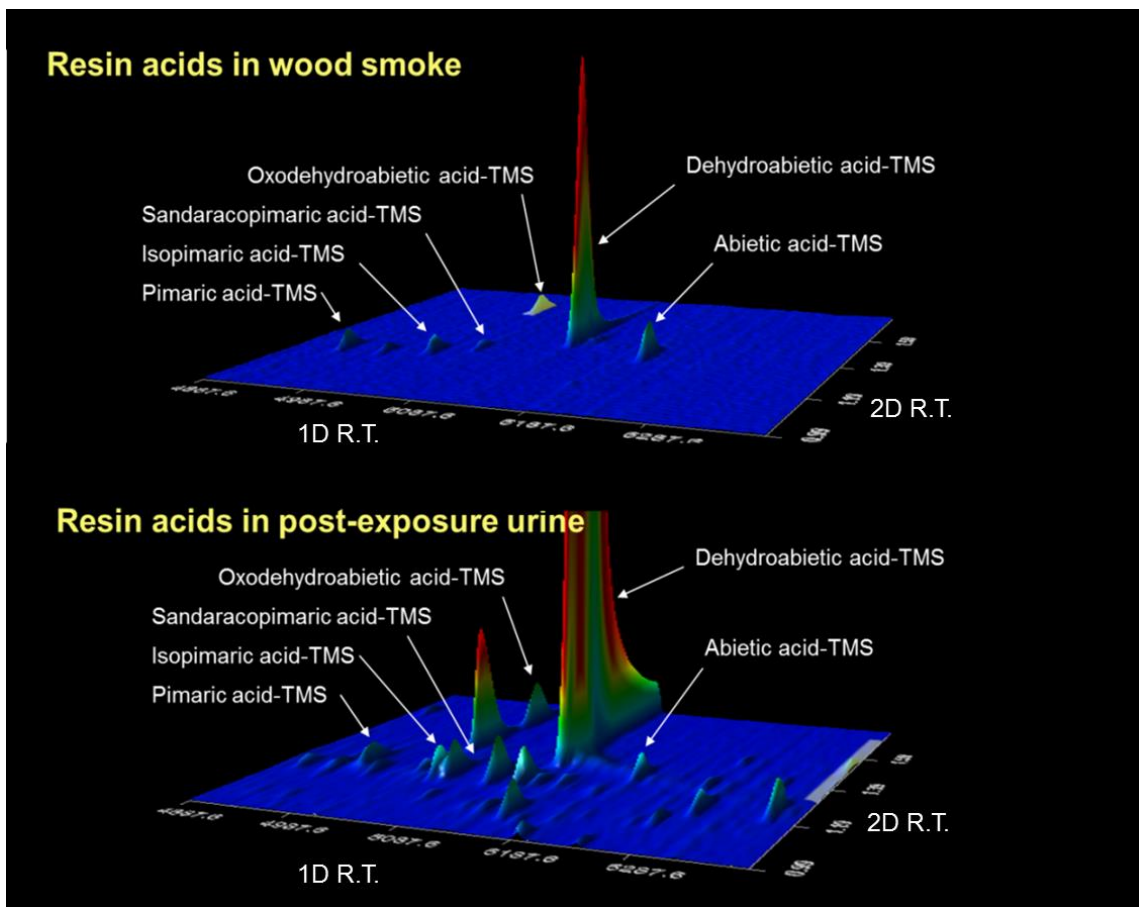


Figure 6. 3D surface plot of the trimethylsilyl (TMS) derivatized resin acids (6) in smoke and in post-exposure urine of an exposed individual.

Figure 7 displays a reconstructed 2D chromatogram of selected wood smoke markers identified in the air and in the post-smoke exposure urine of a single firefighter. The compounds displayed include PAHs, MPs, derivatives of MPs, resin acids and the 60 novel compounds. Of the 122 chemicals identified in the smoke 53 were detected in the post exposure urine in this case (see Table S1). The anhydro sugars along with the alkanols/sterols, alkanolic acids and alkanes/alkenes were excluded due to the ubiquitous nature of these compounds. Since gas phase and particle phase air samples were

collected and analyzed separately, it was possible to distinguish compounds present predominately in the gas phase (>80%) from those present predominately in the particle phase (>80%). One interesting observation from figure 7 is that a number of particle phase compounds from the smoke were also detected in the urine which includes the 6 resin acids. This was significant since most wood smoke markers currently used are found predominantly in the gas-phase. While gas-phase chemicals are thought to penetrate the lungs and cross into the blood through the alveoli, particulate matter has the potential to be embedded in the alveoli and result in a slow release of the bound organic chemicals into the blood thus increasing the potential exposure risk³².

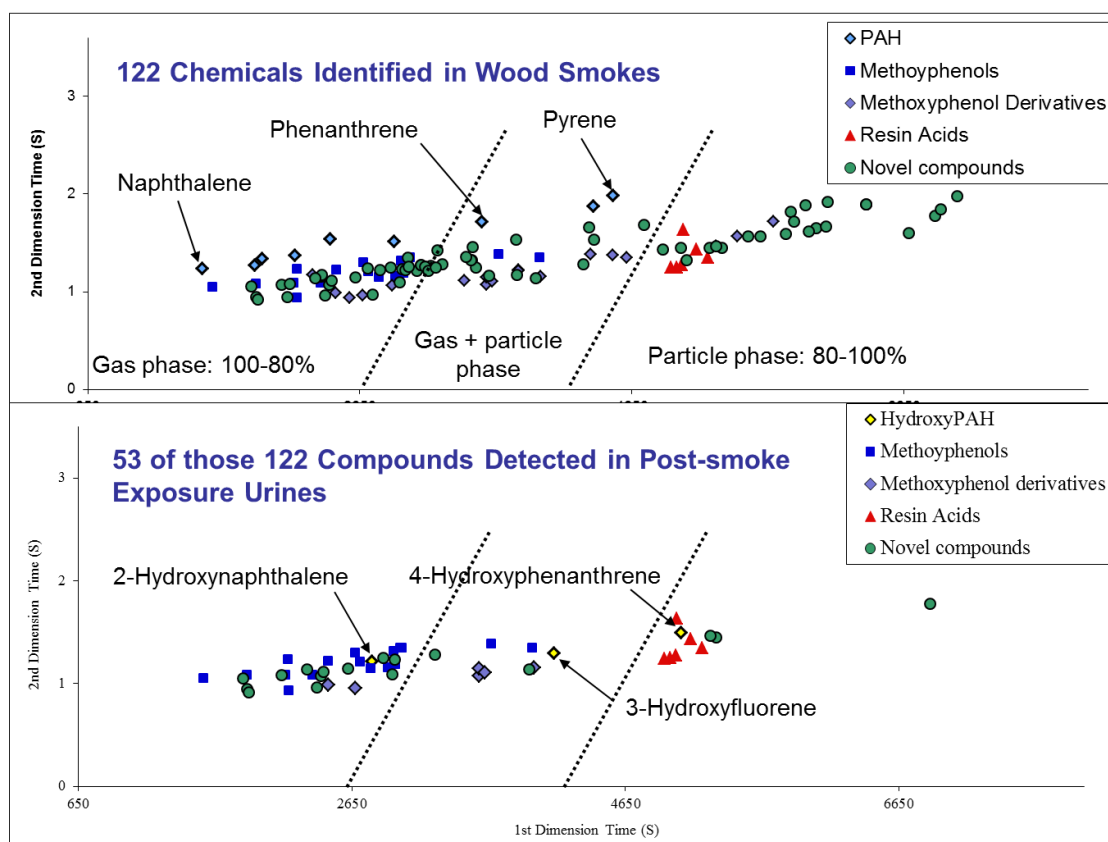


Figure 7. A reconstructed 2D chromatogram of selected wood smoke markers identified in the air and in the post-smoke exposure urine of a single firefighter.

The resin acids and the pentylguaiacols were monitored in the pre and in all 24hrs post-exposure urines of a single firefighter. Figure 8 displays the fold increase (in peak area) for the sum of the 6 resin acids, 3 pentylguaiacols, along with the specific markers selected in Chapter 2 which include 3 syringols (syringol, methylsyringol, ethylsyringol) and 8 hydroxyPAHs (metabolites of naphthalene, fluorene and phenanthrene). In this case the pentylguaiacols show the biggest fold increase of nearly 150-fold while the resin acids show a 100-fold increase. The syringols show a 15-fold increase while the hydroxyPAHs show only a 1.5-fold increase. The resin acids and pentylguaiacols appear to be more sensitive markers than the previously monitored markers.

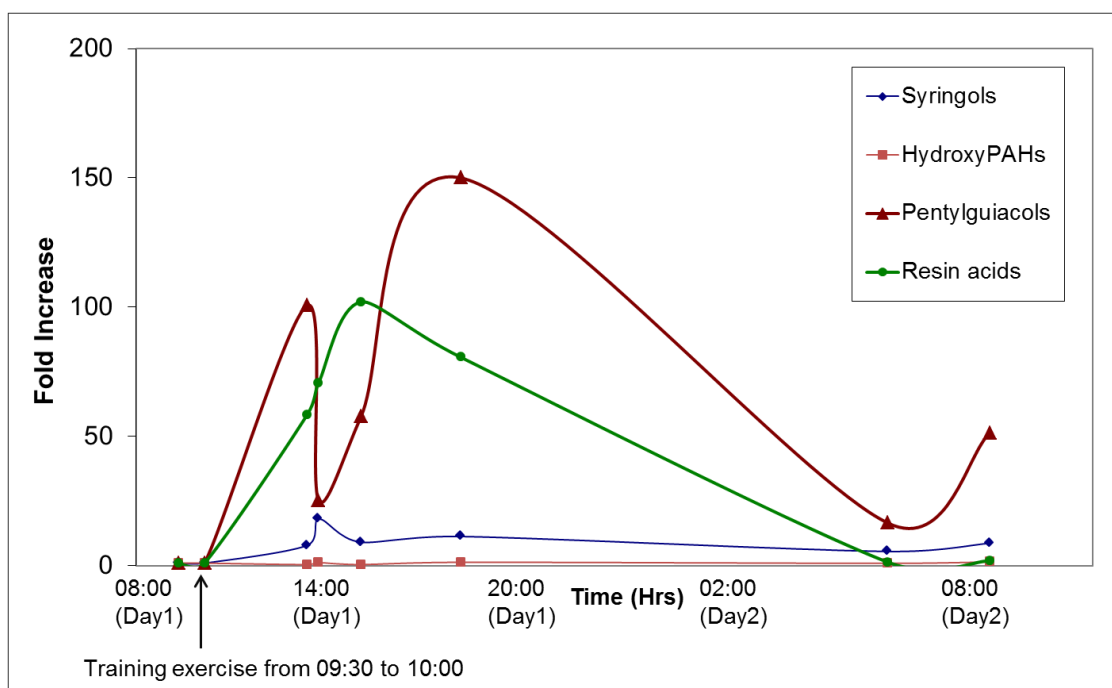


Figure 8. The fold increase (in peak area) for the sum of the 6 resin acids, 3 pentylguaiacols, along with the specific markers selected in Chapter 2 which include 3 syringols (syringol, methylsyringol, ethylsyringol) and 8 hydroxyPAHs (metabolites of naphthalene, fluorene and phenanthrene). Pre-exposure urine samples were collected at approximately 9am before the training exercises were conducted which lasted for approximately 30 minutes. All post-exposure urine samples were collected for the next 24hrs and analyzed.

Target analysis using Multiple Reaction Monitoring

The resin acids were monitored in the pre-exposure and post-exposure urines of the 18 firefighters in the follow-up study along with the 3 syringols and 8 hydroxyPAHs using multiple reaction monitoring (MRM) on a Bruker 320MS triple quadrupole mass spectrometer attached to a Varian CP3800 GC. The use of a triple quadrupole instrument for target analysis resulted in better sensitivity towards the target compounds as well as rapid analysis times. The GC×GC-TOF-MS run times were in excess of 2 hours whereas the MRM runs were approximately 20 minutes in length.

The pre and post-exposure urinary concentration of the syringols, hydroxyPAHs and resin acids for the group of 18 firefighters is displayed as a box-whisker plot in Figure 9. As was the case with the first study in Chapter 2, there is a subset of firefighters with elevated concentrations of the marker compounds in the post exposure urines compared to the rest of the group. In the case of the syringols no significant increase was detected in the post exposure urine samples compared to the pre-exposure for all firefighters with the exception of one individual ($p > 0.05$). In the case of the hydroxyPAHs a significant increase ($p < 0.05$) was observed in the 0-6hr post-exposure period but the levels returned towards the pre-exposure levels by the 6-12 and 12-24hr post exposure period. For the resin acids, the post-exposure levels began to increase during the 0-6hr post-exposure period and peaked during the 6-12hr period ($p < 0.05$). In fact, some of the firefighters continued to excrete elevated levels of resin acids even during the 12-24hrs post-exposure period. This trend is different from the syringol and hydroxyPAH markers used which are found exclusively in the gas-phase. This finding

appears to support the fact that particle bound chemicals are released into the blood at a slower rate than gas-phase chemicals and are thus excreted in the urine at a slower rate as well.

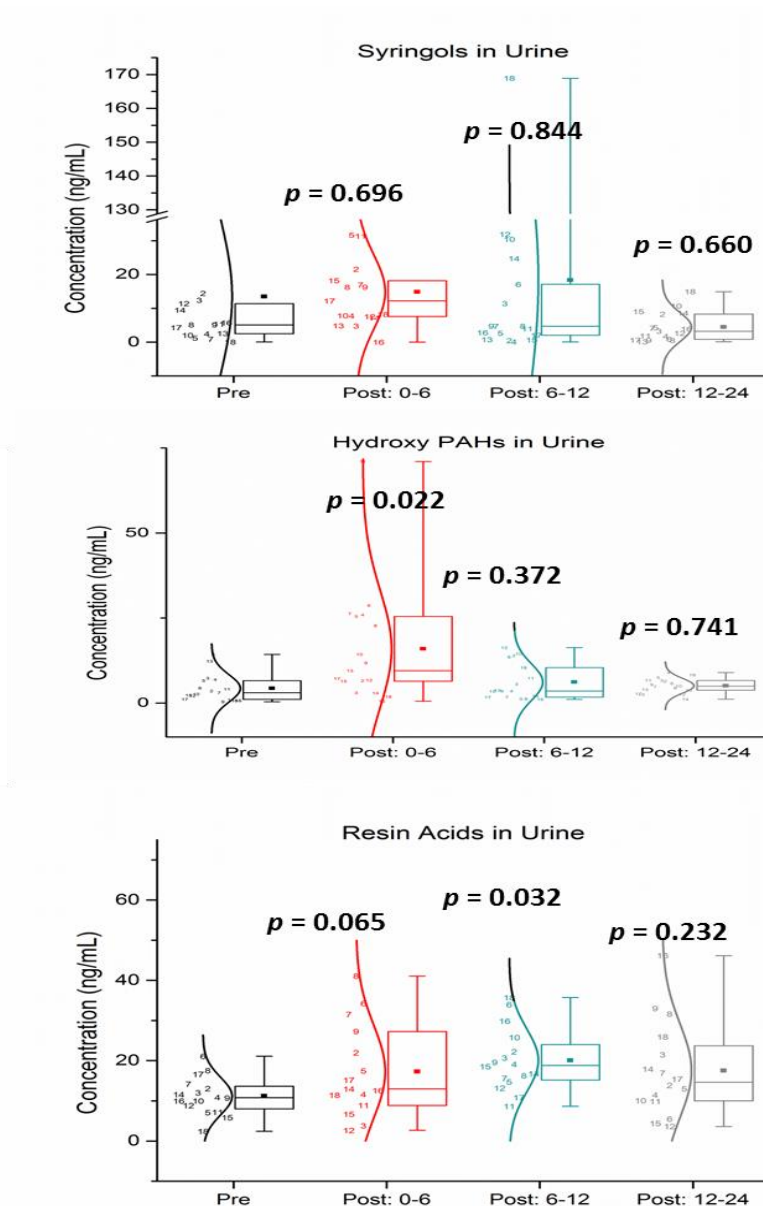


Figure 9. Box-whisker plot of the pre and post-exposure urinary concentrations of MPs, hydroxyPAHs and resin acids in a group of 18 firefighters.

Conclusions

Approximately 1100 compounds were detected in wood smoke air sample extracts using a GC×GC-TOF-MS. Only a small fraction of the compounds were identified using authentic standards and NIST mass spectral library which included PAHs, methoxyphenols and derivatives, resin acids, anhydro sugars, and aliphatic species. A subset of the unknown chemicals was detected in the post-exposure urine of a group of firefighters that were exposed to the wood smoke during training exercises. Some of these novel chemicals have been tentatively identified based on mass spectral interpretation and similarity to known compound spectra.

Also detected in the urine were a group of resin acids which are known particle-bound wood smoke markers but previously not monitored in urine. As a result a multiple reaction monitoring method was created to monitor the resin acids in the urines of a group of firefighters along with specific MP and PAH metabolites monitored in a previous study (Chapter 2). The resin acid markers increased in concentration in the post-exposure urines of the firefighters indicative of exposure to particle bound organics. Furthermore, the post-exposure urinary concentrations appear to remain elevated for a longer period of time than the gas-phase MP and PAHs markers in some of the firefighters. This finding seems to support the fact that particle bound chemicals are excreted more slowly thus could be potentially more toxic. Since highly toxic compounds such as dioxins and furans are also found in the particle-phase, this finding has significant implications.

References

1. Vendevre C, Bertocini F, Duval L, Duplan J-L, Thiébaud D, Hennion M-C. Comparison of conventional gas chromatography and comprehensive two-dimensional gas chromatography for the detailed analysis of petrochemical samples. *J Chromatogr A*. 2004;1056(1-2):155-162.
2. Focant J-F, Sjödin A, Patterson DG. Improved separation of the 209 polychlorinated biphenyl congeners using comprehensive two-dimensional gas chromatography–time-of-flight mass spectrometry. *J Chromatogr A*. 2004;1040(2):227-238.
3. Ohura T. Environmental behavior, sources, and effects of chlorinated polycyclic aromatic hydrocarbons. *ScientificWorldJournal*. 2007;7:372-380.
4. Kouremenos KA, Pitt J, Marriott PJ. Metabolic profiling of infant urine using comprehensive two-dimensional gas chromatography: Application to the diagnosis of organic acidurias and biomarker discovery. *J Chromatogr A*. 2010;1217(1):104-111.
5. Górecki T, Panić O, Oldridge N. Recent Advances in Comprehensive Two-Dimensional Gas Chromatography (GC×GC). *J Liq Chromatogr Relat Technol*. 2006;29(7-8):1077-1104.
6. Evans CR, Jorgenson JW. Multidimensional LC-LC and LC-CE for high-resolution separations of biological molecules. *Anal Bioanal Chem*. 2004;378(8):1952-1961.
7. Edam R, Blomberg J, Janssen H-G, Schoenmakers PJ. Comprehensive multi-dimensional chromatographic studies on the separation of saturated hydrocarbon ring structures in petrochemical samples. *J Chromatogr A*. 2005;1086(1-2):12-20.
8. Özel MZ, Göğüş F, Lewis AC. Comparison of direct thermal desorption with water distillation and superheated water extraction for the analysis of volatile components of *Rosa damascena* Mill. using GC×GC-TOF/MS. *Anal Chim Acta*. 2006;566(2):172-177.

9. Seeley J V, Seeley SK, Libby EK, McCurry JD. Analysis of biodiesel/petroleum diesel blends with comprehensive two-dimensional gas chromatography. *J Chromatogr Sci.* 2007;45(10):650-656.
10. Mao D, Lookman R, Van De Weghe H, et al. Detailed analysis of petroleum hydrocarbon attenuation in biopiles by high-performance liquid chromatography followed by comprehensive two-dimensional gas chromatography. *J Chromatogr A.* 2009;1216(9):1524-1527.
11. Welthagen W, Schnelle-Kreis J, Zimmermann R. Search criteria and rules for comprehensive two-dimensional gas chromatography–time-of-flight mass spectrometry analysis of airborne particulate matter. *J Chromatogr A.* 2003;1019(1-2):233-249.
12. Cavagnino D, Magni P, Zilioli G, Trestianu S. Comprehensive two-dimensional gas chromatography using large sample volume injection for the determination of polynuclear aromatic hydrocarbons in complex matrices. *J Chromatogr A.* 2003;1019(1-2):211-220.
13. Tran TC, Marriott PJ. Characterization of incense smoke by solid phase microextraction—Comprehensive two-dimensional gas chromatography (GC×GC). *Atmos Environ.* 2007;41(27):5756-5768.
14. Panić O, Górecki T. Comprehensive two-dimensional gas chromatography (GC x GC) in environmental analysis and monitoring. *Anal Bioanal Chem.* 2006;386(4):1013-1023.
15. Silva AI, Pereira HMG, Casilli A, Conceição FC, Aquino Neto FR. Analytical challenges in doping control: Comprehensive two-dimensional gas chromatography with time of flight mass spectrometry, a promising option. *J Chromatogr A.* 2009;1216(14):2913-2922.
16. Rocha SM, Caldeira M, Carrola J, Santos M, Cruz N, Duarte IF. Exploring the human urine metabolomic potentialities by comprehensive two-dimensional gas chromatography coupled to time of flight mass spectrometry. *J Chromatogr A.* 2012;1252:155-163.
17. Schwilke EW, Karschner EL, Lowe RH, et al. Intra- and intersubject whole

blood/plasma cannabinoid ratios determined by 2-dimensional, electron impact GC-MS with cryofocusing. *Clin Chem.* 2009;55(6):1188-1195.

18. Dallüge J, van Stee LLP, Xu X. Unravelling the composition of very complex samples by comprehensive gas chromatography coupled to time-of-flight mass spectrometry. Cigarette smoke. *J Chromatogr A.* 2002;974(1-2):169-184.
19. Cardeal ZL, de Souza PP, da Silva MDRG, Marriott PJ. Comprehensive two-dimensional gas chromatography for fingerprint pattern recognition in cachaça production. *Talanta.* 2008;74(4):793-799.
20. Neitzel R, Naeher LP, Paulsen M, Dunn K, Stock a, Simpson CD. Biological monitoring of smoke exposure among wildland firefighters: a pilot study comparing urinary methoxyphenols with personal exposures to carbon monoxide, particulate matter, and levoglucosan. *J Expo Sci Environ Epidemiol.* 2009;19(4):349-358.
21. Slmonelt BRT, Rogge WF, Mazurek MA, Standley LJ, Hildemann LM, Cass GR. Lignin Pyrolysis Products , Lignans , and Resin Acids as Specific Tracers of Plant Classes in Emlssions from Biomass Combustion. 1993;(12):2533-2541.
22. Nolte CG, Schauer JJ, Cass GR, Simoneit BR. Highly polar organic compounds present in wood smoke and in the ambient atmosphere. *Environ Sci Technol.* 2001;35(10):1912-1919.
23. Clark M, Paulsen M, Smith KR, Canuz E, Simpson CD. Urinary methoxyphenol biomarkers and woodsmoke exposure: comparisons in rural Guatemala with personal CO and kitchen CO, levoglucosan, and PM2.5. *Environ Sci Technol.* 2007;41(10):3481-3487.
24. Dills RL, Paulsen M, Ahmad J, Kalman D a, Elias FN, Simpson CD. Evaluation of urinary methoxyphenols as biomarkers of woodsmoke exposure. *Environ Sci Technol.* 2006;40(7):2163-2170.
25. Soldera S, Sebastianutto N, Bortolomeazzi R. Composition of phenolic compounds and antioxidant activity of commercial aqueous smoke flavorings. *J Agric Food Chem.* 2008;56(8):2727-2734.

26. Dobbins R, Fletcher R, Benner B, Hoefft S. Polycyclic aromatic hydrocarbons in flames, in diesel fuels, and in diesel emissions. *Combust Flame*. 2006;144(4):773-781.
27. Grainger J, Huang W, Patterson DG. Reference range levels of polycyclic aromatic hydrocarbons in the US population by measurement of urinary monohydroxy metabolites. *Environ Res*. 2006;100(3):394-423.
28. Li Z, Sandau CD, Romanoff LC, et al. Concentration and profile of 22 urinary polycyclic aromatic hydrocarbon metabolites in the US population. *Environ Res*. 2008;107(3):320-331.
29. Fent KW, Eisenberg J, Evans D. Evaluation of Dermal Exposure to Polycyclic Aromatic Hydrocarbons in Fire Fighters. NIOSH. 2013. Report No. 2010-0156-3196.
30. Bergauff MA, Ward TJ, Noonan CW. Urinary levoglucosan as a biomarker of wood smoke: results of human exposure studies. *J Expo Sci Environ Epidemiol*. 2010;20(4):385-392.
31. Simpson CD, Naeher LP. Biological monitoring of wood-smoke exposure. *Inhal Toxicol*. 2010;22(2):99-103.
32. Nurkiewicz TR, Porter DW, Barger M, et al. Systemic Microvascular Dysfunction and Inflammation after Pulmonary Particulate Matter Exposure. *Environ Health Perspect*. 2005;114(3):412-419.

Supplementary Information

GCxGC-TOF-MS method for the analysis of wood smoke air samples and urines.

The multi-dimensional chromatography system used in the current research is a comprehensive two-dimensional gas chromatograph coupled to a time-of-flight mass spectrometer (GCxGC-TOF-MS, LECO Pegasus 4D).

Primary Column Agilent J&W DB-5MS (60m x 0.25mm x 0.25µm)	Secondary Column Agilent J&W DB-17ht (1m x 0.1mm x 0.1µm)
Primary oven temperature: Initial temp: 40°C (Hold 0.5min) Rate: 20°C/min Target temp: 90°C (Hold 0.5min) Rate: 2°C/min Final temp: 310°C (Hold 20min) Total run time 133.5 minutes	Secondary oven temperature: Initial temp: 45°C (Hold 0.5min) Rate: 18°C/min Target temp: 90°C (Hold 0.5min) Rate: 2°C/min Final temp: 310°C (Hold 20min) Total run time 133.5 minutes
Injector temp: 250°C	
Modulator offset: 50°C	
Transfer-line temp: 280°C	
Modulation period: 3.6 seconds	
MS Parameters: Electron ionization, Full scan (50-800amu) at 200 spectra/second	

GC-MS/MS method for the analysis of smoke exposure markers in urine.

Analysis was carried out on a Bruker CP-3800GC coupled to a Bruker 320MS triple quadrupole MS. Analysis was carried out on an Agilent J&W DB-17ht column (30 m x 0.25 mm x 0.15 µm). The injector was set to 250°C and operated in splitless mode. A 1 µL injection of the sample was made. The starting oven temperature was 40°C and increased to 300°C using a continuous gradient of 8°C/min. Temperature was held at

300°C for 2 min resulting in a total run time of 35 min. The MS was operated in multiple reaction monitoring (MRM) mode. The collision gas used was argon at a collision cell pressure of 1.5 torr. The MRM transitions for the target compounds are listed below. The target compounds were the trimethylsilyl derivatives of the listed compounds.

Compounds	MRM Transition	Collision Energy (V)
Methoxyphenols		
Syringol	226-->211	10
Methylsyringol	240-->210	10
Ethylsyringol	254-->239	10
Resin acids		
Abietic acid	256→241	10
Pimaric acid	374→257	15
Isopimaric acid	256→241	10
Oxodehydroabietic acid	268→253	10
Dehydroabietic acid	372→239	10
Sandaracopimaric acid	374→257	15
Hydroxy-PAHs		
1-OH Naphthalene	216-->201	10
2-OH Naphthalene	216-->201	10
9-OH Fluorene	254-->165	15
3-OH Fluorene	254-->165	15
2-OH Fluorene	254-->165	15
4-OH Phenanthrene	266-->235	25
3-OH Phenanthrene	266-->235	25
2-OH Phenanthrene	266-->235	25
3-OH Fluoranthene	290-->259	30
1-OH Pyrene	290-->259	30

Table S1. The metabolites of PAHs, methoxyphenols/derivatives, resin acids and selected novel compounds detected in the post-exposure urine of a single firefighter. Also provided are the concentrations of the compounds in the smoky air and the fold increase in post-exposure urine in comparison to the pre-exposure urinary level.

Compound Name	1D R.T	2D R.T	*Source of ID	**Concentration in Air (ug/m3)	***Fold increase in Urine
Polycyclic aromatic hydrocarbons					
Naphthalene	1489	1.24	A	139	10
Fluorene	2565	1.58	A	25	2
Phenanthrene	3548	1.72	A	70	5
Methoxyphenols and Derivatives					
Guaiacol	1568	1.05	A	548	4
Methylguaiacol	1885	1.08	A	480	1
Ethylguaiacol	2166	1.09	A	411	7
Syringol	2188	1.24	A	124	13
Syringylaldehyde	2191	0.94	A	877	8
Propylguaiacol	2364	1.09	A	134	1
4-Hydroxybenzoic Acid	2476	0.99	A	99	8
Methylsyringol	2479	1.22	A	510	19
4-hydroxyphenylethanol	2573	0.94	A	99	2
4-Hydroxyphenylpropanol	2674	0.96	L	299	2
Vanillin	2677	1.30	A	274	4
Ethylsyringol	2713	1.21	A	370	6
Eugenol	2792	1.15	A	62	9
Homovanillyl Alcohol	2886	1.06	A	76	2
Isoeugenol	2915	1.16	A	15	2
Acetovanillone	2958	1.32	A	106	13
Propylsyringol	2972	1.19	A	71	34
Guaiacyl Acetone	3019	1.35	A	145	2
3-Guaiacylpropanol	3581	1.08	L	221	4
cis/trans-Coniferyl Alcohol	3624	1.11	L	118	15
Coniferyl Aldehyde	3671	1.39	A	60	2
Homosyringyl Alcohol	3818	1.23	L	9	2
Sinapyl Aldehyde	3973	1.35	A	28	12
3-Syringylpropanol	3980	1.16	L	26	10

Table S1 (Continued)

Compound Name	1D R.T	2D R.T	*Source of ID	**Concentration in Air (ug/m ³)	***Fold increase in Urine
Resin Acids					
Abietic acid	4938	1.25	A	21	12
Pimaric acid	4978	1.25	A	8	67
Isopimaric acid	5017	1.28	A	23	85
oxodehydroabietic acid	5028	1.64	A	9	2
Dehydroabietic acid	5125	1.44	A	174	97
Sandaracopimaric acid	5212	1.35	A	33	13
Novel compounds	1D R.T	2D R.T	*Tentative ID	**Concentration in Air (ug/m ³)	***Fold increase in Urine
Compound 1	1885	0.95	Unknown	149	2
Compound 2	1900	0.92	Unknown	32	12
Compound 3	2137	1.08	C2 guaiacol	2	9
Compound 4	2324	1.14	Unknown	286	6
Compound 5	2396	0.97	Unknown	94	19
Compound 6	2422	1.08	C3 guaiacol	17	24
Compound 7	2443	1.12	Eugenol isomer	60	4
Compound 8	2455	1.08	C4 guaiacol 1	24	19
Compound 9	2560	1.09	C5 guaiacol-1	12	25
Compound 10	2570	1.09	C5 guaiacol-2	13	24
Compound 11	2585	1.09	C5 guaiacol-3	54	100
Compound 12	2796	1.22	Unknown	89	8
Compound 13	2879	1.25	Unknown	19	26
Compound 14	2944	1.10	Unknown	48	20
Compound 15	2962	1.24	Unknown	54	35
Compound 16	3257	1.29	Unknown	39	8
Compound 17	3581	1.15	Unknown	118	14
Compound 18	3944	1.14	Unknown	181	17
Compound 19	5269	1.47	Unknown	18	35
Compound 20	6878	1.78	Unknown	15	16

*Compound identification was carried out using authentic standards (A), NIST 2008 mass spectral library (L). Tentative identification of novel compounds was based on mass spectral interpretation based on similarity to known compound spectra.

**The air concentration of syringol was known from a previous study (Chapter 2) and was used to infer the concentrations of the other compounds based on peak areas from the TIC chromatogram.

***The fold increase in urine was based on peak areas between the pre-exposure urine and the post-exposure urine for the individual.

CHAPTER FOUR

Identification of the halogenated compounds resulting from the 1997 Plastimet Inc. fire in Hamilton, Ontario, using comprehensive two-dimensional gas chromatography and (ultra)high resolution mass spectrometry

Sujan Fernando¹, Karl J. Jobst*^{1,2}, Vince Y. Taguchi², Paul A. Helm²,
Eric J. Reiner^{2,3} and Brian E. McCarry¹

Published: *Environ. Sci. Technol.* 2014, 48, 10656-10663.

Author Affiliations:

¹McMaster University, 1280 Main Street West, Hamilton, ON, L8S 4M1

²Ministry of the Environment and Climate Change, 125 Resources Road, Toronto, ON, M9P 3V6

³University of Toronto, 80 St. George Street, Toronto, ON, M5S 3H6

Author contributions:

Manuscript prepared by Sujan Fernando with editorial comments provided by Karl J. Jobst and Brian E. McCarry. The sample was provided by Karl J. Jobst and Eric J. Reiner from the Ontario Ministry of the Environment. Sample extraction, cleanup and analysis by FT-ICR-MS and GCxGC-TOF-MS were carried out by Sujan Fernando along with data interpretation. Collaborative contributions from Vince Y. Taguchi, Paul A. Helm, and Eric J. Reiner were greatly appreciated.

ABSTRACT

Between July 9 – 12, 1997, at least 400 tonnes of polyvinyl chloride (PVC) were consumed in a fire at the Plastimet Inc. plastics recycling facility in Hamilton, Ontario, Canada. This led to the release of contaminants, including highly toxic polychlorinated dibenzo-p-dioxins (PCDD) and dibenzofurans (PCDF). This study re-examines a composite soil sample collected shortly after the fire using state-of-the-art FT-ICR (Fourier transform ion cyclotron resonance) and GC×GC-TOF (comprehensive two dimensional gas chromatography-time of flight) mass spectrometry. The FT-ICR experiments led to the identification of approximately 150 molecular formulae, corresponding to chlorinated and mixed chloro/bromo compounds. The majority of these are halogenated polycyclic aromatic hydrocarbons (halo-PAHs), including highly substituted (e.g. $C_{14}HCl_9$ and $C_{16}HCl_9$) and high molecular weight (e.g. $C_{28}H_{12}Cl_4$) Cl-PAHs that have not been reported previously in environmental samples. Complementary GC×GC-TOF experiments resolved individual halo-PAHs, some of which were confirmed with available standards. The concentrations of the most abundant halo-PAH groups, $C_{14}H_8Cl_2$ (22 $\mu\text{g/g}$) and $C_{16}H_8Cl_2$ (20 $\mu\text{g/g}$) are much higher than reported dioxin values and comparable to the corresponding PAH groups $C_{14}H_{10}$ (12 $\mu\text{g/g}$) and $C_{16}H_{10}$ (19 $\mu\text{g/g}$). The high abundance of the halo-PAHs identified in this study highlights the need for further investigation into their environmental occurrence and risk.

INTRODUCTION

The Plastimet Inc. fire in Hamilton, Ontario, Canada is recognized as one of the largest industrial fires in North America. The fire began at approximately 7:45pm on July 9th, 1997 at the Plastimet Inc. plastics recycling facility. During the course of the following three days, at least 400 tonnes of polyvinyl chloride (PVC) and polyurethane plastics were consumed. There was, understandably, significant concern among local residents and health officials regarding the nature and concentrations of chemical compounds released to the air, surrounding lands, vegetation and harbour ^{1,2}.

Fires involving the combustion of PVC and other plastics materials can pose a risk to human health and the environment, in part due to the toxic chemical compounds that are generated therefrom ³. Hydrogen chloride released to the air peaked at 930 $\mu\text{g}/\text{m}^3$ during the Plastimet fire, and it was the probable cause of most acute health effects reported during the incident¹. Combustion of PVC also generates polychlorinated dibenzodioxins (PCDD) and polychlorinated dibenzofurans (PCDF) ³, whose long-term health effects and environmental impact are sources of considerable debate and concern ^{4,5}.

In an effort to assess the risk and extent of exposure, samples of air, water, soil, soot and vegetation were collected from the Plastimet Inc. site, and surrounding areas by the Ontario Ministry of the Environment. These samples were subjected to targeted analytical tests for dioxin as well as a range of (volatile) organic and inorganic chemical analyses ¹. Professor Brian McCarry (McMaster University) was also at the scene, only 100 m east of the blaze, where he set up an air monitoring station ². A sample collected from this vantage point during July 11th holds the distinction of containing over 1000 pg/m^3 TEQ

(Toxic Equivalent Quantity) of dioxin, the highest concentration measured during the incident. This was estimated to exceed background levels by 2,500 – 25,000 fold. Elevated concentrations of dioxin were also observed in soil and undiluted runoff close to the site ¹.

Since the late 1970s, high resolution mass spectrometry, hyphenated with gas chromatography (GC-HRMS), has served as the workhorse for the trace analysis of dioxin and related persistent organic pollutants (POPs)⁶. In the years following the Plastimet fire, mass resolution, chromatographic resolution, and therefore the potential number of compounds identified in a single analysis, has increased dramatically. The study of Taguchi et al. ⁷, which employed a custom-built Fourier transform ion cyclotron resonance (FT-ICR) mass spectrometer, serves as a case in point. Aside from the dioxin and furan ions of interest, a range of chlorinated polycyclic aromatic hydrocarbons were also tentatively identified from a single mass spectrum. Visualization of the mass spectral information in the form of a mass defect plot ^{7,8,9} eased the interpretation.

Mass spectrometry is a powerful tool for structure analysis ^{10,11} but isobaric species and structural isomers are usually only distinguishable chromatographically. Separation is important because isomers can exhibit varying toxicities. A prime example is the 2,3,7,8-chlorine substituted dibenzo-p-dioxin, the corresponding dibenzofuran, as well as 15 other congeners that exhibit markedly higher toxicity than the remaining family of ~200 congeners^{4,5}. A recent study by Myers et al.¹² underlines the importance of chromatography for the analysis of dioxin and related compounds. Using tandem mass spectrometry, a suite of mixed bromo/chloro dioxins and furans (PXDD/Fs) were

measured in soil contaminated by the Plastimet fire. The inclusion of bromine, whose source may well have been the ubiquitous brominated flame retardants, increases the number of potential PXDD/F congeners to c. 5000. Total congener class concentrations of the PXDD/Fs were significant, between 6% and 10% of the corresponding chlorinated compounds. However, individual congeners could not be resolved using standard capillary GC.

Comprehensive two dimensional gas chromatography (GC×GC) offers greatly enhanced peak capacity compared to traditional capillary GC experiments¹³, and whose benefits are recently demonstrated for the analysis of PXDD/Fs¹⁴. GC×GC has also been coupled to high resolution time-of-flight (HRTOF) mass spectrometry^{15,16,17,18,19}. Enhanced mass resolution can mitigate the effects of matrix interferences and significantly improve the confidence of target compound identification. Perhaps more interestingly, such experiments can also facilitate the identification of unknown compounds. The pioneering studies of Hashimoto and Zushi et al. have recently developed and employed strategies to selectively identify organohalogen contaminants in environmental and biological samples using GC×GC-HRTOF^{17,18,19}.

Taguchi et al.⁷ and Myers et al.¹² were the first to identify organic contaminants in a Plastimet derived sample outside of the legacy contaminants reported by Socha et al.¹. The present study reports on the analysis of a composite of soil samples from the site of the Plastimet Inc. fire using state-of-the-art FT-ICR mass spectrometry as well as GC×GC coupled to TOF and HRTOF mass spectrometry. Using these complementary experimental techniques, the range of halogenated organic compounds in the mixture are

characterized and, where analytical standards are available, determined semi-quantitatively.

EXPERIMENTAL

Chemicals and Sample Preparation

The PAH standards (Table 1) were purchased from Chiron AS (Norway). The halogenated PAHs (Table 1) were purchased from Sigma-Aldrich (Canada & USA). Naphthalene-d₈ (98%), phenanthrene-d₁₀ (98%), pyrene-d₁₀ (98%), chrysene-d₁₂ (98%) and benzo[*ghi*]perylene-d₁₂ (98%) were purchased from Cambridge Isotope Laboratories (USA). Dichloromethane (distilled-in-glass), water (HPLC), hexane (HPLC), toluene (HPLC) and hydrochloric acid (Reagent, 37% wt) were purchased from Caledon (Canada). Alumina (activated, 80-200 Mesh) was purchased from Anachemia Canada Inc. (Montreal, QC).

Soil samples contaminated by fly ash were collected from the site of a fire that took place in Hamilton, Ontario, Canada at a plastic recycling plant (Plastimet Inc.) in 1997¹. The composite sample (16 g) was grounded to a fine powder using a mortar and pestle. The samples was divided into two 8 g portions and extracted separately. Samples were extracted using dichloromethane (DCM) in an Accelerated Solvent Extractor (ASE 350, Dionex). Prior to extraction 1 µg of naphthalene-d₈, phenanthrene-d₁₀, chrysene-d₁₂ and benzo[*ghi*]perylene-d₁₂ were added to the samples to serve as recovery standards. 1 mL of hexane was added to the resulting DCM extract, which was then concentrated using a rotary evaporator to the 1 mL level. The extract (now in hexane) was loaded onto an

activated alumina column. 20g of alumina was mixed with 200mL of water to form a slurry. The slurry was adjusted to pH 3 using concentrated HCl (37% wt) while stirring with a magnetic stir bar. The water was then decanted and the alumina was dried in an oven at 200°C for 72hrs. The alumina was then packed into a column for use. The aliphatic compounds were first eluted by flushing the column with 100 mL of hexane. The aromatic compounds were then eluted with 200 mL of DCM. 1 mL of toluene was added to the DCM fraction and the sample concentrated to 1 mL. A 150 μ L aliquot of this sample was concentrated to 15 μ L to which was added 5 μ L of pyrene-d₁₀ (4ng/ μ L) to serve as an injection standard. 3 μ L of the sample was introduced to the FTICR using a direct insertion probe (DIP). The injection volume was 1 μ L for the GC \times GC-TOF and GC \times GC-HRTOF experiments.

Instrumental analysis

FTICR experiments were performed using a Varian TQ-FTICR (triple quadrupole-Fourier transform mass spectrometer) consisting of a Varian CP-8400 autosampler, a Varian CP-3800 GC, a Varian 920-MS and a Varian 9.4 Tesla superconducting magnet. The FTMS system was operated in the EI mode (70 eV) at a mass resolution of 80,000 full width half maximum (FWHM) at m/z 400. The ion source was held at 250°C. Mass spectra were obtained using arbitrary waveform excitation and detection from m/z 150 – 650. External mass calibration was obtained using perfluorotributylamine (PFTBA). Each mass spectrum was internally calibrated using a background phthalate ion at m/z 419.3156. Elemental compositions were obtained from measured m/z values using a software package developed by Varian Inc.

GC×GC-HRTOF experiments were performed using a Waters GCT time-of-flight instrument modified with a Zoex ZX2 loop modulator. The GCT was operated in the EI mode at a mass resolution of 7000 FWHM. The GC was equipped with a 15 m DB-5HT primary column (0.25 mm i.d., 0.10 µm film thickness; J&W Scientific, USA) coupled to a 2.3 m Rtx-50 secondary column (0.18 i.d., 0.18 µm film thickness; Restek Corporation, USA). The modulation period and hot pulse duration were 4s and 400ms respectively. The source was held at 250°C. The injector was held at 280°C and the oven temperature program was 120°C for 1 min, ramp to 330°C at 3 °C/min, and hold for 10 min. The secondary column was installed in the main oven and the temperature of the hot pulse (400ms in duration) was held at a +20°C offset to the GC oven.

GC×GC-TOF experiments were also performed for identification and quantification purposes. The instrument used was a LECO Pegasus 4D system. The TOF was operated in EI mode at an acquisition rate of 200 spectra/second. The source was held at 200°C and the injector was held at 280°C. The GC×GC was configured with a 30m DB-17ht primary column (0.25 mm i.d., 0.15 µm film thickness; J&W Scientific, USA) coupled to a 1m DB-5MS secondary column (0.1 mm i.d., 0.1 µm film thickness; J&W Scientific, USA). The primary oven temperature was set to 50°C initially, ramped to 300 °C at 6°C/min and held for 35 mins. A 10°C offset was used for the secondary oven temperature. A modulation period of 5s was used.

The identification of targeted PAH and halogenated PAH (halo-PAH) compounds were based upon GC×GC-TOF experiments using the following criteria: (i) GC×GC retention

times match those of available standards within ± 0.1 min in the 1st dimension and ± 0.1 sec in the 2nd dimension; (ii) target peaks have signal-to-noise ratios of at least 10:1; (iii) Molecular ion isotope ratios are within 15% of theoretical values.

QA/QC

Isotopically labelled halo-PAH standards were not available at the time samples were analyzed. Matrix spike tests using clean Ottawa Sand ($n = 3$) were performed to evaluate if the target compounds were extracted, cleaned, and fractionated quantitatively. Mean recoveries of the PAH and halo-PAH standards were between 60-94%. Surrogates added to the samples prior to extraction and clean-up yielded mean recoveries of 60% for naphthalene-d₈, 76% for phenanthrene-d₁₀, 87% for chrysene-d₁₂ and 110% for benzo[ghi]perylene-d₁₂. The data presented is the average of the 2 extracted samples, which are within 20% of one another.

Data Processing

Raw FT-ICR data was processed using Omega (v. 9.2.3), and peaks lists (using signal:noise threshold 3:1) were exported to Microsoft Excel. FT-ICR mass spectra (Figure 1) were visualized by constructing Kendrick mass defect plots²⁰ using the H/Cl mass scale prescribed for the identification of polychlorinated compounds^{7,21}. Each mass spectral peak, normally measured using the mass scale defined by IUPAC (International Union of Pure and Applied Chemistry), is converted using Equation 1:

$$(1) \text{ H/Cl mass} = \text{IUPAC mass} \times 34 / 33.96102$$

The plot is constructed by graphing the nominal mass of each mass spectral peak (x-axis) against the corresponding mass defect (MD). For example, the IUPAC masses of tetrachloro, pentachloro and hexachlorodibenzofuran are 303.901, 337.862 and 371.823, respectively. The corresponding H/Cl masses are 304.250, 338.250 and 372.250, which are displayed as coordinates (x=304, y=0.250), (x=338, y=0.250) and (x=372, y=0.250), in the MD plot of Figure 2.

GC×GC-TOF and GC×GC-HRTOF data were visualized using the ChromaTOF (Version 4.50, LECO Corporation) and GCImage (Version R2.3, Zoex Corporation) suites of programs.

RESULTS & DISCUSSION

Characterization of the halogenated compounds using FT-ICR

The introduction of the composite soil sample extract to the FT-ICR using a direct insertion probe (DIP) gave rise to more than 3000 peaks in the resulting mass spectrum (Figure 1a). The ultrahigh mass resolution of the FT-ICR is highlighted in Figure 1b: fourteen peaks sharing the same nominal mass-to-charge ratio (m/z) of 320 are resolved. The task of screening target compounds among the great many introduced to the spectrometer is relatively straight forward: the peak at m/z 319.8976 (Figure 1b) and associated ^{37}Cl isotope peaks (not shown) corresponds to the elemental composition of

tetrachlorodibenzo-p-dioxin. On the other hand, the interpretation of the remaining peaks is much more challenging.

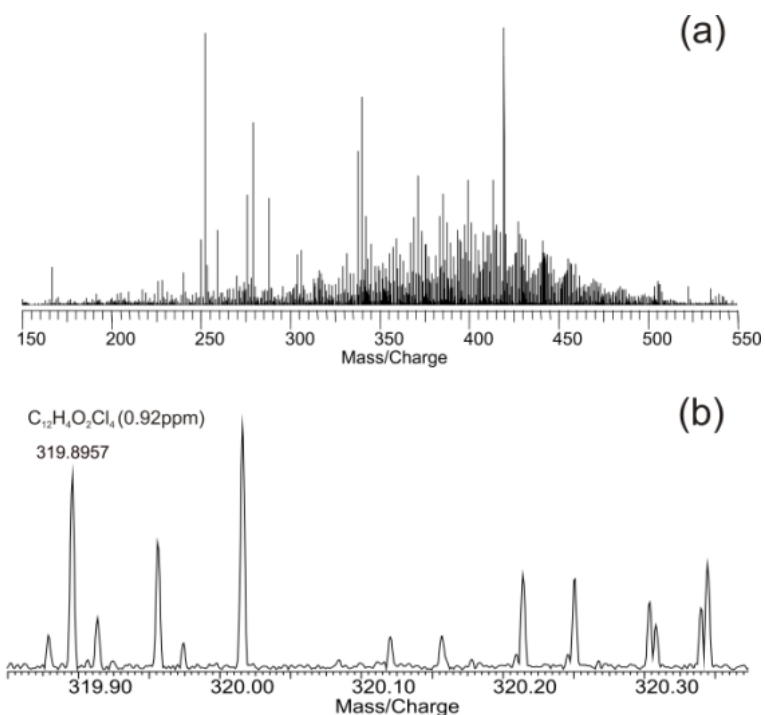


Figure 1. (a) FT-ICR mass spectrum obtained from an extract of the composite soil sample; (b) Expanded view of the m/z 320 region of the spectrum.

A convenient way to visualize the complex mass spectrum of Figure 1 is to construct a MD plot (Figure 2). In the MD plot, clusters of ions along the x-axis for a given series are indicative of congeneric species differing by H/Cl substitution. In this case each cluster is separated by 34Da increments. Each cluster consists of isotopic peaks separated by 1.997Da which corresponds to the exact mass difference between ^{35}Cl and ^{37}Cl . Once a series of compounds has been identified in the MD plot, the exact masses and isotope ratios can be used to derive elemental compositions from which structure proposals can be made. Possible structures are displayed in Figure 2a along with the corresponding

formulae. The ions observed in the mass spectrum correspond to both the molecular ions as well as fragments and this point is discussed further below.

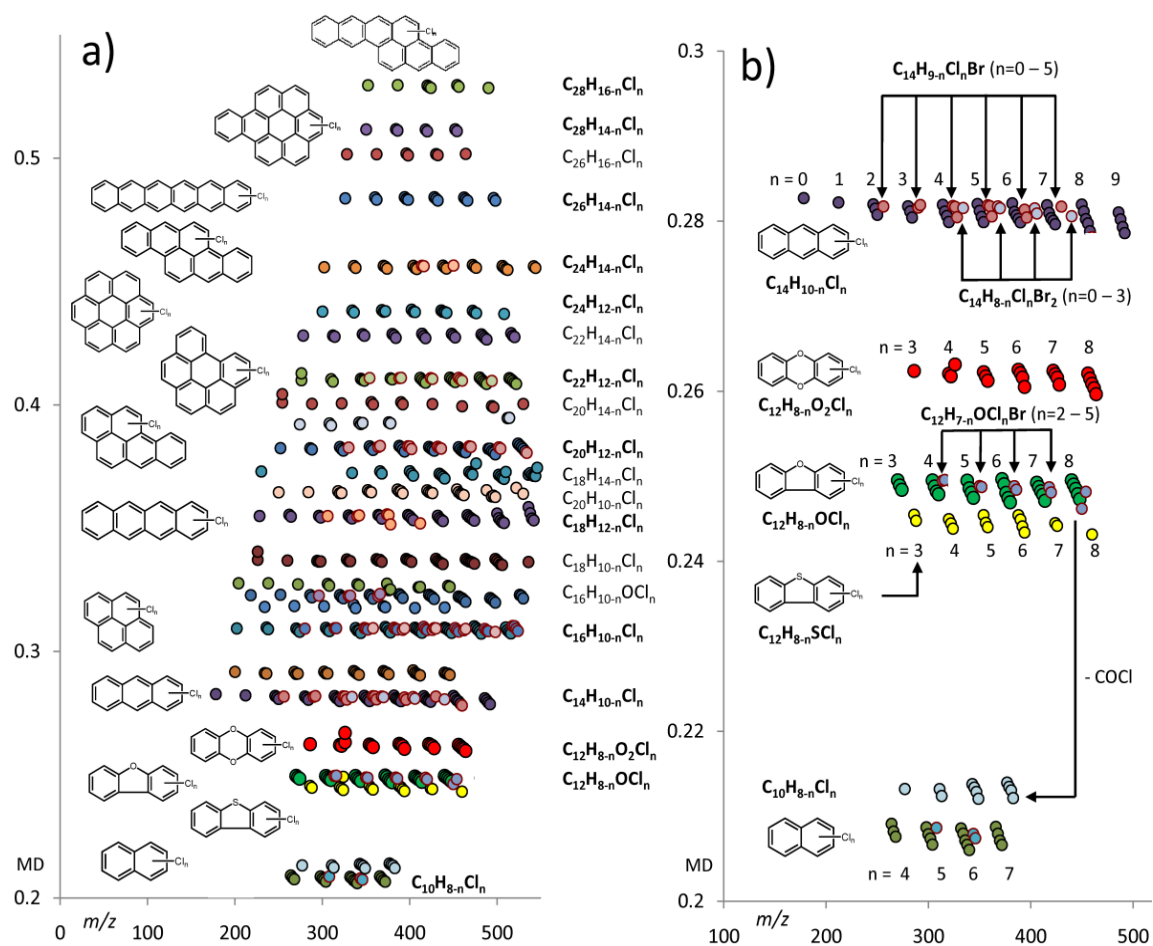


Figure 2. (a) Mass defect plot constructed from the FT-ICR mass spectrum of the soil extract. The structures (left) are tentatively proposed from accurate mass derived elemental compositions (right); (b) Expanded view of the plot focusing on the MD scale between 0.2 and 0.3.

Figure 2b is an expanded view focusing on the MD scale between 0.2 and 0.3. The series of markers across the x-axis at MD of 0.28 begins with a marker at m/z 178.0783, which was assigned a molecular formula of $C_{14}H_{10}^{\bullet+}$. This was determined by an elemental composition calculator with a mass accuracy of 3ppm compared to the theoretical value.

$C_{14}H_{10}$ most likely corresponds to structural isomers anthracene and/or phenanthrene (ANT/PHE), which are two common PAHs found in nature. The next marker along the x-axis at the same MD has an m/z of 212.0388. This corresponds to a mass difference of 33.9605 which is the exact mass difference of H/Cl substitution, and was therefore assigned as a monochlorinated ANT/PHE. This approach led to the identification of ANT/PHE congeners from Cl_1 to Cl_9 substitutions ($C_{14}H_9Cl_1$ to $C_{14}H_1Cl_9$). Along with the chlorinated series, mixed bromo/chloro ANT/PHE congeners are also observed: A series of chlorine substituted monobromo and dibromo analogues were identified ranging from $C_{14}H_8Br_1Cl_1$ to $C_{14}H_4Br_1Cl_5$ and $C_{14}H_7Br_2Cl_1$ to $C_{14}H_5Br_2Cl_3$.

Figure 2b displays series of markers at MD values 0.26, 0.25, 0.24 and 0.21, whose assigned compositions point the presence of PCDDs, PCDFs, polychlorinated dibenzothiophenes and polychlorinated naphthalenes (PCNs). These compounds exhibit intense molecular ions under EI conditions, but a number of fragments are also observed. In Figure 2b, the series at MD 0.21 corresponds to the structure diagnostic loss of a COCl group from the chlorinated dibenzofurans.

Halo-PAHs were detected for parent compounds from mass 128Da ($C_{10}H_8$) to 352Da ($C_{28}H_{16}$). Highly chlorinated species were detected up to Cl_9 for PAHs from 178Da ($C_{14}H_1Cl_9$) up to 228Da ($C_{18}H_3Cl_9$). Also, Cl_8 substituted species were detected up to the 252Da PAHs ($C_{20}H_4Cl_8$) and Cl_7 substituted species were detected up to the 302Da PAHs ($C_{24}H_7Cl_7$). The largest chlorinated PAH (Cl-PAH) detected was a Cl_4 species belonging to the 352Da group ($C_{28}H_{12}Cl_4$). In all 106 chlorinated molecular formulae were detected. Halo-PAHs are of interest because a number of the compounds are known to

exhibit carcinogenic and mutagenic properties^{22,23,24}, but relatively few studies have appeared on their analysis, in part due to the lack of authentic standards. Certain Cl-PAHs are reported to have other toxic effects, such as tumorigenicity and oncogene activation as reviewed by Fu et al.²⁴

In addition, 37 mixed halogenated (Br/Cl) molecular formulae were also detected for this group of PAHs. These included Br/Cl-naphthalenes, ANT/PHE and fluoranthenes/pyrenes (FLU/PYR). The largest mixed halogenated compositions detected were $C_{22}H_7Br_1Cl_4$ and $C_{24}H_{11}Br_1Cl_2$. Mixed halogenated compounds are of particular interest because they may be more toxic than the chlorinated versions⁵ and the large number of potential congeners poses a significant analytical challenge. Two groups of chlorinated sulfur containing PAHs (PASH) were also detected in the sample. These are tentatively proposed to be chlorinated dibenzothiophenes ranging from Cl_3 to Cl_8 ($C_{12}H_5S_1Cl_3$ to $C_{12}S_1Cl_8$) and chlorinated benzonaphthothiophenes ranging from Cl_1 to Cl_6 ($C_{16}H_9S_1Cl_1$ to $C_{16}H_4S_1Cl_6$).

Halo-PAHs have been detected in various environmental matrices, including fly ash²⁵ urban air²⁶, automobile exhaust²⁷, kraft pulp mill wastes²⁸ and sediment^{29,30}. Halo-PAHs have also been detected in various foods including rice, vegetables and meats^{23,31}. These studies were limited to a suite of selected mono- and di-halogenated compounds with available standards. Ieda et al.¹⁵ recently applied GC×GC-HRTOF for the non-targeted analysis of soil contaminated by a former chlor-alkali plant and observed highly substituted Cl-PAHs with molecular formulas $C_{14}H_{10-n}Cl_n$ and $C_{16}H_{10-n}Cl_n$ ($n = 0 - 7$). The composite soil sample of the present study contains both highly chlorinated and high

molecular weight halo-PAH compounds. The observation of the extensive range of halo-PAH compounds shown in Figure 2 is facilitated by the DIP and ultrahigh resolution MS techniques used in this study.

Isomer separation and structure analysis using GC×GC-HRTOF

The high mass resolution and accuracy of the FT-ICR experiments enabled the tentative identification of a large number of halo-PAH classes, but separation of isomers can only be achieved by chromatography. Such an analysis is ideally performed using a GC×GC-HRTOF instrument. Although GC×GC chromatograms are structured, the task of identifying the many unknown compounds is not trivial. Figure 3a displays the total ion chromatogram of the soil extract, and it is seen that there is separation of compounds in the two dimensional space. However, the interpretation of this data remains a challenge because of the sheer number of compounds, the majority of which do not match with library mass spectra. The ability to extract out the ions of interest using the FT-ICR formula assignments as a guide, makes the interpretation more practical.

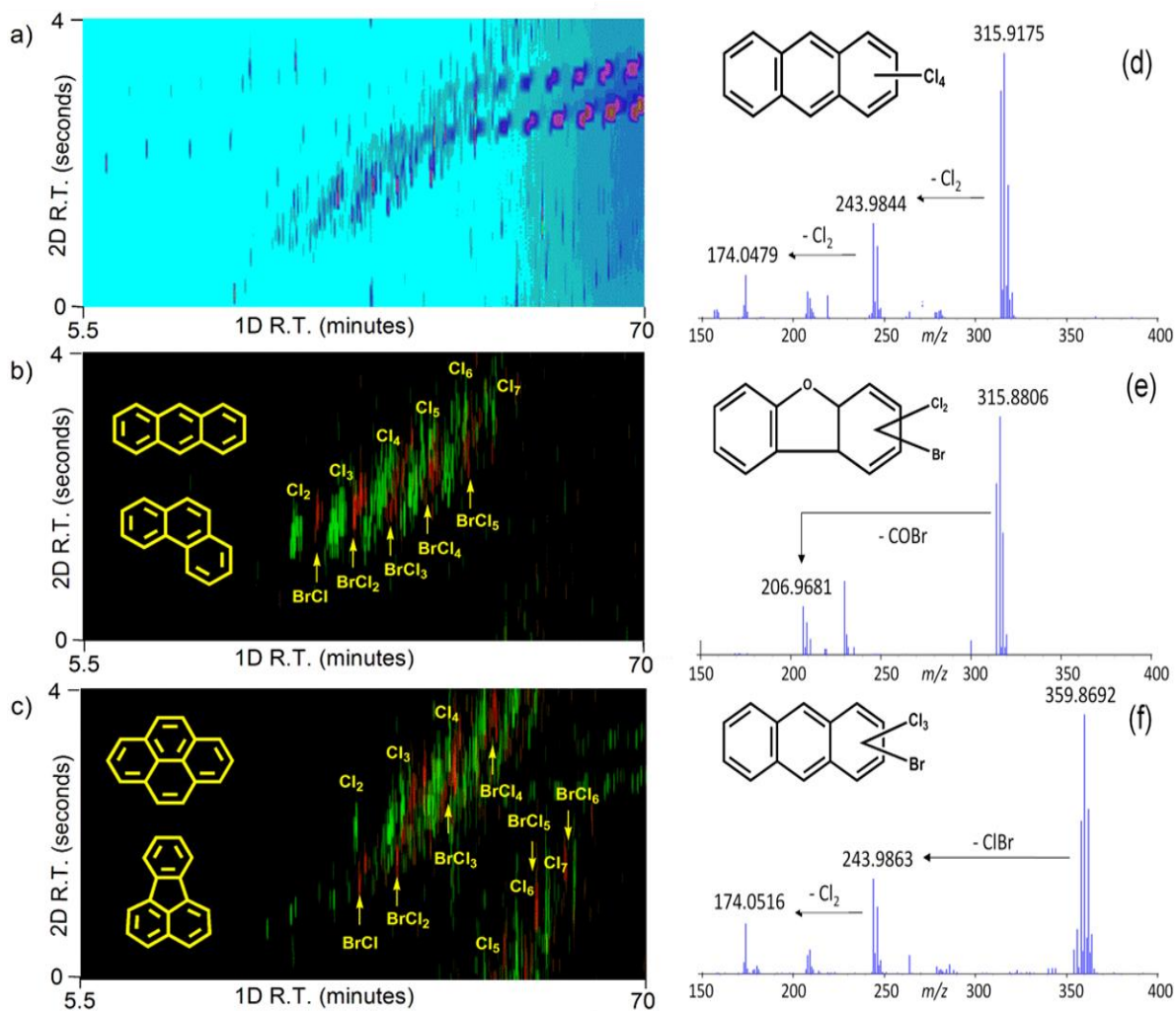


Figure 3. LEFT (a) Total ion and (b-c) Extracted ion chromatograms of the molecular ions of the (mixed) halogenated ANT/PHE and FLU/PYR isomers from GCxGC-HRTOF analysis. RIGHT : Mass spectra with (d) $C_{14}H_6Cl_4^{*+}$ molecular ions; (e) $C_{12}H_5OCl_2Br^{*+}$; and (f) $C_{14}H_6Cl_3Br^{*+}$. The structures are tentatively proposed on the basis of exact mass measurements and EI dissociation behaviour.

Figures 3b and 3c display extracted ion chromatograms corresponding to the Cl and Br/Cl congeners of ANT/PHE (Cl₂ to Cl₇) and FLU/PYR groups (Cl₂ to Cl₇). In both cases, the Cl and mixed Br/Cl congeners appear as bands of peaks across the two-dimensional plane. Further support of the structure proposals is provided by chromatographically resolved mass spectra. Figure 3d and 3e shows the mass spectra of a tetrachloro-

ANT/PHE isomer and that of a bromotrifluoro-dibenzofuran isomer respectively. The molecular ions for both species have the same nominal mass (316 Da) and yet, the two species were separated by GC×GC. The mass resolution necessary to distinguish ions $C_{14}H_6Cl_4$ (m/z 313.9128) and $C_{12}H_5Cl_2BrO$ (m/z 313.8895) by MS alone is greater than 10 000 FWHM. The two species are also differentiated by their characteristic dissociation behaviour. The Cl-PAH undergoes consecutive losses of Cl_2 , whereas the dibenzofuran dissociates by structure diagnostic loss of COBr. The mass spectrum of Figure 3f corresponds to one of the $C_{14}H_6Cl_3Br$ (m/z 357.8718) peaks in the mass chromatogram of Figure 3b. There is no satisfactory match with a library mass spectrum, but the formula assignment and structure proposal is supported by accurate mass measurement, isotope ratios and fragmentation: the molecular ion undergoes losses of ClBr and Cl_2 .

Based upon the above approach, it was possible to obtain the EI mass spectra for many of compounds proposed in Figure 2. Chromatographic separation also enabled the differentiation of isomeric structures, whose mass spectra are virtually identical. Ultimately, confirmation of the identities of individual chromatographic peaks necessitates experiments with additional analytical standards, which are not (yet) available.

Determination of the (relative) levels of halogenated PAH using GC×GC-TOF

A limitation of the GC×GC-HRTOF instrument used in the current study is its slow scan speed (10 spectra/second) and dynamic range. As a result, the peak shapes were not well defined, which introduces considerable uncertainty in quantitative measurements. Therefore, a GC×GC-TOF of nominal mass resolution, but capable of a scan rate of 200

spectra/second, was used instead. A disadvantage of a nominal mass analyzer is the increase in chemical noise. However, this was compensated by the enhanced separation afforded by GC×GC. The identification and quantification of 1,3,6,8-tetrachloropyrene (Figure S1) would have been difficult if not for the chromatographic resolution.

A total of 25 PAHs and halo-PAHs (Table 1) were identified and quantified using authentic standards. (Response factors were measured relative to the injection standard pyrene-d₁₀, and concentrations quoted in Table 1 are not corrected for recoveries, which ranged from 60 – 94%, see Experimental). In addition, a larger suite of halo-PAHs and isomers were detected in the sample for which standards are not available. These compounds were tentatively identified based on the degree of chlorination (tetrachloropyrene, pentachloropyrene, etc). The concentrations of these compounds were also estimated using the average response factor (1.05) of structurally related authentic standards, see Supporting Information Table S1.

Table 1. Concentration of PAH and corresponding halo-PAHs identified in the soil sample.

PAHs Identified	MW (Da)	PAH Conc. (µg/g)	Target HaloPAHs Identified	Target HaloPAH Conc. (µg/g)	Non-target HaloPAHs Identified	# of Congeners Detected		Total PAH Conc. (µg/g)	Total HaloPAH Conc. (µg/g)
						TO F	HRTO F		
Naphthalene	128	11	1,2,3,4-Cl ₄	1	X = Cl ₃ -Cl ₆	18	22	11	42
Phenanthrene Anthracene	178	9 3	1,4-Cl ₂ -Anth 1,5-Cl ₂ -Anth 2,3-Cl ₂ -Anth 9-Br-Anth 9-Br-Phen	0.7 22 20 ND 2	X = Cl ₁ -Cl ₅ X = Br-BrCl	17 5	47 4	12	73 5
Fluoranthene Pyrene	202	11 8	1,3,6,8-Cl ₄ -Pyr	4	X = Cl ₁ -Cl ₅ X = Br-BrCl	11 2	50 0	19	63 9
Phenylnaphthalene	204	9	-	-	X = Cl ₁ -Cl ₂	2	0	9	4
Benzo[c]phenanthrene, Benz[a]anthracene, Chrysene	228	0.5 6 5	-	-	X = Cl ₁ -Cl ₄	6	0	12	14
Benzo[b]fluoranthene Benzo[k]fluoranthene Benzo[a]pyrene	252	5 2 1	-	-	X = Cl ₁ -Cl ₂	10	2	8	3
Indeno[1,2,3-cd]pyrene	276	0.5	-	-	X = Cl ₁	2	ND	0.5	0.1
Dibenz[a,h]anthracene	278	0.5	-	-	ND	ND	ND	0.5	ND
Coronene	300	0.2	-	-	ND	ND	ND	0.2	ND

Halo-PAHs were detected for parent compounds from mass 128 Da ($C_{10}H_8$) to 276 Da ($C_{22}H_{12}$) using the GC×GC-TOF. Among the PAHs naphthalene (MW 128 Da) had the highest degree of chlorination (up to Cl_6). The heaviest halo-PAH identified was a $C_{22}H_{11}Cl_1$ species. Many highly chlorinated and high molecular weight halo-PAHs (278-352 Da) detected by the FT-ICR probe analysis were not observed using GC×GC-TOF. It is likely that these compounds do not elute from the columns used in the GC×GC experiments or were below the detection limit of the instrument. Of the halo-PAHs detected, the ANT/PHE group contained the most halogenated congeners (a total of 22). The number of halogenated congeners identified for this group using the HRTOF was 51, which may be explained by the significantly reduced chemical noise in high resolution mass chromatograms.

Among the PAHs quantified, the concentrations of naphthalene, phenanthrene, fluoranthene and pyrene were the highest ranging from 9 to 11 $\mu\text{g/g}$. Even higher concentrations were observed for the halo-PAHs : 1,5 and 2,3-dichloroanthracene concentrations were 22 and 20 $\mu\text{g/g}$ respectively.

Halogenated congeners of ANT/PHE and FLU/PYR groups yielded the highest total concentrations at 78 and 71 $\mu\text{g/g}$ of ash respectively. This may be significant because Cl -PAHs with three or more fused aromatic rings have been shown to be toxic^{24,30}, the halogenated derivatives of 3-ring PAHs such as ANT/PHE exhibit increasing aryl hydrocarbon receptor (AhR)-mediated activity with increasing chlorine substitution²⁵. Chlorinated ANT/PHE congeners were detected up to Cl_5 in the GC×GC-TOF analysis and up to Cl_9 in the FT-ICR analysis.

In an experiment performed by Wang et al, PVC was combusted in a laboratory scale tube-type furnace and the resulting PAHs and halo-PAHs were monitored^{32,33}. The results showed that mostly monochlorinated derivatives were observed for parent PAHs in the range of 128 to 202 Da. Further, the amount of halogenated derivatives was significantly lower than the corresponding PAHs : the ratio of halo-PAHs/PAHs for the ANT/PHE and FLU/PYR groups were below 0.004. In ash samples obtained from the Plastimet fire, the same ratio is approximately 5:1.

Wang et al. also observed that the levels of both PAHs and halo-PAHs increased with increasing furnace temperature, but the halo-PAHs/PAHs ratios were similar throughout the experiment³³. It has been proposed that PAHs as well as halo-PAHs are formed from the combustion of PVC: incomplete combustion of PVC yields PAHs, which are in turn chlorinated by the HCl that is released from the PVC³³. The HCl levels¹ in the air near the vicinity of the fire were as high as 930 $\mu\text{g}/\text{m}^3$. This value was approximately 450 fold higher than the background levels in the same area measured a few weeks after the fire was extinguished. The high HCl concentrations combined with the PAH concentrations (up to 5000 ng/m^3 , a value 2000 times greater than typical urban background²), provided favourable conditions for the formation of the wide range of halo-PAHs identified in the soil sample.

Halogenated dioxin/furan analysis of the same sample previously have shown that the most prevalent mixed halogenated compounds detected were from the monobromo-hexachlorodibenzo-p-dioxin and monobromo-pentachlorodibenzo-p-dioxin groups at concentrations of 47 ng/g and 41 ng/g respectively¹². The most abundant mixed halo-PAH detected in the current analysis was a monochloro-monobromo-FLU/PYR at a

concentration of 4 $\mu\text{g/g}$ (Supporting Information, Table S1). This level is approximately 100 fold higher than the most abundant Cl/Br dioxins quantified. Although the absolute concentrations of the Br/Cl PAHs were significantly higher than the corresponding PXDD/Fs, the total concentrations of the mixed Br/Cl PAHs were between 6% and 13% of the chlorinated PAHs, a value very similar to the corresponding Br/Cl dioxins and furans. It is suspected that the source of bromine was most likely flame retardants present in the plastics and polyurethane foam.

The toxicity of combustion by-products resulting from fires and subsequent residues in the surrounding environment are of concern to first responders and neighboring citizens. Benzo[a]pyrene (BaP) is regarded as one of the more toxic PAH compounds of its class, but its potency is only a fraction of that of 2,3,7,8-TCDD³⁴. Nevertheless, its high concentration in the sample (0.9 $\mu\text{g/g}$) indicates a toxic equivalency quantity (TEQ) in the soil sample that is significantly higher than that for the PCDDs/Fs determined previously¹. In an early study, Poland et al.²² remarked that while both PAHs and halogenated aromatic hydrocarbons induce AhR activity, the characteristic spectrum of toxic responses are only observed with halogenated compounds. Recent studies have shown that 3,8-dichlorofluoranthene and 6-chlorochrysene exhibit AhR activities that are 2 and 5.7 times greater than that of BaP in the YCM3 cell assay system²⁵. Many of the halo-PAHs resulting from the Plastimet fire, especially the 3-4 ring compounds (ANT/PHE and FLU/PYR), were present at concentrations substantially higher than that of BaP. The high abundance of the halo-PAHs identified in this study, and indications of their bioaccumulation potential^{21,35}, highlights the need for further investigations of their environmental occurrence and risk.

References

1. Socha, A., Abernethy, S., Birmingham, B. Plastimet Inc. Fire. Ontario Ministry of the Environment, October. 1997.
2. McCarry, B.E. McMaster Chemical Extracts. vol. 1, September, 1998.
3. Hutzinger O, Choudhry GG, Chittim BG, Johnston LE. Formation of polychlorinated dibenzofurans and dioxins during combustion, electrical equipment fires and PCB incineration. *Environ Health Perspect.* 1985;60:3–9.
4. Van den Berg M, Birnbaum LS, Denison M, De Vito M. The 2005 World Health Organization reevaluation of human and Mammalian toxic equivalency factors for dioxins and dioxin-like compounds. *Toxicol Sci.* 2006;93(2):223–41.
5. Van den Berg M, Denison MS, Birnbaum LS. Polybrominated dibenzo-p-dioxins, dibenzofurans, and biphenyls: inclusion in the toxicity equivalency factor concept for dioxin-like compounds. *Toxicol Sci.* 2013;133(2):197–208.
6. Reiner EJ, Clement RE, Okey AB, Marvin CH. Advances in analytical techniques for polychlorinated dibenzo-p-dioxins, polychlorinated dibenzofurans and dioxin-like PCBs. *Anal Bioanal Chem.* 2006;386(4):791–806.
7. Taguchi VY, Nieckarz RJ, Clement RE, Krolik S, Williams R. Dioxin analysis by gas chromatography-Fourier transform ion cyclotron resonance mass spectrometry (GC-FTICRMS). *J Am Soc Mass Spectrom.* 2010;21(11):1918–21.
8. Hughey CA, Hendrickson CL, Rodgers RP, Marshall AG, Qian K. Kendrick mass defect spectrum: a compact visual analysis for ultrahigh-resolution broadband mass spectra. *Anal Chem.* 2001;73(19):4676–81.
9. Sleno L. The use of mass defect in modern mass spectrometry. *J Mass Spectrom.* 2012;47(2):226–36.
10. McLafferty, F.W., Tureek, F. *Interpretation of Mass Spectra*; University Science Books, Sausalito, CA, 1993.
11. Lebedev, A, Editor. *Comprehensive Environmental Mass Spectrometry*. ILM Publications, Hertfordshire, U.K., 2012.
12. Myers AL, Mabury SA, Reiner EJ. Analysis of mixed halogenated dibenzo-p-dioxins and dibenzofurans (PXDD/PXDFs) in soil by gas chromatography tandem mass spectrometry
13. Ramos, L, Editor. *Comprehensive Analytical Chemistry*. Elsevier, Oxford, U.K., 2009.
14. Dorman, F., Organtini, K., Myers, Anne., Jobst, K., Reiner, E., Cochran., J., Ladak., A., Stevens, D. Comprehensive Characterization of Mixed-Halogen Dioxins and Furans Generated in Fire Debris Using GC×GC-TOFMS and APGC-

TQS. Proceedings from the 62nd ASMS Conference on Mass Spectrometry and Allied Topics. Baltimore, June 15-19, 2014. (www.asms.org)

15. Ieda T, Ochiai N, Miyawaki T, Ohura T, Horii Y. Environmental analysis of chlorinated and brominated polycyclic aromatic hydrocarbons by comprehensive two-dimensional gas chromatography coupled to high-resolution time-of-flight mass spectrometry. *J Chromatogr A*. 2011;1218(21):3224–32.
16. Ochiai N, Ieda T, Sasamoto K, Takazawa, Y, Hashimoto, S, Fushimi, A, Tanabe, K.. Stir bar sorptive extraction and comprehensive two-dimensional gas chromatography coupled to high-resolution time-of-flight mass spectrometry for ultra-trace analysis of organochlorine pesticides in river water. *J Chromatogr A*. 2011;1218(39):6851–60.
17. Hashimoto S, Takazawa Y, Fushimi A, Tanabe, K, Schibata, Y, Ieda, T, Ochiai, N, Kanda, H, Ohura, T, Tao, Q, Reichenbach, SE.. Global and selective detection of organohalogenes in environmental samples by comprehensive two-dimensional gas chromatography-tandem mass spectrometry and high-resolution time-of-flight mass spectrometry. *J Chromatogr A*. 2011;1218(24):3799–810.
18. Hashimoto S, Zushi Y, Fushimi A, Takazawa Y, Tanabe K, Shibata Y. Selective extraction of halogenated compounds from data measured by comprehensive multidimensional gas chromatography/high resolution time-of-flight mass spectrometry for non-target analysis of environmental and biological samples. *J Chromatogr A*. 2013;1282(October 2011):183–9.
19. Zushi Y, Hashimoto S, Fushimi A, Takazawa Y, Tanabe K, Shibata Y. Rapid automatic identification and quantification of compounds in complex matrices using comprehensive two-dimensional gas chromatography coupled to high resolution time-of-flight mass spectrometry with a peak sentinel tool. *Anal Chim Acta*. 2013;778:54–62.
20. Kendrick E. A Mass Scale Based on CH₂, = 14.0000 for High Resolution Mass Spectrometry of Organic Compounds. *Anal. Chem.* 1963; 35(13):2146-54.
21. Jobst KJ, Shen L, Reiner EJ, Taguchi, VY, Helm, PA, McCrindle, R, Backus, S. The use of mass defect plots for the identification of (novel) halogenated contaminants in the environment. *Anal Bioanal Chem*. 2013;405(10):3289–97.
22. Poland A, Knutson, J.C. 2,3,7,8-Tetrachlorodibenzo-p-dioxin and related Halogenated Aromatic Hydrocarbons: Examination of the mechanism of toxicity. *Ann. Rev. Pharmacol. Toxicol.* 1982;22:517-54.
23. Ding C, Ni H-G, Zeng H. Human exposure to parent and halogenated polycyclic aromatic hydrocarbons via food consumption in Shenzhen, China. *Sci Total Environ*. 2013;443:857–63.
24. Fu PP, Tungeln LS Von, Chiu LH. Reviews Halogenated - polycyclic aromatic hydrocarbons : A class of Genotoxic environmental pollutants. *Environmental Carcinogenesis and Ecotoxicolog* .1999;17(2);71-109

25. Horii Y, Ok G, Ohura T, Kannan K. Occurrence and profiles of chlorinated and brominated polycyclic aromatic hydrocarbons in waste incinerators. *Environ Sci Technol.* 2008;42(6):1904–9.
26. Nilsson UL, Ostman CE. Chlorinated Polycyclic Aromatic Hydrocarbons : Method of Analysis and Their Occurrence in Urban Air. *Environ. Sci. Technol.* 1993;27(9):1826–1831.
27. Haglund, P, Alsberg, T, Bergman, A, Jansson, B. Analysis of halogenated polycyclic aromatic hydrocarbons in urban air, snow and automobile exhaust. *Chemosphere.* 1987;16:2441–2450.
28. Koistinen, J., Paasivirta, J, Nevalainen, T., Lahtipera, M. Chlorinated Fluorenes and Alkylfluorenes in bleached kraft pulp and pulp mill discharges. *Chemosphere.* 1994;28:2139-2150.
29. Ishaq R, Carina N, Zeb Y, Broman D, Järnberg J. PCBs , PCNs , PCDD / Fs , PAHs and Cl-PAHs in air and water particulate samples — patterns and variations. *Chemosphere.* 2003;50:1131–1150.
30. Ohura T. Environmental behavior, sources, and effects of chlorinated polycyclic aromatic hydrocarbons. *ScientificWorldJournal.* 2007;7:372–80.
31. Ding C, Ni H-G, Zeng H. Parent and halogenated polycyclic aromatic hydrocarbons in rice and implications for human health in China. *Environ Pollut.* 2012;168:80–6.
32. Wang D, Xu X, Chu S, Zhang D. Analysis and structure prediction of chlorinated polycyclic aromatic hydrocarbons released from combustion of polyvinylchloride. *Chemosphere.* 2003;53(5):495–503.
33. Wang D, Piao M, Chu S, Xu X. Chlorinated Polycyclic Aromatic Hydrocarbons from Polyvinylchloride Combustion. *Environ. Contam. Toxicol.* 2001;66:326–333.
34. Kawanishi M, Sakamoto M, Ito A, Kishi K, Yagi T. Construction of reporter yeasts for mouse aryl hydrocarbon receptor ligand activity. *Mutat. Res.* 2003;540:99-105
35. Myers A, Watson-Leung T, Jobst K, Shen Li, Besevic S, Mabury S, Reiner E. Determining bioaccumulation of halogenated contaminants in freshwater species using complementary non-targeted and targeted mass spectrometry techniques. *Env. Sci. Technol.* (submitted).

Supplementary Information

Table S1. Concentration of selected PAHs and haloPAHs from the ash sample. Compounds were identified and quantified using authentic standards.

Compound	MW	RRF	Concentration ($\mu\text{g/g}$)
Naphthalene	128	0.75	11
1,8-Dichloronaphthalene	196	1.53	ND
1,2,3,4-tetrachloronaphthalene	264	1.27	1
Phenanthrene	178	0.99	9
Anthracene	178	1.06	3
1,4-Dichloroanthracene	246	0.88	1
1,5-Dichloroanthracene	246	0.62	22
2,3-Dichloroanthracene	246	0.67	20
9-bromophenanthrene	256	2.26	2
9-bromoanthracene	256	0.99	ND
Fluoranthene	202	1.1	11
Pyrene	202	1.18	8
1,3,6,8-tetrachloropyrene	338	1.35	4
Benzo[c]phenanthrene	228	1.25	0.5
Benz[a]anthracene	228	1.12	6
Chrysene	228	0.95	5
Benzo[b]fluoranthene	252	1.31	5
Benzo[k]fluoranthene	252	1.14	2
Benzo[a]pyrene	252	1.26	1
Indeno[1,2,3-cd]pyrene	276	1.01	0.5
Dibenz[a,h]anthracene	278	1.02	0.5
Coronene	300	0.88	0.2

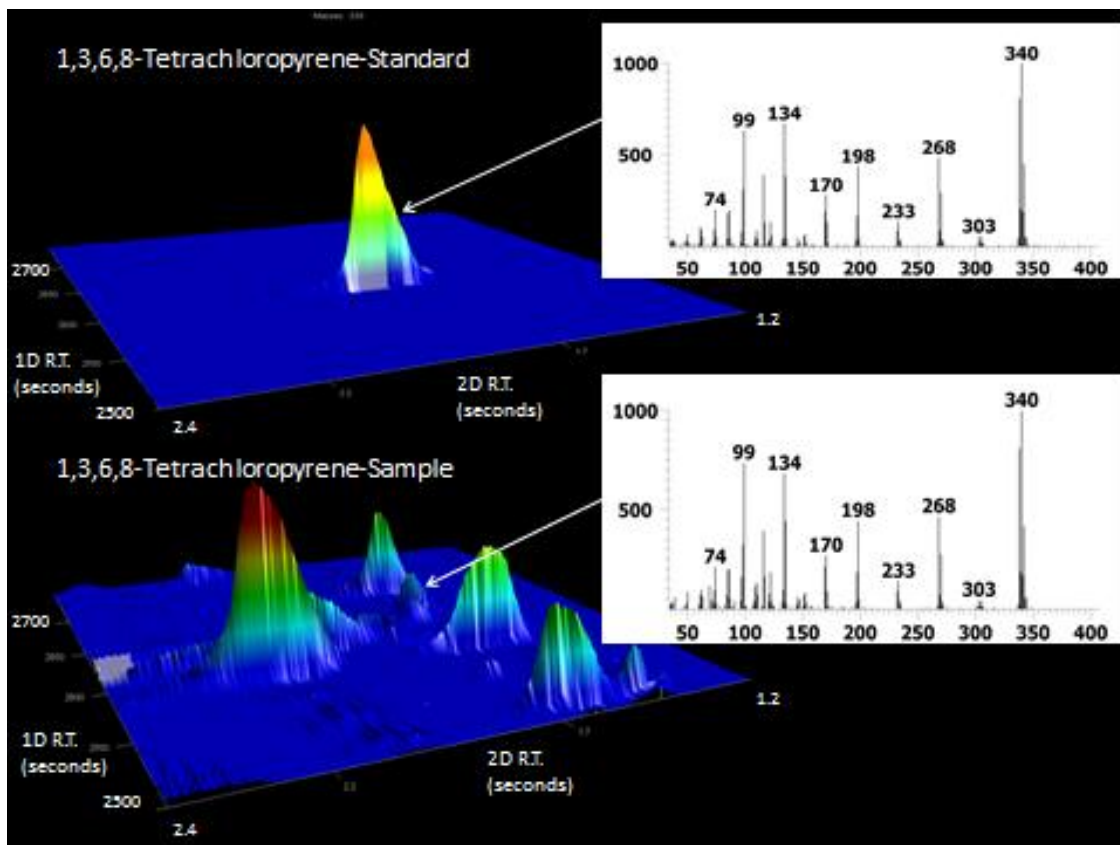


Figure S1. Surface plots of the Plastimet soil extract focusing on the region of interest for the identification of 1,3,6,8-tetrachloropyrene. The plot on the top is that of the authentic standard and the plot at the bottom is from the sample.

Additional Experiments

GCxGC separation of the crude ash extract

The separation capabilities of GCxGC were explored by injecting a crude extract of the ash sample. Approximately 5g aliquot of the sample was grounded to a fine powder using a mortar and pestle. The powdered sample was extracted using dichloromethane (DCM) in an Accelerated Solvent Extractor (ASE, Dionex). Phenanthrene-d₁₀ and chrysene-d₁₂ were added to the sample prior to extraction to serve as recovery standards. To the DCM extract was added 1mL of toluene and the sample was concentrated to 1mL. A 150uL aliquot of the sample was blown down to 15μL to which was added 5uL of pyrene-d10 (4ng/uL) to serve as an injection standard. 1μL of the sample was injected for GCxGC analysis. The GCxGC was configured with a 60m DB-5MS primary column (0.25 mm i.d., 0.15 μm film thickness; J&W Scientific, USA) coupled to a 1m DB-17ht secondary column (0.1 mm i.d., 0.1 μm film thickness; J&W Scientific, USA). The primary oven temperature was set to 50°C initially, ramped to 300 °C at 6°C/min and held for 35 mins. A 10°C offset was used for the secondary oven temperature. A modulation period of 5s was used.

Figure 1 displays the resulting 2D chromatogram as a contour plot along with the reconstructed 1D chromatogram. The reconstructed 1D chromatogram displays a ‘hump’ indicative of an unresolved complex mixture (UCM) of compounds. The 2D chromatogram has been able to differentiate the UCM into distinct bands. In this case the alkanes and alkenes dominate the UCM along with numerous aldehydes and ketones. The aromatic species including PAHs and halo-PAHs are found as a band of compounds

above the aliphatics. Although we were able to identify some of the PAH and halo-PAHs, the chemicals noise from the intense band of aliphatics that smear across the second dimension of the chromatogram makes the task difficult.

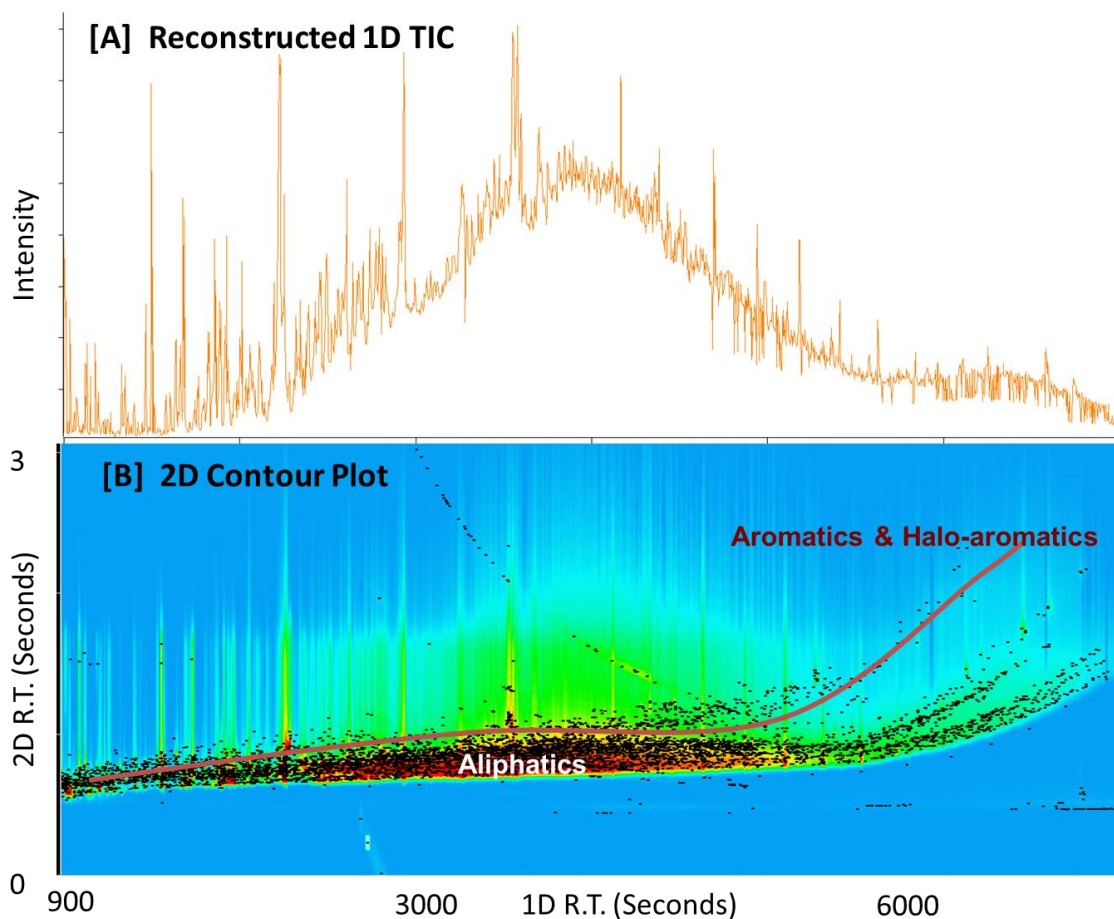


Figure A1. GCxGC analyses of the crude ash extract using a DB-5 (1D column) and a DB-17 (2D column) configuration. [A] Reconstructed 1D total ion current (TIC) chromatogram. [B] 2D chromatogram presented as a contour plot. The 2D chromatogram shows the separation of the aromatic and halo-aromatic compounds from the unresolved complex mixture (UCM) which is not possible on a standard 1D GC-MS system as depicted by the reconstructed 1D TIC.

In order to eliminate the interference from the aliphatic compounds, a reverse column configuration was explored. In this case the GCxGC was configured with a 30m DB-17ht primary column (0.25 mm i.d., 0.15 μm film thickness; J&W Scientific, USA)

coupled to a 1m DB-5MS secondary column (0.1 mm i.d., 0.1 μm film thickness; J&W Scientific, USA). The primary oven temperature was set to 50°C initially, ramped to 300 °C at 6°C/min and held for 35 mins. A 10°C offset was used for the secondary oven temperature. A modulation period of 5s was used.

The resulting 2D chromatogram is displayed in Figure 2. In this case the intense aliphatic band is now on top of the aromatic band. As a result the interference from the intense aliphatic band has been eliminated. It should also be noted that the reverse column configuration has enhanced the separation of the UCM in the second dimension. Distinct bands of aldehydes and ketones are observable between the aromatic band and the intense cluster of alkanes and alkenes at the top of the chromatogram. The reverse column configuration has effectively separated the UCM from the aromatics enabling for the analysis of a crude extract of a complex environmental sample without any cleanup procedures. This is highly beneficial in cases where rapid responses are needed to extreme environmental events such as fires and for the comprehensive analysis of samples.

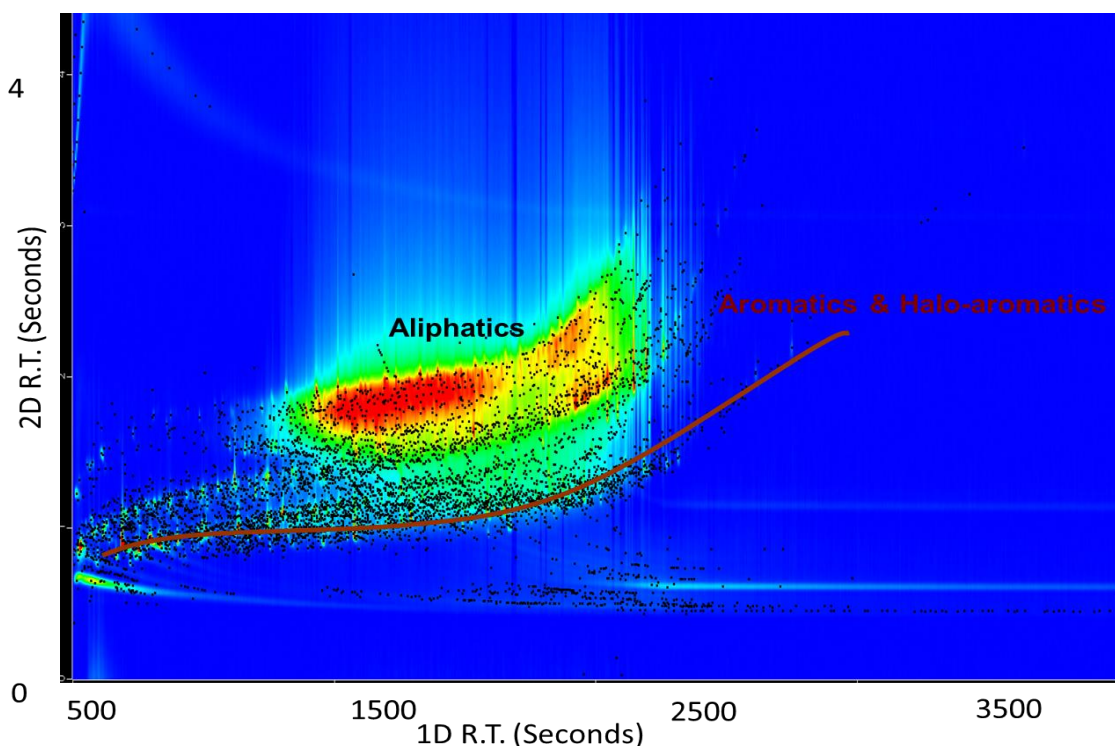


Figure A2. GCxGC analyses of the ash sample crude extract using a DB-17 (1D column) and a DB-5 (2D column) configuration. In this case the UCM is located atop of the aromatic band and thus does not interfere with the aromatics.

Sephadex LH-20 fractionation of the ash extract

The ash sample extract was fractionated in order to isolate the aromatic compounds. The isolated aromatic fraction can be concentrated and further analyzed for novel halogenated compounds that might be present at very low levels. Furthermore, the aromatic fraction can be used to test the toxicity of these compounds in biological assays. The crude extract was separated on a chromatographic medium known as Sephadex LH-20 which separates compounds based on both physical and chemical properties. The procedure was established and previously published by our research group. Briefly, 20g of Sephadex LH20 gel was allowed to soak in 200mL of the elution solvent (hexane:methanol:dichloromethane, 6:4:3, v/v) overnight followed by degassing under vacuum for 1-2 hrs. A stainless steel column (5 cm I.D., 15 cm length) was packed with

the gel by first pouring the slurry into it and then by pumping eluent through it. This procedure was repeated until the column was packed to the top. The column was equilibrated by pumping elution solvent through it at 2 mL/min for 1 hr. Naphthalene (1 mg/mL in elution solvent) was used as a column test standard. A 200 μ L injection of the standard was made and the eluting peak was detected using a Beckman model 153 analytical UV detector at 254nm connected to a strip-chart recorder. The standard was injected until 3 reproducible peaks were observed.

Since naphthalene is the smallest of the PAHs, all peaks eluting from naphthalene onwards were considered to be aromatic and all peaks prior to naphthalene were considered to be aliphatic. A 200 μ L of the crude ash extract was loaded onto the column and eluted at 2 mL/min with the elution solvent. Fractions were collected at 1.5 min time intervals. The aliphatic compounds eluted in fractions 1-6 and the aromatic compounds eluted in fractions 7-12. The heavier PAH and halo-PAHs were eluted in the later fractions (10-12) compared to the low molecular weight compounds. Figure 3 displays the GCxGC chromatogram of the combined aliphatic fractions (1-6) along with the combined aromatic fractions (7-12). In this case the fractions were combined and blown down to 20 μ L for both the aliphatic and aromatics. The Sephadex chromatographic separation has effectively isolated the aromatic fraction containing the many halogenated aromatic species (figure 3c).

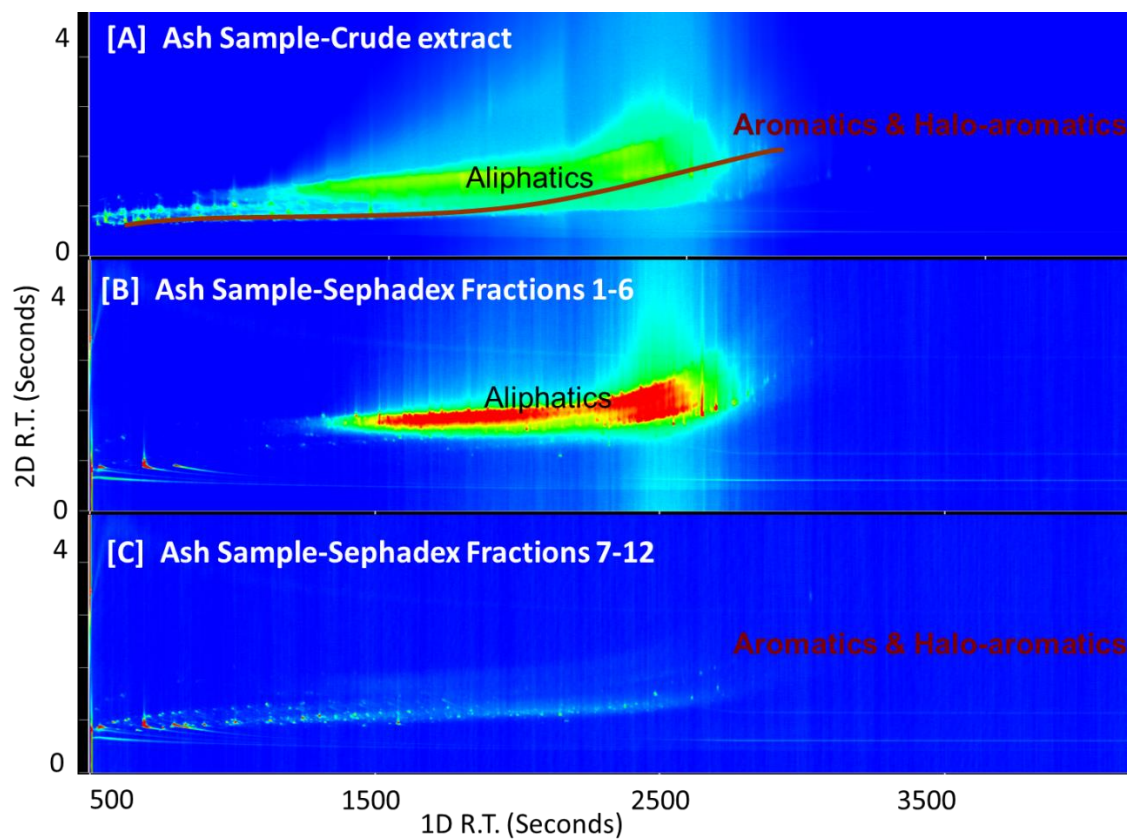


Figure A3. GCxGC analyses of the ash sample crude extract and Sephadex fractions using a DB-17 (1D column) and a DB-5 (2D column) configuration. [A] Crude sample extract displaying both the aliphatic and aromatic compounds. [B] Sephadex fractions 1-6 which contain the majority of aliphatic compounds. [C] Sephadex fractions 7-12 which contain the majority of aromatic and halo-aromatic compounds.

CHAPTER FIVE

Differentiation of (Mixed) Halogenated Dibenzo-*p*-Dioxins by Negative Ion Atmospheric Pressure Chemical Ionization

Sujan Fernando¹, Kirk Green¹, Kari Organitini², Frank Dorman², Rhys Jones³,
Eric J. Reiner^{4,5} and Karl J. Jobst*^{1,4}

Author Affiliations:

¹McMaster University, 1280 Main Street West, Hamilton, ON, L8S 4M1

²Penn State University, 107 Althouse Labs, University Park, PA 16802

³Waters Corporation, Altrincham Road, Wilmslow, UK SK9 4AX

⁴Ministry of the Environment and Climate Change, 125 Resources Road, Toronto, ON,
M9P 3V6

⁵University of Toronto, 80 St. George Street, Toronto, ON, M5S 3H6

Author contributions:

Manuscript prepared by Sujan Fernando with editorial comments provided by Karl J.

Jobst. Method development and sample analysis was carried out by Sujan Fernando.

Collaborative contributions from Kirk Green, Kari Organitini, Frank Dorman, Rhys Jones and Eric J. Reiner were greatly appreciated.

ABSTRACT

Mixed halogenated dibenzo-p-dioxins (PXDDs) may well be more toxic than 2,3,7,8-tetrachlorodibenzo-p-dioxin (2378-TCDD), a compound reputed as one of the most toxic chemicals known to exist. However, studies on the occurrence of PXDDs have been hampered by a lack of authentic standards as well as separation techniques capable of resolving the enormous number of potential isomers. Electron ionization (EI) mass spectrometry-based methods are of limited value due to the lack of isomer specific fragmentation.

Negative ion atmospheric pressure chemical ionization (APCI) of 2378-TCDD was described in this Journal [Mitchum *et al.* Anal. Chem. 54 (1982) 719] over 30 years ago. Under these conditions, the reaction between $O_2^{\bullet-}$ and 2378-TCDD results in structure diagnostic cleavages of the C-O bonds, which can distinguish TCDD isomers. In the present study, the analogous ether cleavages of PCDDs and PXDDs were studied using a gas chromatograph-quadrupole time-of-flight (GC-QTOF) mass spectrometer coupled using APCI. The results indicate comparable detection limits for the positive radical cations $[M^{\bullet+}]$ and negative pseudo-molecular ions $[M-Cl+O]^-$: Approximately 5fg and 10fg respectively for 2378-TCDD and 5-10fg and 10–60fg, respectively for the PXDDs. Detection limits obtained by monitoring the ether cleavage products were somewhat higher (between 100 and 600 fg), but still acceptable for trace analysis of PXDDs. Such reactions effectively resolve co-eluting isomers, which is crucial for the identification of (toxic) PXDDs. The technique is demonstrated by differentiating PXDD isomer classes in

a sample obtained from a major industrial fire that would not be feasible using EI or positive ion APCI⁺.

INTRODUCTION

Polychlorinated dibenzo-*p*-dioxins and furans (PCDD/Fs) have been monitored in the environment for nearly half a century due to their toxic properties and persistent nature¹. These compounds are formed as unintentional products of combustion^{2,3} by thermal conversion processes involving polychlorinated biphenyls (PCBs), polychlorophenols and other polychlorinated chemicals⁴. 2,3,7,8-tetrachlorodibenzo-*p*-dioxin (2378-TCDD) is the most toxic of this class of chemicals and its toxicity is mediated through the aryl hydrocarbon receptor (AhR)⁵. Compounds with similar chemical structures to 2378-TCDD also have the ability to activate the aryl hydrocarbon receptor and thus have the potential to be highly toxic^{5,6}.

The past four decades have witnessed the widespread production, distribution and eventual regulation of brominated diphenyl ethers (PBDEs)⁷, whose degradation and transformation products include polybrominated dibenzo-*p*-dioxins (PBDDs), furans (PBDFs) and their mixed halogenated counterparts (PXDD/Fs). Considering their structural similarity, it is not surprising that the AhR-mediated toxicities of the PCDDs, PBDDs, and PXDDs are comparable⁵. Nevertheless, there are relatively few studies of the environmental impact and human exposure of PBDDs^{8,9} and PXDDs^{10,11,12}.

The Plastimet Inc. fire (July, 1997) in Hamilton, Ontario, Canada^{13,14} is regarded as one the largest industrial fires in North America, and it provides a salutary example of

the generation and release of (mixed) halogenated chemicals. Approximately 400 tonnes of polyvinyl chloride (PVC) and polyurethanes stored at the plastics recycling facility were consumed in the fire. It is suspected that decomposition of brominated flame retardants contributed to the formation of PXDD/Fs, as well as mixed halogenated PAH identified in soil and vegetation from the site^{10,13,15}. The concentrations of the PXDD/Fs were a fraction (6-10%) of the corresponding chlorinated compounds¹⁰, but the increasing reliance on organobromine chemicals in industry and commerce may serve as an indicator of the growing significance of PXDD/Fs.

PXDDs can also be generated under less spectacular conditions, such as during municipal incineration¹⁶ and electronics waste recycling¹⁷. These activities are leading sources of emission of dioxins and furans into the environment¹⁸. In a recent study, analysis of soil samples contaminated by plastic recycling facilities in China¹⁷ revealed PCDD/Fs concentrations that exceeded international guidelines as well as PBDD/Fs and PXDD/Fs concentrations that were even higher. Considerably less information is available about human exposure to PXDD/Fs. However, studies by Fernandes *et al.*^{12,19} have reported on the occurrence of PXDD/Fs in foods and determined that the toxic equivalents (TEQ) resulting from PXDD/Fs and mixed halogenated biphenyls (PXBs) can account for as much as 15% of the corresponding TEQ for the fully chlorinated analogues.

Gas chromatography coupled to high resolution mass spectrometry (GC-HRMS) is the most popular technique used for the analysis of PCDDs²⁰, PBDDs²¹ and PXDDs²². This has been partly driven by the low detection limits afforded by magnetic deflection

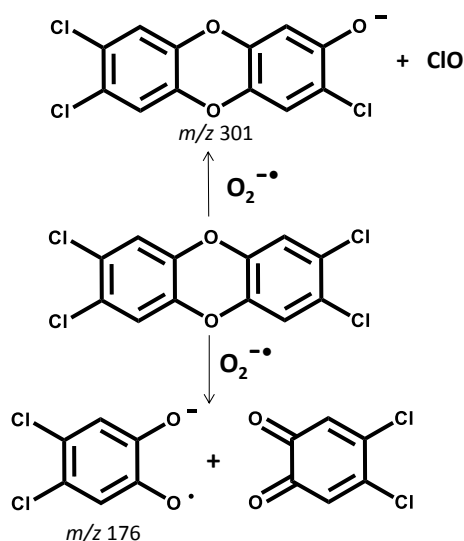
instruments, although reports on the use of tandem mass spectrometry for the analysis of PCDDs have also appeared for over 25 years²³. Isomer differentiation is a critical aspect of dioxin analysis, but separation of the large number of potential PXDD congeners is not feasible using standard capillary GC. There are 1550 possible PXDD congeners and 3050 possible PXDF congeners, of which only a fraction are expected to be toxic. This problem is exacerbated by the lack of structure diagnostic fragments that are formed by electron ionization (EI). Negative chemical ionization (NCI) has demonstrated to be a selective and sensitive technique for the analysis of halogenated organics¹⁶ but like EI, the mass spectra obtained do not yield any structure diagnostic fragments for dioxins using common CI gases²⁴.

In 1975, Hunt *et al.*²⁵ discovered that under NCI conditions, 2378-TCDD undergoes a structure-diagnostic reaction with $O_2^{\bullet-}$, resulting in cleavage of the C-O bonds and formation of the m/z 176 ion $C_6H_2Cl_2O_2^{\bullet-}$. This reaction (see Scheme 1) differentiates TCDD isomers on the basis of the distribution of Cl atoms across the two aromatic rings. For example, 1234-TCDD cannot produce m/z 176 by the analogous ether cleavage. The main reaction pathway shared by all congeners is the formation of [M-Cl+O]⁻ pseudo-molecular ions. Several studies have appeared on various NCI conditions that promote the above structure diagnostic reactions^{24,26}.

The pioneering studies of Mitchum and Korfmacher *et al.*^{27,28,29} explored negative ion atmospheric pressure chemical ionization (NI-APCI) of TCDDs with oxygen as a reagent gas. These conditions minimized the undesirable effects of introducing oxygen into the CI source²⁷. They showed that 2378-TCDD can be distinguished from many

other common interfering species including PCBs, chlorinated methoxybiphenyls and chlorinated pesticides based on the ether cleavage products, even using a low resolution mass spectrometer. This technique was used to measure PCDDs in Great Lakes fish³⁰, animal tissue^{28,29} and other biological samples³¹, but it was not widely adopted.

Recently, the concept of coupling GC-HRMS using atmospheric pressure chemical ionization has attracted renewed interest and its benefits for environmental analysis are being explored³²⁻³⁴. This resurgence is partly the result of the widespread adoption of atmospheric pressure ionization sources (e.g. electrospray) whose development was driven by liquid chromatography and direct analysis applications³⁵. Here, we report on the analysis of a selection of chlorinated, brominated and mixed halogenated dioxin/furan standards using a quadrupole time-of-flight (QTOF) mass spectrometer coupled to GC using APCI. The technique is demonstrated by differentiating PXDD isomer classes in a soil sample contaminated by the Plastimet Inc. fire that would not be feasible using EI.



Scheme 1. The reaction between 2378-TCDD and $O_2^{\bullet-}$

EXPERIMENTAL

The chemical standards used in this study (Table 1) were provided by Wellington Laboratories (Guelph, Ontario). The soil samples contaminated by the fallout of a plastics fire (Plastimet Inc., Hamilton, Ontario, Canada 1997) have been described previously¹³.

The experiments were performed using a Waters Xevo G2-XS quadrupole time-of-flight mass spectrometer (Manchester, UK) coupled to an Agilent 7890B gas chromatograph (GC) using an atmospheric pressure chemical ionization (APCI) source. Separations were performed using Agilent J&W DB-5 (40m x 0.18mm x 0.18um) and DB-5 (15m x 0.18mm x 0.18um) columns. The injector was operated in the splitless mode at a temperature of 280°C. The injection volume was 1 μ L. The oven temperature program for the 40m column was as follows: Initial temperature 140°C (held 2.5 minutes) and increased to 200°C at 40°C/minute and then to 235°C at 3°C/minute and

then to a final temperature of 300°C at 6°C/minute and held for 14.17 minutes for a total run time of 40 minutes. The oven temperature program for the 15 m column was as follows: Initial temperature 100°C and increased to 200°C at 40°C/minute and then to a final temperature of 330°C at 15°C/minute and held for 3.5 minutes for a total run time of 15 minutes.

The ion source parameters were as follows: Corona current 10µA, sampling cone 20V, auxiliary gas flow 100L/hr and cone gas flow 175L/hr. Nitrogen from a generator (Parker Balston) was used for cone and auxiliary gas. Ultrahigh purity (UHP) nitrogen (Praxair) was used as the GC make-up gas at 350 mL/min. The mass acquisition range was set to 30-1000 m/z with a resolving power of 25,000 FWHM. The target enhancement mode was used to increase signal intensity of the target pseudo-molecular ions and product ions during the analysis. Additional experimental information can be found in the supplementary information (SI), which includes an expanded discussion on optimization of ion source flow rates and its effect on sensitivity (Figure S1).

RESULTS AND DISCUSSION

APCI of (Mixed) Halogenated Dioxins and Furans

Twenty-one PCDD, PBDD and PXDD/F standards were investigated in this study (Table 1). In general, reactions between dioxins and O_2^{\bullet} occur via two main pathways. In almost all cases, the base peak of the mass spectrum corresponds to $[M-X+O]^+$, where $X=Br/Cl$. This is in line with the behaviour of other halogenated compounds studied under various CI and APCI conditions²⁴. Cleavages of the C-O bonds also occur akin to

the reaction shown in Scheme 1 for 2378-TCDD. Table 1 lists the relative intensities of the $[M-X+O]^-$ ions and ether cleavage products (ECP), if detected.

Table 1. A list of the 21 PCDD, PBDD and PXDD/F standards analyzed using APCI. Listed are the observed pseudomolecular ions in NI-APCI mode along with the ether cleavage products (ECP) and its relative abundance (in parenthesis). Also listed are the positive radical cations $[M\bullet+]^+$ observed by APCI+ mode as well as the estimated instrument detection limits (I.D.L.) for the observed ions. Note that for certain ECP which were detected below 1%, IDLs could not be calculated from the 1pg of material injected on column.

Compound	ECP 1	ECP 2	Neg	Pos ($M\bullet+$)	I.D.L. (fg/uL)			
					ECP 1	ECP 2	Neg	Pos ($M\bullet+$)
1234-TCDD	245.86 (Cl_4) (0.03%)	ND	300.92 (M-Cl+O)	321.89			9	6
1378-TCDD	175.94 (Cl_2) (35%)	ND	300.92 (M-Cl+O)	321.89	390		10	6
2378-TCDD	175.94 (Cl_2) (75%)	ND	300.92 (M-Cl+O)	321.89	250		10	5
1Br-DD	ND	ND	277.99 (M+O)	261.96			33	7
27/28Br-DD	ND	ND	276.95 (M-Br+O)	341.87			61	3
237Br-DD	265.84 (Br_2) (1%)	ND	356.86 (M-Br+O)	419.78	680		33	5
1234TBDD	423.66 (Br_4) (0.005%)	ND	434.77 (M-Br+O)	499.69			20	6
1378TBDD	265.84(Br_2) (15%)	ND	434.77 (M-Br+O)	499.69	150		20	5
2378TBDD	265.84(Br_2) (20%)	ND	434.77 (M-Br+O)	499.69	130		33	6
12478B-DD	265.84(Br_2) (1%)	343.75 (Br_3) (1%)	514.68 (M-Br+O)	577.60	500	150	12	9
12378B-DD	265.84(Br_2) (1%)	343.75 (Br_3) (1%)	514.68 (M-Br+O)	577.60	660	130	13	9
Heptabromo-DD	343.75 (Br_3) (0.02%)	423.66 (Br_4) (0.03%)	672.50 (M-Br+O)	735.42			500	66
Octabromo-DD	423.66 (Br_4) (0.02%)	ND	750.41 (M-Br+O)	815.33			980	500
7B,23C-DD	175.94 (Cl_2) (10%)	185.93(Br_1) (1%)	266.96 (M-Br+O)	331.88	130		25	4
2B,378C-DD	175.94 (Cl_2) (10%)	221.89 (ClBr) (20%)	300.92 (M-Br+O)	365.84	150	660	28	4
23Br, 78Cl-DD	175.94 (Cl_2) (10%)	265.84(Br_2)(30%)	346.87 (M-Br+O)	409.79	140	500	11	5
2B,1378C-DD	175.94 (Cl_2) (1%)	255.85 (Br Cl_2) (5%)	380.83 (M-Cl+O)	399.80	170	120	4	4
12Br, 78Cl-DF	ND	ND	330.87 (M-Br+O)	393.80			5	4
23Br, 78Cl-DF	ND	ND	330.87 (M-Br+O)	393.80			6	4
3B, 278Cl-DF	ND	ND	284.93(M-Br+O)	349.85			10	4
8B, 234Cl-DF	ND	ND	330.87(M-Cl+O)	349.85			4	4

The APCI mass spectrum of 2378-TCDD, (Figure 1a), displays a significant peak at m/z 176 corresponding to the ECP shown in Scheme 1, $C_6H_2Cl_2O_2\bullet^-$. The intensity of m/z 176 is comparable to the $[M-Cl+O]^-$ peak, in agreement with the observations of Hunt *et al.*²⁵. 1378-TCDD also gives rise to an m/z 176 peak, at about 35% the intensity of the $[M-Cl+O]^-$ peak (Table 1). Hass *et al.*²⁶ noted that this difference in reactivity may be

related to 2378-TCDD being the only TCDD isomer that does not contain any chlorines at the *peri*-positions of the aromatic rings (i.e. 1, 4, 6, or 9). In contrast, the mass spectrum of 1234-TCDD does not display m/z 176, but rather a low intensity peak at m/z 246 $C_6Cl_4O_2^{\bullet}$ because all four chlorine atoms are located on the same ring structure. The spectrum is instead dominated by $[M-Cl+O]^-$. Hass *et al.*²⁶ proposed that one can determine the number of chlorines per ring and the presence of *peri* chlorines in an unknown dioxin by monitoring the products of the above two reaction pathways.

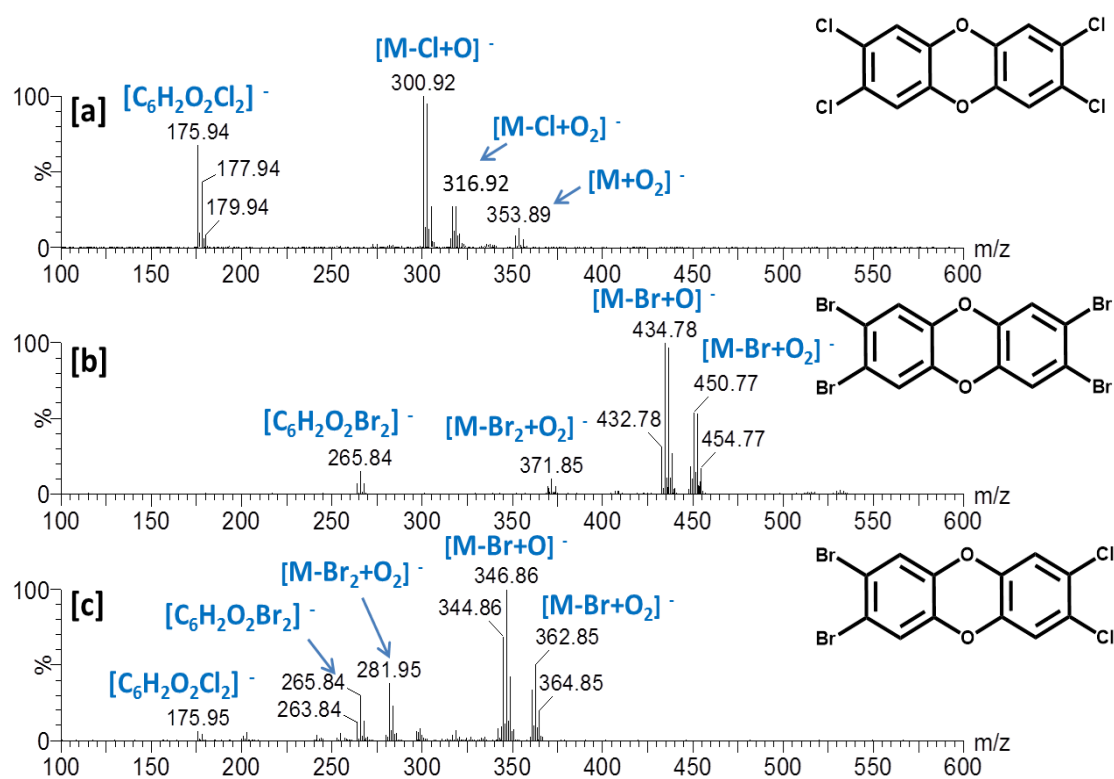


Figure 1. The NI-APCI spectra of 2378-TCDD, 2378-TBDD and 2,3-Br₂-,7,8-Cl₂DD. ECPs are observed at m/z 176, and 266 for the 2378-TCDD and 2378-TBDD species. Both of these ECPs are observed for the 2,3-Br₂-,7,8-Cl₂DD

The results of the present study indicate that PBDDs and PXDDs undergo analogous processes. Both 2378-TBDD and 1378-TBDD generate the m/z 266 ether cleavage product $C_6H_2Br_2O_2^{\bullet}$ along with $[M-Br+O]^-$. The intensity of the ECP is 15% of the $[M-Br+O]^-$ peak for 1378-TBDD and 20% for 2378-TBDD (Figure 1). The marginal difference in ratios (~5%) contrasts with that of the chlorinated analogues, which suggests the ratio of the two pathways may not be helpful for structure analysis of PBDDs. Nevertheless, the presence (or absence) of ECP ions can still easily distinguish isomers. For example, 1234-TBDD does not produce m/z 266, unlike its isomers 2378-TBDD and 1378-TBDD. Instead, it reacts with O_2^{\bullet} to generate m/z 424 ions $[C_6Br_4O_2^{\bullet}]$, resulting in a mass spectral peak that is less than 1% relative to $[M-Br+O]^-$. The pentabrominated compounds (123788-PeBDD and 124788-PeBDD) also undergo ether cleavages into $C_6HBr_3O_2^{\bullet}$ and $C_6H_2Br_2O_2^{\bullet}$, but the yield is low (~1%). Hexabrominated dioxins were not available for this study, but the hepta- and octabrominated dioxins (Table 1) produced ECPs consistent with the reaction in Scheme 1.

The behaviour of the PXDDs parallels that of the PCDDs and PBDDs. For 2,3-Cl₂-7-BrDD, peaks corresponding to ECPs at m/z 176 $C_6H_2Cl_2O_2^{\bullet}$ and m/z 186 $C_6H_3BrO_2^{\bullet}$ were observed with relative intensities of 10% and 1%. Interestingly, the weak yield of $C_6H_3BrO_2^{\bullet}$ ions coincides with the observation that the base peak of the spectrum corresponds to $[M-Br+O]^-$. In contrast, the relative intensity of the $[M-Cl+O]^-$ peak was negligible (<1%). This provides supporting evidence that the *peri* Br atom is the preferred site of attack for O_2^{\bullet} . The preference for Br/O exchange is also observed for the tetrahalo PXDDs 2,3-Br₂-,7,8-Cl₂DD and 2-Br-3,7,8-Cl₃DD. However, the spectrum of

the pentahalogenated dioxin 2-Br-1,3,7,8-Cl₄DD displays a peak for [M-Cl+O]⁻ that is 4x more intense than that of [M-Br+O]⁻. In this case, the *peri* positions are occupied by Cl.

Ether cleavages of 2,3-Br₂-,7,8-Cl₂DD result in peaks at *m/z* 176 C₆H₂Cl₂O₂^{•-} and at *m/z* 266 C₆H₂Br₂O₂^{•-}. In the same vein, the mass spectrum of 2-Br-3,7,8-Cl₃DD displays *m/z* 176 C₆H₂Cl₂O₂^{•-} and *m/z* 222 C₆H₂BrClO₂^{•-}. Neither compound contains a *peri* halogen, which is consistent with the observation that the combined intensities of the ECP peaks is high (~30-40%) relative to [M-Br+O]⁻. On the other hand, 2-Br-1,3,7,8-Cl₄DD does contain a *peri* Cl. It undergoes ether cleavages into C₆H₂Cl₂O₂^{•-} and C₆H₂BrClO₂^{•-}, but the intensities (1% and 5%) are diminished relative to [M-Cl+O]⁻. These observations indicate that the reactivity of the PBDDs and PXDDs towards O₂⁻ follows essentially the same scheme proposed by Hass *et al* for the PCDDs, *viz.*, the number of halogens per aromatic ring can be determined by monitoring the ECP(s). Additionally, the formation of [M-X+O]⁻ is preferred if a *peri* halogen is present. Otherwise, Br/O exchange is preferred over Cl/O exchange.

Four PXDFs were also investigated, but not surprisingly, ECPs were not observed because a C-C bond connects the two aromatic rings. Nevertheless, some structure diagnostic information was apparent from the ratio of [M-X+O]⁻ ions. For example, the mass spectrum of 3-Br-2,7,8-Cl₃DF displays [M-Br+O]⁻ as the base peak with the [M-Cl+O]⁻ at 70% relative intensity, but its isomer 8-Br-2,3,4-Cl₃DF mainly produces [M-Cl+O]⁻ with the [M-Br+O]⁻ at only 5% relative intensity. The mass spectra of isomers 1,2-Br₂-7,8-Cl₂DF and 2,3-Br₂-7,8Cl₂DF displays [M-Br+O]⁻ as the base peak in both

cases but the relative intensity of the $[M-Cl+O]^-$ peak are significantly different at 5% and 40% respectively.

Selectivity and Sensitivity Considerations

The presence of ECPs in the APCI mass spectrum of an unknown dioxin can be used to determine the distribution of halogen atoms among the aromatic rings. Similarly, monitoring carefully selected ECP ions can be used to distinguish isomeric dioxins, which would otherwise be difficult to separate chromatographically and may exhibit very different toxicities. A prime example is the separation of 2378-TCDD and 1234-TCDD, which has long been used as an indicator of column performance for the analysis dioxins by GC-HRMS³⁶. Figure 2a and 2b are extracted ion chromatograms of the molecular ions (APCI⁺) and m/z 176 ether cleavage product (APCI) obtained from a mixture of 1378-, 1234- and 2378-TCDD. In positive ion mode, an intense molecular ion is observed for all three compounds. However, only 1378-TCDD and 2378-TCDD share a 2:2 chlorine distribution, and therefore produce m/z 176 ions upon reaction with O_2^{\bullet} . As a result, two chromatographic peaks are observed in Figure 2b. This result mirrors the early experiments by Mitchum and Korfmacher²⁷, who realized that APCI could improve the separation of PCDDs.

Figures 2c and 2d displays extracted ion chromatograms of the analogous TBDDs. In Figure 2c intense peaks for the positive molecular ions of 1378, 1234- and 2378-TBDD are observed. However, 1234-TBDD and 2378-TBDD co-elute under the experimental conditions used. Highly brominated compounds can be difficult to analyze using conventional GC techniques due to their thermal lability. For this reason, short GC

columns are often chosen for the analysis, but this is at the cost of reduced separation. Figure 2d displays the extracted ion chromatogram of ions $C_6H_2Br_2O_2^{\bullet-}$, which are generated by 2:2 bromine substituted isomers 1378-TBDD and 2378-TBDD under APCI conditions. In this way 2378-TBDD is completely resolved from its co-eluting isomer. This raises the possibility that APCI⁻ could be used to reduce co-elutions and decrease analysis time for PBDDs and PXDDs.

The instrument detection limits (IDLs) for the standards analyzed were estimated by injecting 0.5pg of 2378-TCDD and 1pg on column for all other compounds in Table 1. For this study, detection limit was defined as a peak with a signal-to-noise ratio (S/N) of 10. Table 1 lists the estimated IDLs for the positive radical cations $[M^{+\bullet}]$ and negative pseudo-molecular ions $[M-Cl+O]^-$ along with the ECPs. In general, the IDLs for positive and negative ions mode experiments are comparable. The IDLs for 2378-TCDD were approximately 5 fg and 10 fg for the $[M^{+\bullet}]$ and $[M-Cl+O]^-$ traces respectively. The IDLs for the TBDDs and PXDDs ranged between 5-10 fg and 10–60 fg, respectively. ECP ions typically represent a small fraction (< 30%) of the ions detected. Nevertheless, detection limits for the ECPs were reasonably low. All four tetrahalogenated compounds 2378-TCDD, 2378-TBDD, 2Br-378-CDD and 23B-78-CDD were detectable at levels around 200fg injected, which is sufficient for analysis of environmental samples²³.

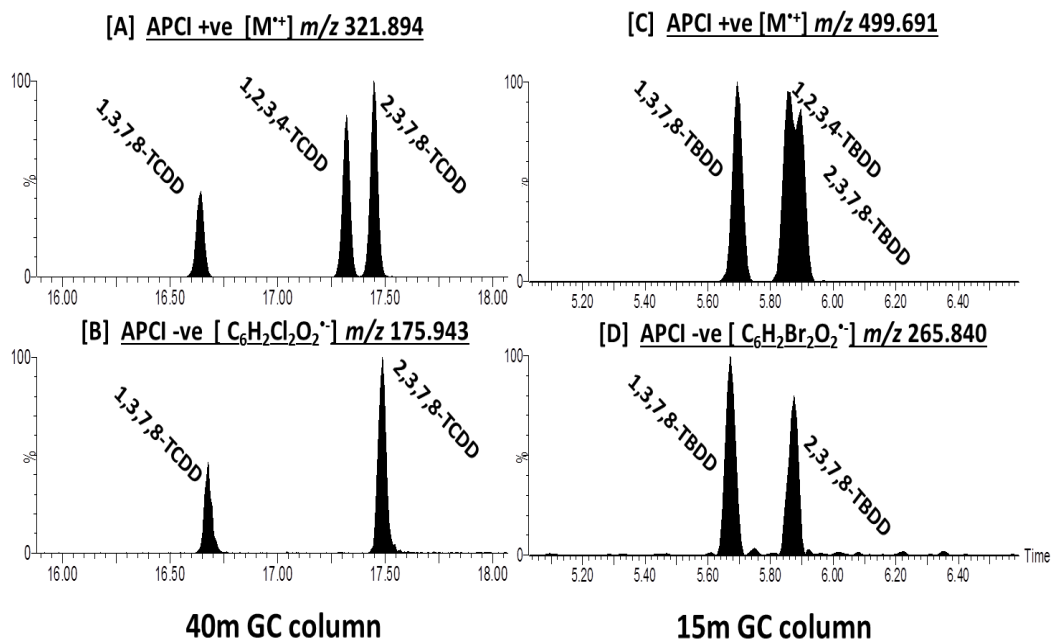


Figure 2. The positive and negative ion APCI analysis of the 1378-, 1234- and 2378-tetra chlorinated dioxins (TCDD) and tetra brominated dioxins (TBDD). [A] displays the molecular ion trace (APCI +ve) for the TCDD isomers and [B] displays the Cl₂ ether cleavage product trace (APCI –ve). [C] displays the molecular ion trace (APCI +ve) for the TBDD isomers and [D] displays the Br₂ ether cleavage product trace (APCI –ve). Note that the TCDDs were separated on a 40m column (DB5-MS) whereas the TBDDs were separated on a 15m column (DB5-MS).

The supply of O₂ was air purified using a nitrogen generator and introduced as the cone and auxiliary gases in the ion source. The effects of oxygen content in the ion source on yield of ECPs were investigated as follows. When O₂ is introduced to the ion source at concentrations of 0.05% and ~1% (using previously characterized nitrogen generators), the yield and ratio of the [M-X+O] and ECP ions do not change. However, the background noise increases significantly with O₂ concentration. Figure S2 displays the mass spectra of 2378-TBDD using nitrogen (top panel) and using dry compressed air (bottom panel) as the cone gas. A significant increase in the relative intensity of the [M+O]⁻ peak is observed when using compressed air. However, the absolute intensity of the ECP at *m/z* 266 as well as the other ions in the spectrum decreases approximately

five-fold when using compressed air. It is gratifying that best quality spectra were obtained under normal operating conditions, with trace quantities of O₂ introduced as an impurity in the N₂ supply.

Identification of (Mixed) Halogenated Dioxins Resulting from the Plastimet Inc. Fire

The sample characterized in the following section was collected from the site of the Plastimet Inc. plastic recycling plant fire in Hamilton, Ontario (1997). The fire consumed more than 400 tonnes of PVC and polyurethane plastics. The presence of brominated flame retardants may well explain why mixed bromo/chloro substituted organics have been identified from soil and vegetation collected from the site¹³, including PXDDs¹⁰.

Figure 3a displays the extracted ion chromatogram of ions [M-Cl+O]⁻ generated by hexachlorinated dioxins (HxCDD) present in the soil extract. Also displayed are the mass chromatograms of the Cl₂, Cl₃ and Cl₄ ECPs (Figure 3b-d). Based upon the alignment of the peaks in the [M-Cl+O]⁻ and ECP chromatograms, the distribution of the chlorines among the 2 aromatic rings of the HxCDDs can be deduced. Peaks 1,3,4 and 6 are displayed in Figures 1a, b and d. Thus these peaks must have a 2:4 distribution of chlorines. Similarly, peaks 2,5 and 7 correspond to HxCDDs that have a 3:3 distribution of chlorines. We also note that the peak pairs 4-5 and 6-7, which co-elute in the [M-Cl+O]⁻ trace, are resolved in the ECP chromatograms, thereby providing for an additional separation mechanism beyond traditional methods.

Inclusion of Br in the structure dramatically increases the number of potential dioxin isomers. Concentrations of PXDD/Fs in soil obtained from the Plastimet fire have

been measured using tandem mass spectrometry coupled to EI¹⁰. However, concentrations of individual compounds were not reported due to the lack of isomer specific fragments generated by EI and insufficient chromatographic separation. The complexity of a PXDD mixture is nicely illustrated by the chromatogram in Figure 4a. Twelve monobromo-trichloro-dioxin (Br₁Cl₃-DD) isomers were detected from the soil extract by monitoring the dissociation $M^{\bullet+} \rightarrow [M - COBr]^+$, see Figure 4a. Only 7 of these peaks are detected when monitoring the Br₁Cl₁ ECP, which is generated by 2:2 halogen substituted isomers. Comparison with a genuine standard indicates that peak 6 corresponds to the highly toxic 2,3,7,8-substituted congener. It is interesting to note that the relative intensity of peak 6 is actually lower in the negative ion mode experiment. This may be because the yield of ECP can fluctuate depending on the structure. Another possibility is that peak 6 observed in the positive ion mode experiment (Figure 4a) actually corresponds to a mixture of co-eluting isomers.

Figure 5a displays the APCI (+ve) molecular ion chromatogram for the Br₁Cl₅-DD congener class. Its appearance is very close to that of the [M-Cl+O]⁻ (Figure 5b) and MS/MS chromatograms (not shown)¹⁰. Of the 8 partially-resolved peaks detected, peaks 3 and 5 correspond to compounds that dissociate into the BrCl ECP (figure 5c) and peaks 4 and 7 correspond to compounds that dissociate into the BrCl₃ ECP (figure 5e), which is indicative of 4:2 halogen distribution. Similarly, peaks 1, 2, 6 and 8 (Figure 5d) correspond to 3:3 halogen substituted congeners. Not every isomer is separated due to the complexity and chromatographic conditions, but the ECP reactions permit sorting isomers on the basis of halogen distribution. Using this information, we attempted to

determine the relative ratios of the various congener groups (e.g. 3:3 vs. 4:2 halogen substitutions). Based upon peak area ratios obtained from Figure 5a, it is proposed that the 3:3 and 4:2 substituted congeners constitute 67% and 33% respectively of the total $\text{Br}_1\text{Cl}_5\text{-DD}$ concentration. This compares well with the statistical distribution³⁷, which suggests the formation of the PXDDs during the fire results in a random distribution of isomers. Similar breakdowns are observed for the $\text{BrCl}_3\text{-DD}$ and $\text{BrCl}_4\text{-DD}$ congener classes (Figure 6). In all cases, it appears the formation of PXDDs with symmetrical halogen distributions (2:2, 3:2 and 3:3) is favoured over those with asymmetric distributions.

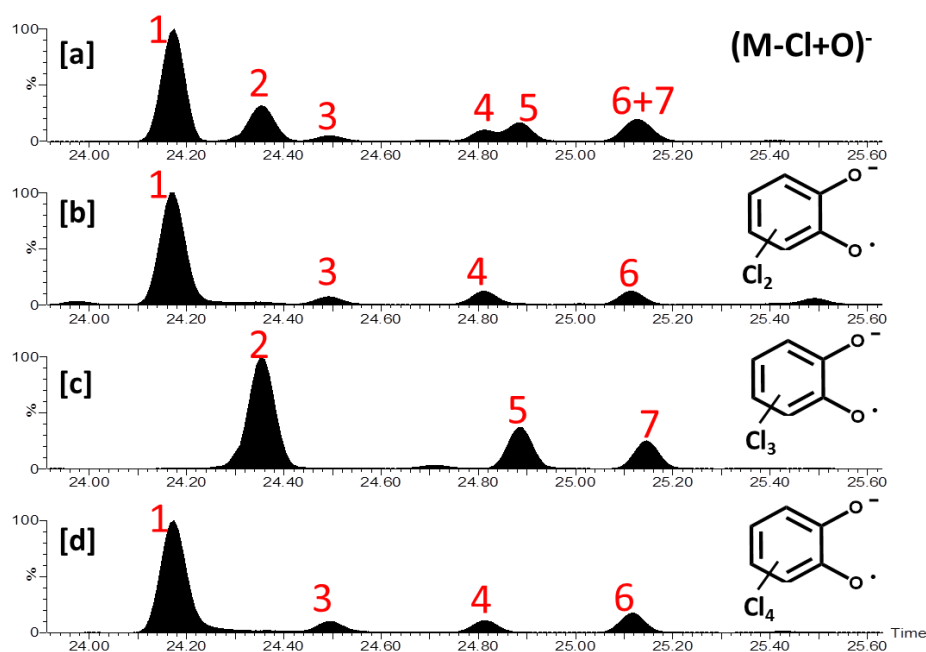


Figure 3. [a] The $(\text{M-Cl+O})^-$ chromatogram of the hexachlorinated dioxins (HxCDD) in the Plastimet ash sample along with the Cl_2 , Cl_3 and Cl_4 ether cleavage product chromatograms (b-d). The ether cleavage product chromatograms yield the distribution of the chlorines across the 2 aromatic rings of the dioxin backbone.

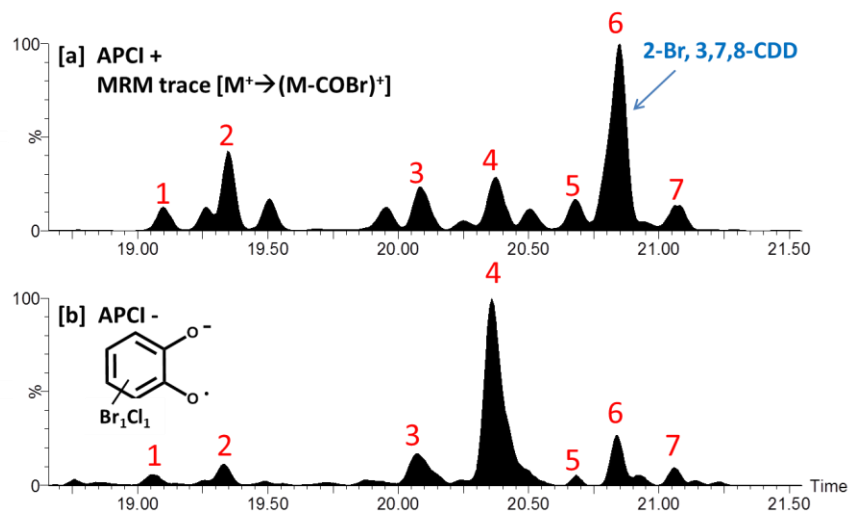


Figure 4. [a] The APCI⁺ MRM trace $[M^+ \rightarrow (M-COBr)^+]$ transition for the monobromo-trichloro-dioxins (Br_1Cl_3 -DD) in the Plastimet ash extract. [b] The NI-APCI Br_1Cl_1 ether cleavage product trace for the same sample. The ether cleavage product trace shows the number of Br_1Cl_3 -DD species that have a 2:2 halogen distribution. The toxic 2-Br, 3,7,8-CDD isomer has been identified using an authentic standard.

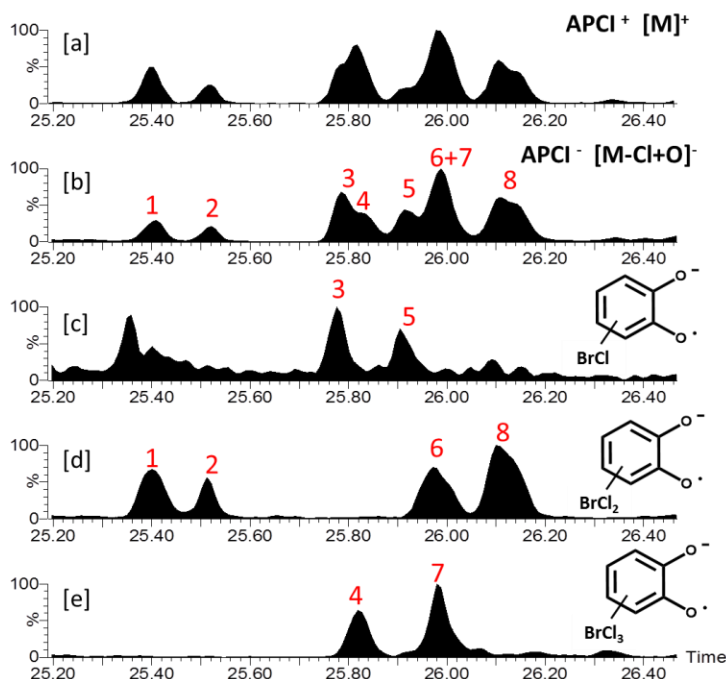


Figure 5. [a] The APCI⁺ molecular ion chromatogram of the Br_1Cl_5 -DD congener class along with the corresponding $[M-Cl+O]^-$ chromatogram [b], Br_1Cl_1 ECP chromatogram [c], Br_1Cl_2 ECP chromatogram [d] and the Br_1Cl_3 ECP chromatogram [e]. The ECP chromatograms yield information on the halogen distribution for the 8 unresolved peaks observed.

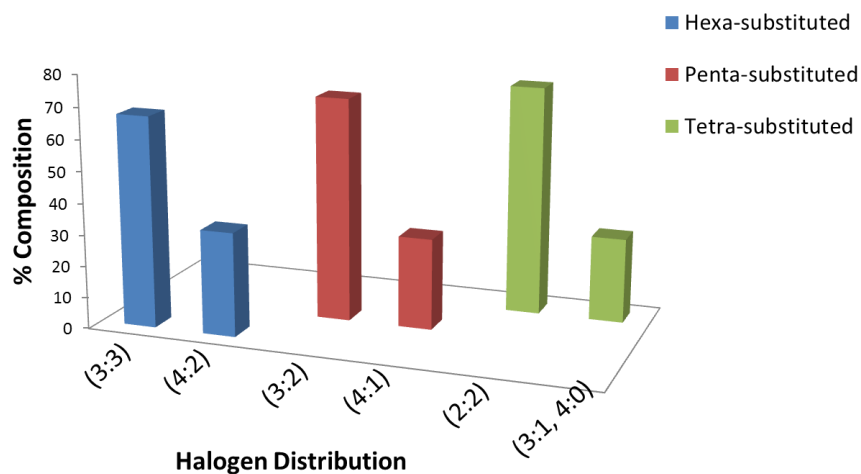


Figure 6. The percent composition of the halogen distribution for the hexa-, penta- and tetra substituted Br_1Cl_x species. In this case the percent composition for the symmetrical distributions (3:3, 3:2 and 2:2) was favoured over the asymmetrical distributions (4:2, 4:1, 4:0 and 3:1) of the halogens for these congener classes.

The results reported by Myers et al.¹⁰ indicated that the total concentration of the monobromopolychloro-dioxin ($\text{Br}_1\text{Cl}_x\text{-DD}$) congeners were approximately 10% of the corresponding chlorinated dioxins¹⁰. It was also determined that the TEQ in surrounding residential areas (air, soil vegetation) returned to normal urban background levels within a few days after the fire¹⁴. Thus, the threat posed by the PXDDs in this case was minimal. However it should be noted that an air sample taken within close proximity to the fire was measured to contain 1000pg TEQ/m³, which exceeds typical background levels by 2,500-25,000 fold. These conditions were likely encountered by first responders. With the increased use of brominated chemicals in manufactured products, PBDDs and PXDDs are becoming increasingly important¹⁷.

CONCLUSIONS

APCI was explored as an alternative, structure diagnostic ionization technique for the analysis of PBDDs and PXDDs. The results of this study indicate that the reactivity of the PBDDs and PXDDs towards $O_2^{\bullet-}$ follows essentially the same scheme proposed by Hass *et al*²⁶ for the PCDDs.

- (i) $O_2^{\bullet-}$ reacts with PBDDs and PXDDs by cleaving the C-O bonds, essentially cleaving the dioxin molecules into two halves. The reaction also results in the formation of pseudo-molecular ions $[M-X+O]^-$ (where X=Br/Cl).
- (ii) The number of halogens per aromatic ring can be determined by monitoring the ether cleavage product ions.
- (iii) The yield of ether cleavage product ions is high for 2378-substituted compounds, which are the most toxic congeners.
- (iv) Formation of $[M-X+O]$ is preferred over ether cleavage for compounds which have at least one *peri* position (1,4,6,9) occupied by a halogen. If a *peri* halogen is not present, Br/O exchange is preferred over Cl/O exchange.

Using APCI, it was possible to differentiate unknown dioxins and resolve dioxin isomers that would otherwise co-elute. For example, this could be highly beneficial for the analysis of PBDDs, which constitute the same number congeners as the PCDDs, but the choice of GC column is limited by the volatility of the heavier congeners. The enhanced separation of isomers is demonstrated through the analysis of a complex mixture of PXDDs in a soil extract obtained from a major industrial fire. Deconvolution of isomeric

PXDDs was made possible by monitoring selected ECP ions generated by reactions with O_2^{\bullet} . These reactions are observed under typical operating conditions of the instrument, using standard API gas supplies. Further, the estimated IDLs for the ECPs are between 110 and 675fg injected. APCI is a promising, complementary technique for the analysis and identification of PCDD, PBDD, and PXDD compounds in environmental samples.

References

1. Alcock RE, Jones KC. Dioxins in the Environment: A Review of Trend Data. *Environ Sci Technol.* 1996;30(11):3133.
2. Ishaq R, Carina N, Zeb Y, Broman D, Ulf J. PCBs , PCNs , PCDD / Fs , PAHs and Cl-PAHs in air and water particulate samples - patterns and variations. *Chemosphere.* 2003;50:1131-1150.
3. Morital M, Nakagawa JI, Rappe C. Polychlorinated Dibenzofuran (PCDF) Formation From PCB Mixture by Heat and Oxygen. *Bull. Environm. Contam. Toxicol.* 1978;19:665-670.
4. Hutzinger O, Choudhry GG, Chittim BG, Johnston LE. Formation of polychlorinated dibenzofurans and dioxins during combustion, electrical equipment fires and PCB incineration. *Environ Health Perspect.* 1985;60:3-9.
5. Van den Berg M, Birnbaum LS, Denison M. The 2005 World Health Organization reevaluation of human and Mammalian toxic equivalency factors for dioxins and dioxin-like compounds. *Toxicol Sci.* 2006;93(2):223-241.
6. Van den Berg M, Denison MS, Birnbaum LS, et al. Polybrominated Dibenzop-dioxins (PBDDs), Dibenzofurans (PBDFs) and Biphenyls (PBBs)-inclusion in the Toxicity Factor Concept for Dioxin-like Compounds. *Toxicological Sciences.* 2013;133:197-208.
7. Hites RA. Polybrominated Diphenyl Ethers in the Environment and in People : A Meta-Analysis of Concentrations. *Environ Sci Technol.* 2004;38(4):945-956.
8. Van den Berg M, Denison MS, Birnbaum LS, et al. Polybrominated dibenzo-p-dioxins, dibenzofurans, and biphenyls: inclusion in the toxicity equivalency factor concept for dioxin-like compounds. *Toxicol Sci.* 2013;133(2):197-208.
9. Weber, LWD. Greim, H. THE TOXICITY OF BROMINATED AND MIXED-HALOGENATED DIBENZO-p-DIOXINS AND DIBENZOFURANS: AN OVERVIEW. *J Toxicol Environ Health.* 1997;50(3):195-216.
10. Myers AL, Mabury SA, Reiner EJ. Analysis of mixed halogenated dibenzo-p-dioxins and dibenzofurans (PXDD/PXDFs) in soil by gas chromatography tandem mass spectrometry (GC-MS/MS). *Chemosphere.* 2012;87(9):1063-1069.

11. Myers AL, Watson-Leung T, Jobst KJ. Complementary Nontargeted and Targeted Mass Spectrometry Techniques to Determine Bioaccumulation of Halogenated Contaminants in Freshwater Species. *Environ Sci Technol.* 2014;48:13844-54.
12. Fernandes A. Investigation into the Occurrence of Mixed Halogenated Dioxins, Furans and Biphenyls in Food. *Food and Environmental Research Agency.* 2010. FD 09/08.
13. Fernando S, Jobst KJ, Taguchi VY, Helm PA, Reiner EJ, Mccarry BE. Identification of the Halogenated Compounds Resulting from the 1997 Plastimet Inc. Fire in Hamilton, Ontario, using Comprehensive Two-Dimensional Gas Chromatography and (Ultra)High Resolution Mass Spectrometry. *Environ Sci Technol.* 2014;48:10656-63.
14. Socha, A., Abernethy, S., Birmingham, B. Plastimet Inc. Fire. Ontario Ministry of the Environment, October. 1997.
15. Taguchi VY, Nieckarz RJ, Clement RE, Krolik S, Williams R. Dioxin analysis by gas chromatography-Fourier transform ion cyclotron resonance mass spectrometry (GC-FTICRMS). *J Am Soc Mass Spectrom.* 2010;21(11):1918-1921.
16. Sovocool GW, Mitchum RK, Tondeurt Y, Munslow WD, Vonnahme TL, Donnellyf JR. Bromo- and Bromochloro-polynuclear aromatic hydrocarbons , Dioxins and Dibenzofurans in Municipal Incinerator Fly Ash. *Biomedical and Environmental Mass Spectrometry.* 1988;15:669-676.
17. Yu, X., Zennegg, M., Engwall, M., Rotander, A., Larson, M., Wong, M.H., Weber, R. E-waste recycling heavily contaminates a Chinese city with chlorinated, brominated and mixed halogenated dioxins. *Organohalogen Compounds.* 2008;70:813-816.
18. Viel J, Arveux P, Baverel J, Cahn J. Soft-Tissue Sarcoma and Non-Hodgkin ' s Lymphoma Clusters around a Municipal Solid Waste Incinerator with High Dioxin Emission Levels. *Am J Epidemiol.* 2000;152(1):13-19.
19. Fernandes AR, Rose M, Mortimer D, Carr M, Panton S, Smith F. Mixed brominated/chlorinated dibenzo-p-dioxins, dibenzofurans and biphenyls: Simultaneous congener-selective determination in food. *J Chromatogr A.* 2011;1218(51):9279-9287.
20. Reiner EJ, Clement RE, Okey AB, Marvin CH. Advances in analytical techniques for polychlorinated dibenzo-p-dioxins, polychlorinated dibenzofurans and dioxin-like PCBs. *Anal Bioanal Chem.* 2006;386(4):791-806.

21. Hagberg J. Analysis of brominated dioxins and furans by high resolution gas chromatography/high resolution mass spectrometry. *J Chromatogr A*. 2009;1216(3):376-384.
22. Zacs D, Rjabova J, Viksna a., Bartkevics V. Method development for the simultaneous determination of polybrominated, polychlorinated, mixed polybrominated/chlorinated dibenzo-p-dioxins and dibenzofurans, polychlorinated biphenyls and polybrominated diphenyl ethers in fish. *Chemosphere*. 2015;118:72-80.
23. Reiner EJ. Analysis of Dioxins and Related Compounds. *Mass Spectrometry Reviews*. 2010;29:526-559.
24. Chernetsova ES, Revelsky AI, Revelsky IA, Mikhasenko IA, Sobolevsky TG. Determination of polychlorinated dibenzo-p-dioxins, dibenzofurans, and biphenyls by gas chromatography/mass spectrometry in the negative chemical ionization mode with different reagent gases. *Mass Spectrom Rev*. 2002;21:373-387.
25. Hunt, D.F., Harvey TM, Russell W. Oxygen as a Reagent Gas for the Analysis of 2,3,7,8-Tetrachlorodibenzo-p-dioxin by Negative Ion Chemical Ionization Mass Spectrometry. *J.C.S. Chem Comm*. 1975:151-152.
26. Hass, R J, Friesen MD, Carolina N. The Mass Spectrometry of Polychlorinated Dibenzo-p-Dioxins. *Organic Mass Spectrometry*. 1979;14(1):9-16.
27. Mitchum R.K., Korfmacher W, Moler, G F. Capillary Gas Chromatography / Atmospheric Pressure Negative Chemical Ionization Mass Spectrometry of the 22 Isomeric. *Anal Chem*. 1982;(7):719-722.
28. Korfmacher WA, Rowland KL, Mitchum RK, Daly JJ, Mcdaniel RC, Plummer M V. Analysis of snake tissue and snake eggs for 2,3,7,8-tetrachlorodibenzo-p-dioxins via fused silica GC combined with atmospheric pressure ionization MS. *Chemosphere*. 1984;13(11):1229-1233.
29. Korfmacher WA, Hansen, E.B., Rowland KL. Tissue distribution of 2,3,7,8-TCDD in bull frogs obtained from 2,3,7,8-TCDD contaminated area. *Chemosphere*. 1986;15(11):121-126.
30. Kleopfer RD, Zirschky J. TCDD distribution in the Spring River, Southwestern Missouri. *Environ Int*. 1983;9:249-253.
31. Hass JR, Friesen MD, Harvan DJ, Parker CE. Determination of polychlorinated dibenzo-p-dioxins in biological samples by negative chemical ionization mass spectrometry. *Anal Chem*. 1978;50(11):1474-1479.

32. Ballesteros-Gomez A, Boer J De, Leonards PEG. Novel Analytical Methods for Flame Retardants and Plasticizers Based on Gas Chromatography, Comprehensive Two-Dimensional Gas Chromatography, and Direct Probe Coupled to Atmospheric Pressure Chemical Ionization-High Resolution Time-of-Flight-Mass Spectrometry. *Anal Chem.* 2013;85:9572-80.
33. Organtini KL, Myers AL, Jobst KJ, et al. Quantitative Analysis of Mixed Halogen Dioxins and Furans in Fire Debris Utilizing Atmospheric Pressure Ionization Gas Chromatography-Triple Quadrupole Mass Spectrometry. *Anal Chem.* 2015;87:10368-77..
34. Li D-X, Gan L, Bronja A, Schmitz OJ. Gas chromatography coupled to atmospheric pressure ionization mass spectrometry (GC-API-MS): Review. *Anal Chim Acta.* 2015;891:43-61.
35. McEwen CN, McKay RG, Larsen BS. Analysis of solids, liquids, and biological tissues using solids probe introduction at atmospheric pressure on commercial LC/MS instruments. *Anal Chem.* 2005;77(23):7826-7831.
36. Ontario Ministry of the Environment and Climate Change. 2014. The determination of polychlorinated dibenzo-p-dioxins, polychlorinated furans and dioxin-like PCBs in environmental matrices by GC-HRMS. Toronto, ON, Canada: Laboratory Services Branch Method E3418.
37. Buser HR. Brominated and Brominated/Chlorinated Dibenzodioxins and Dibenzofurans: Potential Environmental Contaminants. *Chemosphere.* 1987;16(4):713-732.

Supplementary Information

Experimental

The flow rate of gases into the APCI source was found to be an important parameter which influenced sensitivity. There are 4 gas inputs into the source which include helium from the GC column, GC make up gas, cone and auxiliary gas. The pressure within the source is balanced by the amount of gas taken in through the cone into the mass spectrometer and the gas pumped out through the exhaust. In cases where the total flow into the source is lower than the amount drawn in through the cone, exhaust backflow into the source occurs giving rise to high background noise and an overall decrease in sensitivity as illustrated in Figure S1. The figure displays the Br₂ ECP trace at m/z 266 for a suite of halogenated dioxins (1pg injected) analyzed at a cone gas flow of 100L/hr and 175L/hr. The increase in cone gas flow rate dramatically decreased the noise in the trace and increased the signal to noise ratio (S/N) for the 2378-TBDD by nearly 7-fold. In cases where the gas flow into the source is significantly higher than the amount drawn in through the cone, signal intensity decreases as the excess flow is pumped out through the exhaust.

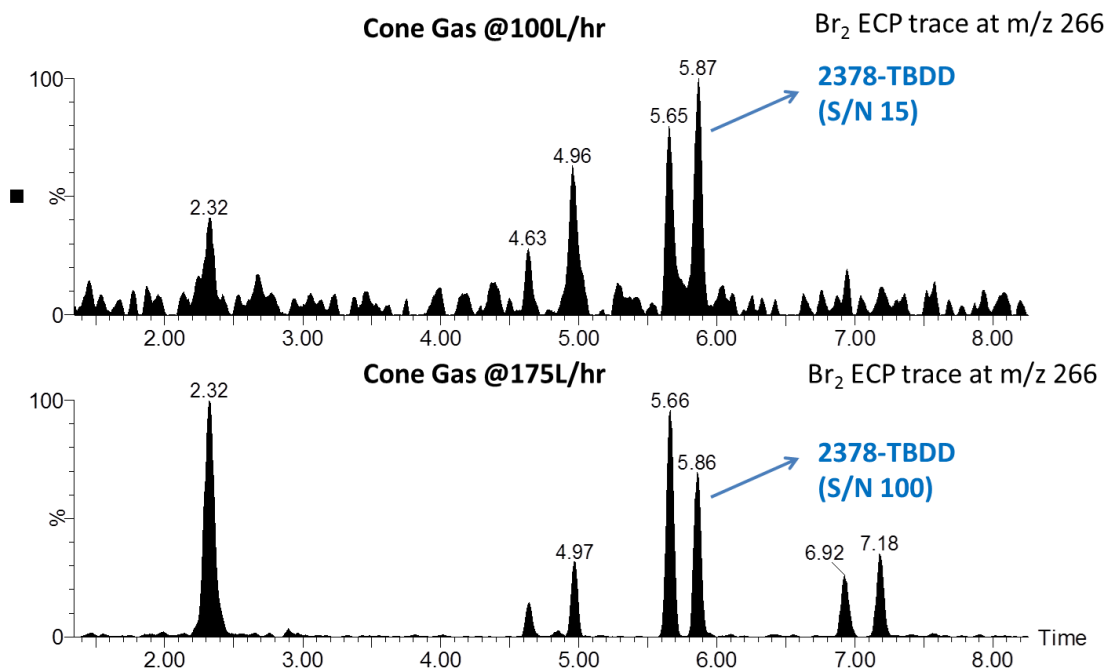


Figure S1. The Br₂ ECP trace at m/z 266 for a suite of halogenated organics analyzed at a cone gas flow rate of 100L/hr and then at 175L/hr. In this case the increased gas flow into the source helped reduce exhaust backflow resulting in an increase in the S/N as shown for the 2378-TBDD species.

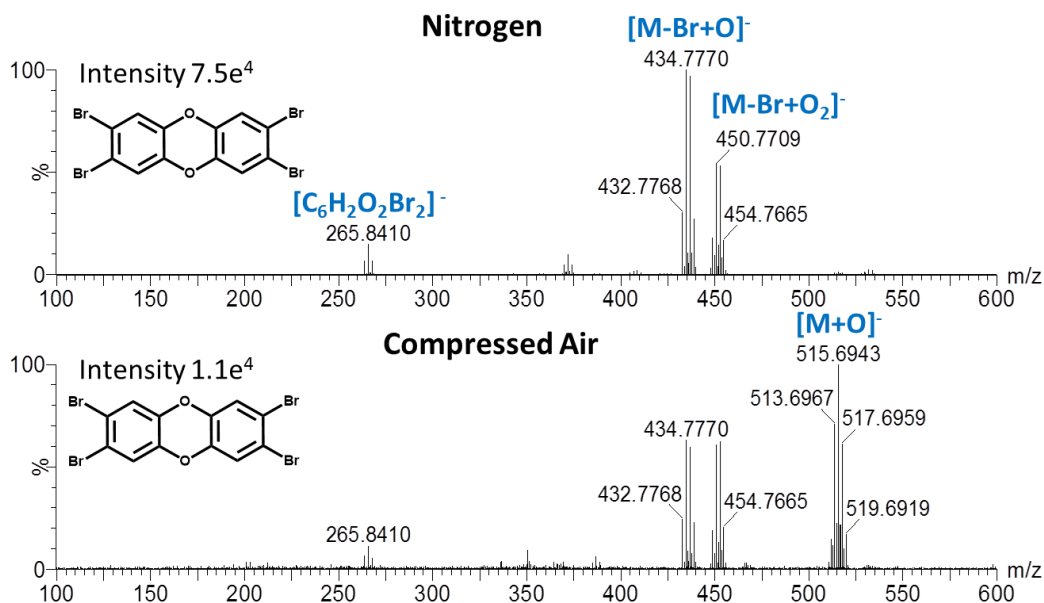


Figure S2. The NI-APCI mass spectrum of 2378-TBDD using nitrogen and then compressed air as the cone gas. The use of compressed air led to a significant increase in the relative abundance of the [M+O]⁻ peak. However, the absolute intensity of the ions including the ECP at m/z 266 was significantly lower compared to the nitrogen spectrum.

CHAPTER SIX

Conclusions

Research Summary

Chapter 2

Air samples, skin wipes and urine samples were collected from a group of firefighters who participated in training exercises in order to evaluate exposure. Wood was the primary fuel used in these training exercises. A suite of wood smoke markers were monitored, which included PAHs and MPs. Skin wipes were obtained from multiple body sites and analyzed for the presence and levels of the marker compounds to evaluate dermal exposure. The concentrations of the marker compounds at the multiple body sites were statistically similar indicating whole-body exposure. Next, both pre- and post-exposure urine samples from each firefighter were analyzed by multiple reaction monitoring (MRM) for metabolites of the marker compounds in an attempt to quantify overall exposure. A group of PAH and MP metabolites were chosen as specific and sensitive urinary markers of smoke exposure. Post-exposure creatinine-normalized levels of these markers were significantly higher ($p < 0.05$) in the urine of some firefighters as compared to the rest of the group. The lack of correlation between smoke-markers measured in the air and on the skin with levels in the urine suggested that exposure likely occurred from inhalation/ingestion despite use of self-contained breathing apparatus (SCBA) and could be related to specific operational roles. This work provides deeper insight into chronic disease risk posed by occupational smoke exposure among

firefighters that can be mediated by improved hygiene practices and protective equipment.

Chapter 3

Comprehensive two-dimensional gas chromatography mass spectrometry (GC×GC-MS) was used for the identification of novel markers of wood smoke exposure by analyzing both smoke and urine samples from the firefighter study described in Chapter 2. More than 1000 components were detected in smoke sample extracts and 4000-20,000 components were detected in urine sample extracts by GC×GC-MS. Novel markers were identified in the smoke, some of which were also detected in the post-exposure urines of the firefighters. A number of these compounds were found to be present exclusively in the particle-phase of smoke, including a group of resin acids. At the moment, most wood smoke markers used are found exclusively in the gas-phase including the specific PAH and MPs monitored in Chapter 2. While gas-phase chemicals are thought to penetrate the lungs and cross into the blood through the alveoli, particulate matter has the potential to be embedded in the alveoli and result in a slow release of the bound organic chemicals into the blood thus potentially increasing the risk of exposure. Multiple reaction monitoring (MRM) experiments were developed and used to monitor the resin acids in the urines of a group of firefighters along with the specific MP and PAH metabolites. The resin acids increased in concentration in the post-exposure urines of the firefighters indicative of exposure to particle bound organics. In combination with the MP and PAH metabolites, the resin acids help provide a more complete picture of exposure to wood smoke.

Chapter 4

The halogenated organic compounds were identified in soil contaminated by a major industrial fire at a plastic recycling plant (Plastimet Inc.). Due to the potential toxic nature of halogenated organics that arise from the burning of plastics, this fire raised significant concerns among local residents and health officials. At the time of the fire (1997) numerous samples (air, soil, water) were collected and analyzed for compounds of concern including PAHs, PCBs and PCDD/Fs. The goal of this study was to identify novel halogenated organics using state-of-the-art analytical instrumentation that was not readily available at the time. Accurate mass measurements obtained from a direct insertion probe experiment using an ultra-high resolution mass spectrometer (FT-ICRMS) were used to construct a mass defect (MD) plot. The MD plot revealed numerous halogenated PAHs including many highly substituted and high molecular weight species that have not previously been identified in the environment. Subsequent analysis of the sample extract on a GC×GC-MS enabled isomer differentiation and quantification. The high concentrations of the halogenated PAHs compared to the PCDDs/Fs along with the high potential toxicity of these compounds highlights the need for further investigation into their environmental occurrence and risk.

Chapter 5

Alternative ionization techniques were explored for the analysis of dioxins and furans including chlorine, bromine and mixed bromo/chloro substituted species. The analysis of mixed halogenated dioxins and furans (PXDD/Fs) have been hampered by a lack of authentic standards as well as suitable analytical techniques required to resolve the

enormous number of potential congeners. Traditional electron ionization (EI) mass spectrometry-based methods are of limited value in part due to the lack of structure diagnostic fragments that are formed. Therefore, differentiation of isomeric species has not been possible in the absence of chromatographic separation. Negative ion atmospheric pressure chemical ionization (NI-APCI) of PXDDs was explored as an alternative ionization technique to derive structure diagnostic fragments using a modern Atmospheric Pressure Gas Chromatography mass spectrometry (APGC) system. NI-APCI of a number of halogenated dioxin standards gave rise to ether cleavage fragments as a result of reaction with residual oxygen in the ion source. These fragments provided structural information since the distribution of halogens on the dioxin backbone could be used to differentiate isomers. The results indicate comparable detection limits for the positive radical cations $[M^{*+}]$ and negative pseudomolecular ions $[M-Cl+O]^-$: Approximately 5 fg and 10 fg respectively for 2378-TCDD and 5-10 fg and 10–60 fg, respectively for the PXDDs. Detection limits for the ether cleavage products were somewhat higher (between 100 and 500 fg), but still acceptable for trace analysis of PXDDs. This method was applied for the analysis of an ash sample from the Plastimet fire known to contain PXDDs and has demonstrated its potential in deconvoluting mixtures of isomers.

6.2 Outcomes and Future directions

Very few studies have attempted to assess firefighter exposures in a comprehensive manner. Most studies have been limited by the choice of marker compounds and analytical methods. The analytical methods developed during the course

of my Ph.D. studies can be used to assess firefighter exposure by monitoring a suite of marker compounds representing both the gas- and particle-phase of the smoke. The identification of particle-phase chemical markers in the post-exposure urines of exposed firefighters provides direct evidence of exposure to particulate matter and the chemicals bound to it. This is an important finding since other highly toxic chemicals, including the haloPAHs, PCDD/Fs and PXDD/Fs identified in the Plastimet ash sample, are predominantly particle-bound. However, due to the lipophilic nature of these halogenated organics, the average half-life of dioxins in humans is approximately 8 years¹. In this case the resin acids can be used as surrogates for particle-bound chemical exposures. However a number of studies have measured dioxins in blood and serum of the general population² as well as those occupationally exposed including firefighters³⁴⁵.

Based on the results of the firefighter study it is believed that a subset of the sampled firefighters was exposed to higher levels of wood smoke via the SCBA. These firefighters may be at increased risk of exposure to more toxic chemicals based on the nature of the fires encountered. Although industrial fires such as Plastimet are rare, a number of the halogenated organics produced in the Plastimet fire may be present in more common household fires. Since households are equipped with numerous electronic devices and plastic based materials, the combustion products are likely to consist of halogenated and mixed halogenated organics. In a study conducted at the Fire and Emergency Services Training Institute (FESTI) in Toronto, Ontario, Canada 2 simulated fires were carried out. One fire involved the burning of mostly electronic items such as televisions, computers and printers while the second fire involved the burning of common

household items such as a mattress, sofa, chairs and a television. Numerous halogenated organics were produced in these fires⁶. As a result, the general population as well as firefighters are at risk of exposure to these chemicals from such common fires. It is therefore imperative that firefighters take all necessary actions to protect themselves during such events.



Sujan Fernando and Professor Brian McCarry assembling air samplers used to monitor the combustion products from the burning of common household materials at FESTI.

The analytical methodologies developed in the current work can be used to evaluate the effectiveness of improved hygiene practices and safety gear to limit firefighter exposures. It was observed that at the moment no standard hygiene practices exist across the province where it concerns cleaning of the personal safety equipment.

The fact that many of the firefighter safety gear, including their SCBA, are not properly cleaned after fires or training exercises raises questions about the prolonged exposures due to the off-gassing of chemicals from the safety gear. Also, in many cases the SCBA may be custom fitted at the time of distribution and may not be tested again for an extended period of time. During this period any physical changes in the firefighter such as change in weight may affect the degree to which the SCBA fits and thus protects against smoke exposure. It is suspected that in some firefighters, the SCBA might have become dislodged momentarily during the training exercises and potentially during actual fires. The design of the study however does not allow us to investigate this suspicion further. A method of sampling inside the SCBA will help evaluate this claim further. Furthermore, the analytical methodologies developed during course of the research can also be readily adopted to assess other occupational exposures.

Combustion products from fires and other anthropogenic sources continue to impact the environment. The use of new formulations in the production of synthetic materials will undoubtedly lead to the emergence of novel contaminants. Therefore, it is necessary to develop improved techniques to monitor legacy contaminants, but it is also important to develop techniques capable of identifying emerging contaminants. The multidimensional chromatography and high resolution mass spectrometry techniques utilized in the current work have proven to be very powerful tools that can be used to conduct comprehensive analysis of complex samples. The construction of MD plots from high resolution data provides a stepping stool for data mining and aids the identification of potentially toxic novel contaminants in a complex sample matrix. The

enhanced separation achieved by GC×GC can be utilized for isomer separation and minimize matrix interference.

The development of modern analytical instruments such as APGC has provided the opportunity to explore the use of non-traditional ionization techniques for the analysis of environmental contaminants. The NI-APCI method developed in the current work for the analysis of mixed halogenated dioxins has proven to be more selective for the identification of the (potentially) toxic isomers compared to traditional electron ionization techniques. Such a selective method could be used to identify toxic isomers/congeners for which authentic standards are not available. NI-APCI has the potential to be more selective and sensitive towards a wide range of halogenated contaminants than traditional ionization techniques and may be applied to the analysis of firefighter exposure to these compounds in the future.

References

1. Geyer HJ, Schramm K, Anton E, Poiger H, Henkelmann B, Kettrup A. Half-lives of tetra-, penta-, hexa-, hepta-, and octachlorodibenzo-p-dioxins in rats, monkeys and humans — a critical review. *Chemosphere*. 2002;48:631-644.
2. Consonni D, Sindaco R, Bertazzi PA. Blood levels of dioxins, furans, dioxin-like PCBs, and TEQs in general populations: A review, 1989–2010. *Environ Int*. 2012;44:151-162.
3. Wittsiepe J, Wilhelm M, Kraus T. Levels of Polychlorinated Dibenzo- *p* -Dioxins and Dibenzofurans (PCDD/F) in Blood Samples of Occupationally Exposed Workers From a Transformer Recycling Plant in Dortmund, Germany—Initial Findings. *J Toxicol Environ Heal Part A*. 2012;75(8-10):423-428.
4. Mannetje A, Eng A, Walls C, et al. Serum concentrations of chlorinated dibenzo-p-dioxins, furans and PCBs, among former phenoxy herbicide production workers and firefighters in New Zealand. *Int Arch Occup Environ Health*. 2015.
5. Shaw SD, Berger ML, Harris JH, et al. Persistent organic pollutants including polychlorinated and polybrominated dibenzo-p-dioxins and dibenzofurans in firefighters from Northern California. *Chemosphere*. 2013;91(10):1386-1394.
6. Organtini KL, Myers AL, Jobst KJ, et al. Quantitative Analysis of Mixed Halogen Dioxins and Furans in Fire Debris Utilizing Atmospheric Pressure Ionization Gas Chromatography-Triple Quadrupole Mass Spectrometry. *Anal Chem*. 2015.